Evaluating the anti-leukemia activity of avocatin B

by

Eric Alexandre Lee

A thesis

presented to the University of Waterloo

in fulfillment of the

thesis requirement for the degree of

Master of Science

in

Pharmacy

Waterloo, Ontario, Canada, 2014

AUTHOR'S DECLARATION

I hereby declare that I am the sole author of this thesis. This is a true copy of the thesis, including any required final revisions, as accepted by my examiners.

I understand that my thesis may be made electronically available to the public.

Abstract

Acute myeloid leukemia (AML) is an aggressive malignant disease characterized by poor patient outcome and suboptimal front-line chemotherapy. To identify novel anti-AML compounds, a high-throughput screen of a natural products library (n=800) was performed. This screen was performed against the AML cell line (TEX), which has several properties of leukemia stem cells, the cells responsible for disease pathophysiology and patient relapse. Here, avocatin B was identified as a potent and novel anti-leukemia agent. Avocatin B, at concentrations as high as 20μM, had no effect on normal peripheral blood stem cell viability. In contrast, it induced death of primary AML cells with an EC50 of 1.5-5.0 μM. Selective toxicity towards a functionally defined subset of primitive leukemia cells was also demonstrated. Avocatin B (3μM) reduced clonogenic growth of AML progenitor cells with no effect on clonogenic growth of normal hematopoietic stem cells. Further, treatment of primary AML cells with avocatin B (3μM) diminished their ability to engraft into the bone marrow of pre-conditioned, NOD/SCID mice (t_{18}=6.5; $p<0.001$). Together, these results confirm that avocatin B is a novel anti-AML agent with selective toxicity towards leukemia and leukemia stem cells.

Mechanistically, avocatin B induced reactive oxygen species (ROS)-dependent leukemia cell apoptosis that was characterized by the release of mitochondrial proteins, cytochrome c and apoptosis inducing factor (AIF). Cytochrome c and AIF were detected in the cytosol of avocatin B treated TEX cells by flow cytometry. Avocatin B-induced apoptosis, as measured by the Annexin V/Propidium iodide assay, DNA fragmentation and PARP cleavage, and was abolished in the presence of anti-oxidants confirming the functional importance of ROS. Next, we further evaluated the role of mitochondria in avocatin B-induced apoptosis. First, we generated leukemia cells lacking mitochondria by successive culturing in media containing ethidium bromide. The drastic (>80%) reduction in mitochondria was confirmed by nonyl acridine orange staining and flow cytometry and a

near absence of the mitochondria specific proteins ANT and ND1, as measured by Western blotting. Avocatin B's activity was abolished in leukemia cells lacking mitochondria. Next, we tested avocatin B in cells engineered to lack CPT1, the enzyme that facilitates transport of 16-20 carbon lipids into mitochondria. Avocatin B's activity was abolished in cells with reduced CPT1 expression (>70% as measured by qPCR analysis). To further confirm the importance of CPT1 in avocatin B-induced death, we chemically inhibited CPT1 with etomoxir. Avocatin B's activity was blocked in the presence of etomoxir, further demonstrating that avocatin B accumulates in mitochondria.

Since avocatin B is a lipid that targets mitochondria and that mitochondria can oxidize fatty acids for energy, we next assessed the impact of avocatin B on fatty acid oxidation, using the Seahorse Bioanalyzer. Avocatin B inhibited leukemia cell fatty acid oxidation (>40% reduction in oxygen consumption at 10μM) and this occurred at a 10-fold less concentration than etomoxir, the standard experimental molecule used to probe this pathway. Further, avocatin B treatment resulted in a 50% reduction in levels of NADPH, an important co-factor generated during fatty acid oxidation that participates in catabolic processes during cell proliferation.

Additionally, we demonstrated that autophagy was functionally important for avocatin B induced leukemia cell death. We reported increased autophagic activity through confocal microscopy and Western Blotting of autophagy specific proteins LC3B, ATG7, SQSTM1(p62) and BNIP3L(Nix). To further confirm the importance of autophagy in avocatin B-induced death, we generated cells with reduced ATG7, the protein involved in autophagosome formation. Avocatin B's activity was abolished in these cells demonstrating that autophagy was essential for avocatin B's activity.

These results show that avocatin B accumulates in mitochondria to inhibit fatty acid oxidation and reduce NADPH to result in ROS-mediated activation of autophagy and apoptosis in leukemia cells. This highlights a novel AML-therapeutic strategy by which mitochondria are targeted to impair cellular metabolism leading directly to AML cell death.

Acknowledgements

First and foremost, I would like to thank my supervisor, Dr. Paul A. Spagnuolo, for his continual guidance and support. The accomplishments that I have achieved over the past two years serve as a testament of his exemplary mentorship. It has been an honour and privilege to have a mentor that I can rely on for both advice and support. I would like to thank my advisory committee members, Dr. Jonathan Blay and Dr. Jamie Joseph, for their feedback and input throughout my masters. I would like to acknowledge the numerous collaborators who have contributed to the success of this thesis: Dr. Schimmer, Dr. Quadrilatero, Dr. Joseph, Dr. Minden, Elliott McMillan, Andrew Mitchell, Elena Kreinin, and Thomas Hanlon. Many thanks to Sarah Rae for her patience and kindness when dealing with my administrative requests. Special thanks to Dr. Murray Cutler Jr., our token post-doc, whose advice and feedback have been invaluable. I would also like to acknowledge and thank Roger Chen, Marina Jalal and Samih Alqawlaq, for both their friendship and their contributions to the success of the project (but will never be formally acknowledged). I would like to thank and acknowledge my lab mates, Leonard Angka, Sarah-Grace Rota and Kevin the fish, for not only being supportive teammates but being my family away from home. I am grateful to have spent almost every day of the last two years with my best friends. Thank you to #loveisonyourside for being the perfect escape to long and unsuccessful days in the lab. Together we have built some unforgettable memories and others that ought to be forgotten. Thank you to the all the graduate students at the School of Pharmacy who welcomed me into their community. I am thankful for your friendship and wish you all success. Thank you Angela Millson for all your love and support. I am eternally grateful to have met you. I am also thankful that you passed the OSCE. Last but not least, thank you to my family for their continual love and support. My successes are yours.

Table of Contents

List of Figures

Chapter 1

Chapter 4

Chapter 5

Chapter 1: General Introduction

1.1 Acute myeloid leukemia (AML)

Acute myeloid leukemia (AML) is a devastating disease characterized by poor patient prognosis. Abysmal patient survival rates are due to high rates of disease relapse and failure to achieve remission due to two factors: 1) the treatment of AML is outdated, having been unchanged for the past 40 years [1-3], and 2) the presence of leukemia stem cells (LSCs), which are responsible for drug resistance, as these are not targeted by current drugs, and disease propagation [4-6].

AML, a type of blood cancer, is a heterogeneous disease which results from the disruption of hematopoiesis resulting in hematopoietic insufficiency (Figure 1.1). The inadequate production of normal blood cells observed in AML is due to the uncontrolled proliferation and accumulation of immature myeloid cells, generally referred to as leukemic blasts, in the bone marrow [7]. AML is observed in 3-8 per 100,000 people, with increasing incidence with age [8]. Approximately 12,000 people are diagnosed with AML in the United States annually, whereby 8,590 of them are predicted to die from the disease [9, 10]. AML patients are faced with extremely poor prognosis, where patients 60 years or older have a 2-year survival rate of less than 10% and median survival of less than 1 year. AML is the most common leukemia observed in adults, with a median patient age of 72 years old, and three quarters of patients with AML are 60 years of age or older [1, 9, 10]. Furthermore, AML accounts for 32% of cancer-related deaths in children [11].

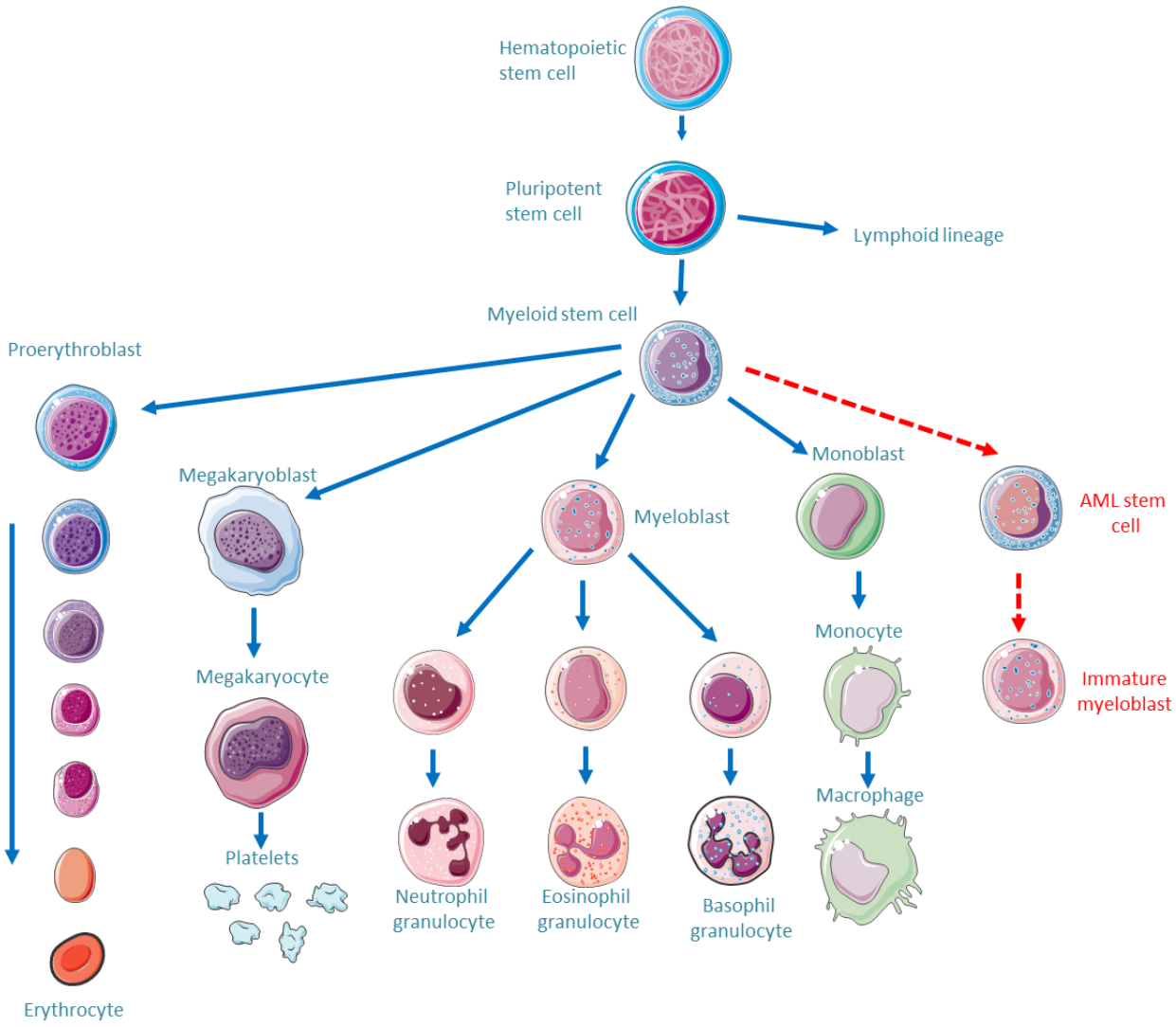

Figure 1.1. Schematic flow diagram of normal hematopoiesis and AML. In AML, myeloid stem cell differentiation is impaired resulting in the accumulation of immature myeloid cells. As a result, AML patients suffer from hematopoietic insufficiency due to lowered leukocyte and erythrocyte counts. Adapted from "Marieb, Elaine Nicpon,Hoehn, Katja. (2010) Human anatomy & physiology /San Francisco : Benjamin Cummings" using Servier Medical Art (Creative Commons Attribution 3.0 Unported License).

1.1.1 Treatment

AML therapy has essentially remained unchanged for the past 40 years. The first step in AML therapy, known as induction therapy, has relied on daunorubicin, an anthracycline, and the pyrimidine analog cytarabine as the backbone of chemotherapeutic treatment. This is known as the "3+7" treatment regimen, which consists of 3 days of daunorubicin (45-90mg/m^2) followed by 7 days of intravenous

cytarabine (100-200 mg/m^2) [1, 3, 11, 12]. Usage of daunorubicin and cytarabine in induction therapy causes remission in 65-75% of cases who are less than 60 years of age and 30-50% in patients older than 60 years of age [1, 11, 13]. Induction therapy aims to achieve remission, which is characterized by the presence of less than 5% blasts in the bone marrow and to prevent the possibility of disease relapse.

Treatment of older AML patients (e.g., >65) is complicated by increased resistance to therapy, and a higher incidence of co-morbidity and as these patients are less tolerant to the cytotoxicities of conventional chemotherapy [11, 13]. Daunorubicin and cytarabine are highly cytotoxic with side effects such as nausea, vomiting, pain, ataxia and haemorrhage. As such, only 30% of older AML patients receive treatment beyond supportive care [14]. This clearly warrants for the development of novel and safer AML treatment strategies. Current efforts have been made to improve complete remission rates whilst reducing cytotoxic side effects -such as increased dosing, the use of alternative anthracyclines (ie. Idarubicin), or the addition of other chemotherapeutic agents such as etoposide (topoisomerase II inhibitor), clofarabine, cladribine, and fludarabine (purine analogues). Unfortunately, no conclusive evidence has been generated to indicate that one treatment or new combinations should become the new chemotherapeutic standard [1, 9, 15].

1.2 Leukemia stem cells (LSCs)

Leukemia is believed to be a hierarchical model similar to that of regular hematopoiesis with leukemia stem cells at the apex [16]. The first study supporting this involved the identification of a subpopulation of CD34+/CD38- AML cells that were capable of transplanting in an immunocompromised mouse, whereas the bulk population of cells were not [17]. Furthermore, serial transplantation of this cell subpopulation in mouse xenograft models displayed long-term engraftment as well as self-renewal properties [18]. This led to the belief that a subpopulation of LSCs is responsible for propagating and initiating disease. The discovery of LSCs that are responsible for the initiation and propagation of leukemia has great implications for the treatment of patients with this disease, as the discovery of LSC targeted therapies could dramatically improve overall patient survival rates [4].

LSCs comprise 0.1-1% of the blasts in AML and can be identified through morphological surface markers which differ from hematopoietic stem cells such as the absence of CD90 and the increased expression of CD34+/CD38- (which has shown initiation activity of leukemia), CD123 (interleukin-3 receptor), CD45RA (naïve T cell marker), CD13 (myeloid antigen), CD44 (involved in cell-cell interactions and adhesion), CLL-1 (novel LSC antigen), CD96 (T cell receptor), TIM3 (T cell receptor), CD47 (involved in proliferation and adhesion), CD32 (B cell signal modulator), and CD25 (interleukin-2 receptor) [4, 10, 19].

Not only are LSCs implicated in disease propagation, they are also responsible for drug resistance resulting in eventual patient relapse. Unlike bulk AML blasts, LSCs possess adaptive properties that enable them to evade the cytotoxic effects of chemotherapeutics. Unlike bulk AML blasts, LSCs comprise 0.1-1% of blasts and reside primarily in the bone marrow, which provides a protective niche from circulating chemotherapeutics [4, 10]. Furthermore, LSCs express the multidrug resistance efflux pump P-glycoprotein (ABCB1) that actively remove chemotherapeutics from the cell. In addition, LSCs have been shown to reside mainly in the G_0 cell cycle phase, implying that they are generally quiescent [4-6]. As current chemotherapeutics generally target fast cycling, proliferating cells, LSCs that are quiescent are generally unaffected. As such, future therapy must target LSCs to overcome drug resistance and disease relapse.

1.3 Metabolic alterations in cancer cells

In general, cancer cells have an altered metabolism allowing for the accumulation of metabolic intermediates that can be used as cellular building blocks to support increased cell division and thus conferring a growth advantage [20]. The most common alteration is the Warburg effect, a perturbation of glucose metabolism, where glycolysis is decoupled from pyruvate oxidation allowing for the collection of glucose-derived carbon molecules rather than oxidizing them to carbon dioxide [20].

Alteration of glutamine metabolism is often observed in cancer cells, where increased glutamine uptake is observed to generate reduced NADPH, which is integral for both lipid synthesis and the Krebs cycle [20, 21].

Another type of metabolic alteration involves the oxidation of lipids and fatty acids (FAs). FAs are composed of a hydrocarbon chain with a terminal carboxyl group and are used as energy sources, membrane components and signaling molecules [20]. FAs originate from 2 sources: 1) exogenous sources or 2) from *de novo* FA synthesis. Normal human cells generally prefer exogenous sources of FAs, whereas tumor cells shift towards *de novo* FA synthesis [20].

The oxidation of fatty acids, also known as fatty acid oxidation (FAO), produces twice as much ATP compared to carbohydrates [21]. FAO takes place in mitochondria and peroxisomes, however; the mitochondria is the main site for FAO [22]. It consists of a cyclical series of reactions which shorten fatty acids (by 2 carbons), generating NADH, $FADH_2$, and acetyl-CoA per cycle [21] (Figure 1.2). NADH and $FADH_2$ enter the electron transport chain (ETC) to produce ATP whereas acetyl-CoA enters the Krebs cycle to generate ATP and further reducing equivalents for the ETC and other biological processes [21]. Chain shortening occurs via a cycle consisting of 4 enzymatic steps (Figure 1.2): (1) acyl-CoA dehydrogenase which dehydrogenates acyl-CoA fatty acid to 2-enoyl-CoA, (2) 2-enoyl-CoA hydratase which produces 3-hydroxyacyl-CoA, (3) 3-hydroxyacyl-CoA which is dehydrogenated by 3-hydroxyacyl-CoA dehydrogenase to produce 3-ketoacyl-CoA and NADH, and (4) 3-ketoacyl-CoA thiolase which cleaves 3-ketoacyl-CoA to produce a 2 carbon-shortened saturated acyl-CoA and an acetyl-CoA [22, 23].

In order for FAs to undergo FAO, they must be transported into the mitochondria. Acyl-CoAs are incapable of crossing the mitochondrial membrane; therefore they must be transported by the carnitine shuttle. This is facilitated by carnitine palmitoyl transferase 1 (CPT1), which is found on the outer mitochondrial membrane and conjugates FAs with carnitine [21]. CPT1 is the rate limiting step of FAO as it exerts about 80% of control over the FAO pathway [23]. Once acyl-carnitines have entered the

mitochondria, CPT2, found on the inner mitochondrial membrane, reconverts the acyl-carnitines into usable acyl-CoAs to undergo FAO [22].

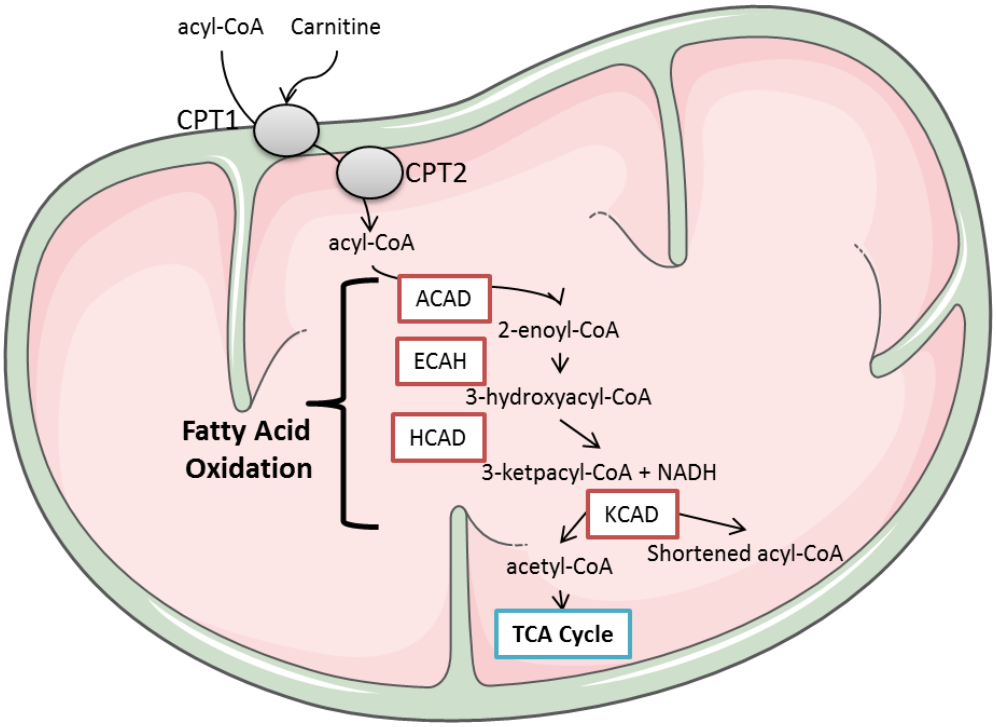

Figure 1.2. Schematic diagram of fatty acid oxidation. Fatty acids are taken up into the mitochondria through CPT1 and CPT2 where they undergo a cyclical series of chain shortening reactions to generate NADH, acetyl-CoA and shortened acyl-CoA. Adapted from Houten *et al*. 2010 and Bartlett *et al*. 2004 using Servier Medical Art (Creative Commons Attribution 3.0 Unported License). ACAD- acyl-CoA dehydrogenase; ECAH- 2-enoyl-CoA hydratase; HCAD- 3-hydroxyacyl-CoA dehydrogenase; KCAD- 3-ketoacyl-CoA thiolase.

FAO is essential for cell survival, whereby inhibition can lead to cell death through the accumulation of lipids (lipotoxicity) as well as deficiencies in metabolic intermediates [21, 24]. FAO is also implicated in the production of NADPH which allows for the recycling of reduced glutathione (GSH), which reduces oxidative stress through its antioxidant properties. Studies have demonstrated that ROS inhibits FAO and can be counteracted by antioxidants [25]. The reduction of NADP+ to NADPH is mediated by isocitrate dehydrogenases (IDHs) 1 and 2, which also catalyze the decarboxylation of

isocitrate to α-ketoglutarate [26]. IDH2 (found in the mitochondria) and IDH1 (found in the cytosol) play a key role in lipid biosynthesis, antioxidant systems and oxidative respiration. NADPH generated by IDHs are provided to fatty acid synthase for *de novo* synthesis of fatty acids [26] and help defend cells against oxidative stress caused by ROS generated from lipid oxidation [26]. As NADPH cannot pass through the inner mitochondrial membrane, NADPH generated by IDH2 serves as a primary source of antioxidants to combat mitochondrial specific ROS [26]. The role of IDHs in protecting against oxidative stress have been confirmed as IDH deficiency results in increased oxidative DNA damage, increased ROS from lipid peroxidation and increased peroxide generation [27].

1.3.1 Metabolic alterations in leukemia cells

Recently, mitochondrial alterations have been observed in leukemia cells. Such alterations include increased mitochondrial biogenesis [28] and mitochondrial uncoupling as a result of increased expression of uncoupling protein 2 (UCP2) [29, 30]. UCPs are mitochondrial anion carriers which dissipate the mitochondrial proton gradient resulting in a reduction in oxidative phosphorylation [21]. As such, mitochondrial uncoupling imparts a metabolic shift to the oxidation of other carbon sources, such as fatty acids and glutamine, to fuel the Krebs cycle [29, 31]. This is evident through increased lactate generation by leukemia cells despite aerobic conditions [31]. This is in stark contrast to normal coupled mitochondria which rely mainly on the oxidation of glucose-derived pyruvate as a primary carbon source. Uncoupled mitochondria display a reduced mitochondrial proton gradient ($\Delta\psi M$) resulting in an inability to generate ATP, forcing cells to rely on glycolysis to meet energy demands [29].

These metabolic alterations confer many advantageous benefits to leukemia cells. First, the use of non-glucose carbon sources acts as a safeguard for biosynthetic capacity. The oxidation of glucose via the Krebs cycle can result in shunting of anabolic pathways [31]. For example, pyruvate transamination can generate products which can block downstream processes such as NADPH and ribose-5-phosphate biosynthesis [31]. Next, depending on glycolysis over oxidative phosphorylation allows leukemia cells to thrive in reduced oxygen environments such as the hypoxic bone marrow niche [31]. Given the fact that

oxidative phosphorylation depends on adequate oxygen concentrations, this would not be sustainable in hypoxic environments. Next, mitochondrial uncoupling promotes resistance to mitochondrial intrinsic apoptosis through up regulation of Bcl-2 and antagonism of Bax/Bak proteins [24, 31]. Recently, LSCs have also been shown to display an overexpression in Bcl-2, where Bcl-2 favors apoptosis resistance, and also displays antioxidant properties through the reduction of ROS generation and facilitating the import of reduced glutathione into the mitochondria [31, 32]. Finally, reduced dependence on oxidative phosphorylation favors the generation of biosynthetic intermediates from the Krebs cycle [20, 31]. A shift towards fatty acid carbon sources over pyruvate results in the production of one less NADH and FADH2, whilst still yielding the same carbon intermediate products [31]. Notably, inhibition of FAO sensitized leukemia cells to chemotherapeutics, and promoted the pro-apoptotic proteins Bax/Bak [24].

Given the numerous metabolic alterations in leukemia and LSCs, this presents novel chemotherapeutic targeting strategies for the eradication of AML.

1.4 Leukemia cell death

Cells can undergo programmed cell death through three distinct pathways – apoptosis, autophagy and necrosis. Autophagy, which constitutes the recycling of cellular components, generally functions as a survival mechanism; however, prolonged autophagic signaling can lead to cell death [33]. Apoptosis is a regulated process by which cells activate catabolic enzymes (i.e., caspases) resulting in cell death [34]. Necrosis, which constitutes the premature death of cells by autolysis, was once thought to be an unregulated form of cell death; however, recent studies have shown that it can be regulated [34].

1.4.1 Apoptosis

Apoptotic cell death is characterized by the shrinking of the cell and nucleus, plasma membrane blebbing, cleavage of cytoskeleton proteins, chromatin condensation, nuclear fragmentation and the formation of apoptotic bodies [34]. It can be induced by many stimulants such as DNA damage, cell starvation, ROS, death receptor ligand binding and/or other cellular stressors [34]. An early indicator for

apoptosis involves the externalization of phosphatidylserine (PS) to the outer leaflet of the plasma membrane. This acts as a signaling mechanism for phagocytes to target apoptotic cells for degradation [35].

Apoptosis can occur via two different but convergent pathways: the death receptor (extrinsic) and the intrinsic mitochondrial pathways (Figure 1.3) [34, 36]. Caspase activation will determine which pathway a cell is to be inducted to. The death receptor pathway is activated by the binding of tumour necrosis factors (TNF) to cell surface death receptors. Binding of the factors to receptors leads to the formation of a death-inducing signaling complex. Aggregation of this complex then triggers an initiator of death receptor apoptosis, caspase 8 [36]. This initiates a caspase cascade by which executioner caspases 3, 6, or 7 are activated. The executioner caspases in turn cleave proteins associated with structural and metabolic processes leading to apoptotic cell death [36]. The DNA repair enzyme poly-ADP-ribose polymerase (PARP) is cleaved by caspases 3 and 7 resulting in DNA fragmentation, a hallmark of apoptosis [34].

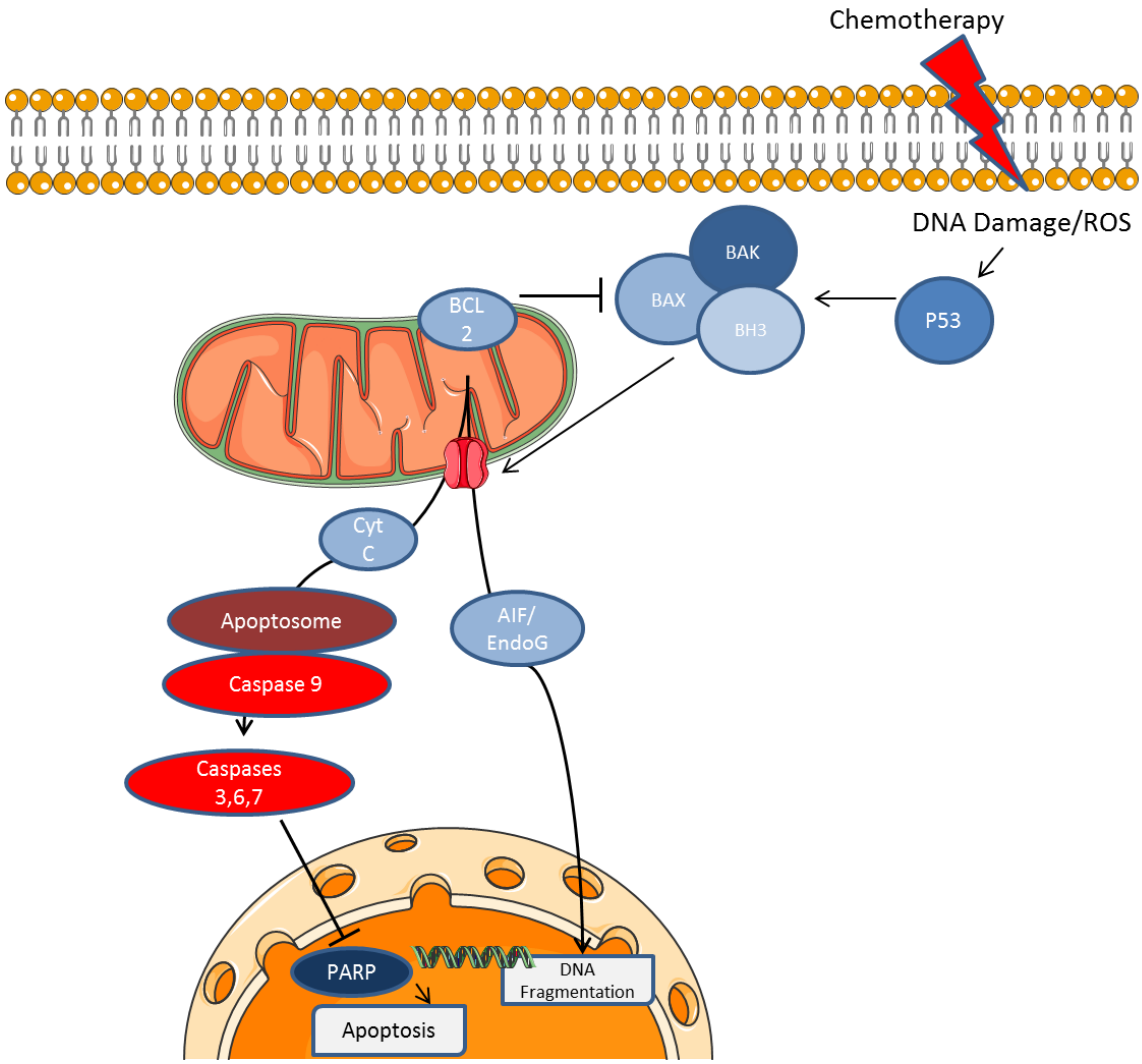

Figure 1.3. Intrinsic mitochondrial pathway of apoptosis. Apoptotic stimuli initiate permeabilization of the mitochondrial membrane pore resulting in the release of pro-apoptotic proteins. This leads to activation of caspases 9, 3, 6 and 7 resulting in apoptosis. Release of AIF and EndoG induce caspase-independent apoptosis through direct DNA fragmentation. Adapted from Samudio *et al.* 2010 using Servier Medical Art (Creative Commons Attribution 3.0 Unported License).

The mitochondrial, or intrinsic, apoptotic pathway occurs as a result of mitochondrial dysfunction and is controlled by members of the BCL2 family [34]. Initiation of this pathway involves changes in the permeability of the outer mitochondrial membrane as a result of changes to the mitochondrial membrane potential, allowing for the release of pro-apoptotic proteins such as cytochrome c, EndoG and apoptosis inducing factor (AIF) [36]. Caspase 9 acts as a central mediator of this pathway, which is initiated by cytochrome c, and is responsible for the formation of a multiprotein complex called the apoptosome [36].

Upon activation, the apoptosome mobilizes caspase 3, 6 and 7 which promote the cleavage of cellular proteins [34].

Interestingly, apoptosis can also be induced independent of caspases. This is mediated by AIF and EndoG, which upon release from the mitochondria, translocates into the nucleus where it enacts large scale DNA fragmentation as well as chromatin condensation [36, 37]. AIF, is a flavoprotein which resides in the mitochondrial intermembrane space. Upon apoptosis induction and the permeabilization of the mitochondrial outer membrane, AIF is cleaved by cysteine proteases where is released into the cytosol to translocate into the nucleus [37]. AIF then interacts directly with DNA through its negatively charged surface, causing chromatin condensation and DNA fragmentation [38]. Activation of AIF induced cell death is strongly associated with exitotoxin drug treatment and growth factor deprivation [37, 39].

1.4.2 Autophagy

Autophagy constitutes the recycling of non-essential cellular components, damaged organelles or macromolecules and is a response mechanism to cellular stress that can arise from nutrient starvation, hypoxia, or drug treatment [33, 40-44]. Autophagy plays a role in tumour growth suppression, microorganism elimination and antigen presentation. Recycling of organelles or macromolecules is conducted by lysosomes in three different forms. In macroautophagy (generally referred to, and hereafter as autophagy) the double-membrane bound autophagosome, derived from the isolation membrane, envelops the material to be consumed and is then fused with a lysosome to form a single membrane bound unit called the autophagolysosome. In microautophagy, the lysosome engulfs the recyclable material via invagination of its membrane. In chaperone-mediated autophagy, cargo is delivered directly into the lysosomes by heat-shock proteins. Once delivered into the lysosome, acid hydrolases breakdown the ingested material into usable metabolic substrates. The formation of the autophagosome is closely regulated by a set of autophagy-related proteins (ATGs) [34].

Most autophagy stimuli converge at the mammalian target of rapamycin (mTOR) and the class III phosphatidylinositol 3-kinase complex (PI3K), which serve as key autophagy regulators [42, 45]. The

core autophagy machinery required for autophagosome formation can be divided into four distinct groups: 1) ATG9 membrane protein, 2) unc-51-like kinase 1/2 (ULK1/2), 3) the PI3K complex, and 4) the microtubule-associated protein 1 light chain 3 alpha (LC3) and ATG12, a ubiquitin-like protein. Together, these proteins regulate the process of autophagy vesicle generation which can be divided into four steps: 1) initiation and nucleation, 2) elongation and closure, 3) maturation, and 4) degradation (Figure 1.4) [42, 44].

Initiation and nucleation. The beginning step to autophagy involves the formation of the isolation membrane. In starvation conditions, or another cell stressor conditions (such as oxidative stress), mTOR is inhibited resulting in dephosphorylation of ATG13. ATG13 then activates ULK1/2 via autophosphorylation resulting in the recruitment of focal adhesion kinase family interacting protein (FIP2000). The activated ULK-ATG-FIP2000 complex (mTORC) localizes to the developing isolation membrane to participate in elongation to promote a progression towards the complete autophagosome structure. In contrast, mTOR phosphorylates ATG13 preventing recruitment and activation of the ULK1/2 complex during nutrient rich condition [42, 43]. Following initiation of the isolation membrane, nucleation arises when the PI3K complex binds to its core units such as Beclin 1 and p150. This complex resides on the isolation membrane and facilitates recruitment of other ATGs to the unit as well as produces phosphatidylinositol 3-phosphate, which is necessary for nucleation [8, 33, 42]. According to current consensus, the developing isolation membrane originates from the endoplasmic reticulum, the plasma membrane and the mitochondria [42].

Elongation and closure. The next step in autophagosome formation involves the development of the double-membrane-bound autophagosome from the precursor isolation membrane through the action of two ubiquitin-like conjugation systems: ATG12 and LC3 [8, 42, 43]. ATG12 is conjugated to ATG5 by ATG7 and ATG10. Following, ATG16 conjugates to the complex and directs it to the phagophore. This complete complex is known as ATG16L (ATG12-ATG5-ATG16), and is essential for the formation of the autophagosome. ATG16L is also involved in aiding with the delivery of LC3 to the phagophore along with its lipidation [42]. The ubiquitin-like LC3 is a known marker of autophagy required for

generation of the autophagosome. LC3 undergoes post-translational c-terminal cleavage by the protease ATG4 to become its cytoplasmic form LC3-I. LC3-I is then conjugated with phosphatidylethanolamines (PE) to become LC3-II. This conjugation is mediated by ATG7, ATG3 and ATG16L. Upon lipidation, LC3-II can be inserted onto the surface of the autophagosomal membrane via its lipid moiety [33, 42-44].

Maturation and degradation. This step involves the formation of the autophagolysosomes which consists of the fusion of autophagosomes to lysosomes. Unlike autophagosomes, autophagolysosomes are single-membrane bound vesicles which degrade the autophagosomes contents by acidic hydrolases and lysosomal proteases such as cathepsins. This fusion is mediated by RAB7 (RAS related protein), Beclin-1 and LAMP-2 (lysosomal associated protein 2), however their mechanistic involvement remains to be well understood [42, 43]. Following degradation, broken down products are released into the cytosol as nutrients and pre-cursor building blocks [44].

Autophagy can be a highly selective process with adaptor molecules such as p62 (also known as sequestosome 1) which binds to ubiquinated targets, transports the targets to the lysosome, and binds to LC3-II to promote degradation [33, 43]. This highlights the importance of the ubiquitin-proteasome system in managing the selective targeting of autophagy.

The role of autophagy in leukemia remains controversial as both the inhibition and activation of autophagy have been reported as promising treatment strategies [46]. Several reports suggest that activating autophagy leads to tumourigenesis by favoring atypical cell survival. Indeed, autophagy has been reported to promote tumour survival by restricting necrosis and inflammation and preventing cell death [47]. Additionally, autophagy-related gene (Atg)5 and Atg7 have been reported to promote cell survival [48] by allowing cancer cells to survive metabolic stress in response to nutrient deprivation. Further, in response to cell damage, autophagy can promote survival by removing damaged organelles. Given that many current chemotherapeutics induce metabolic stress and nutrient deprivation, the inhibition of autophagy is a promising strategy to increase treatment efficacy [49]. In contrast, there is strong evidence that autophagy induction acts as a tumor suppressor mechanism. Beclin 1, a regulator of autophagy responsible for autophagosome formation, has been linked to the stability and function of p53

[50], which is a crucial tumor suppressor protein that can initiate apoptosis [34]. Further, Atg12 promotes intrinsic apoptosis through inactivation of proteins of the anti-apoptotic Bcl-2 family [51]. In acute myeloid leukemia (AML), PI3K-Akt-mTOR, which is an essential signaling pathway for the activation of autophagy, is constitutively activated in 70-90% of patients and has been shown to contribute towards cell proliferation and drug resistance [52, 53]. Further, it has been experimentally demonstrated that rapamycin, a potent activator of autophagy, and rapamycin derivatives induce selective AML cell death [54, 55].

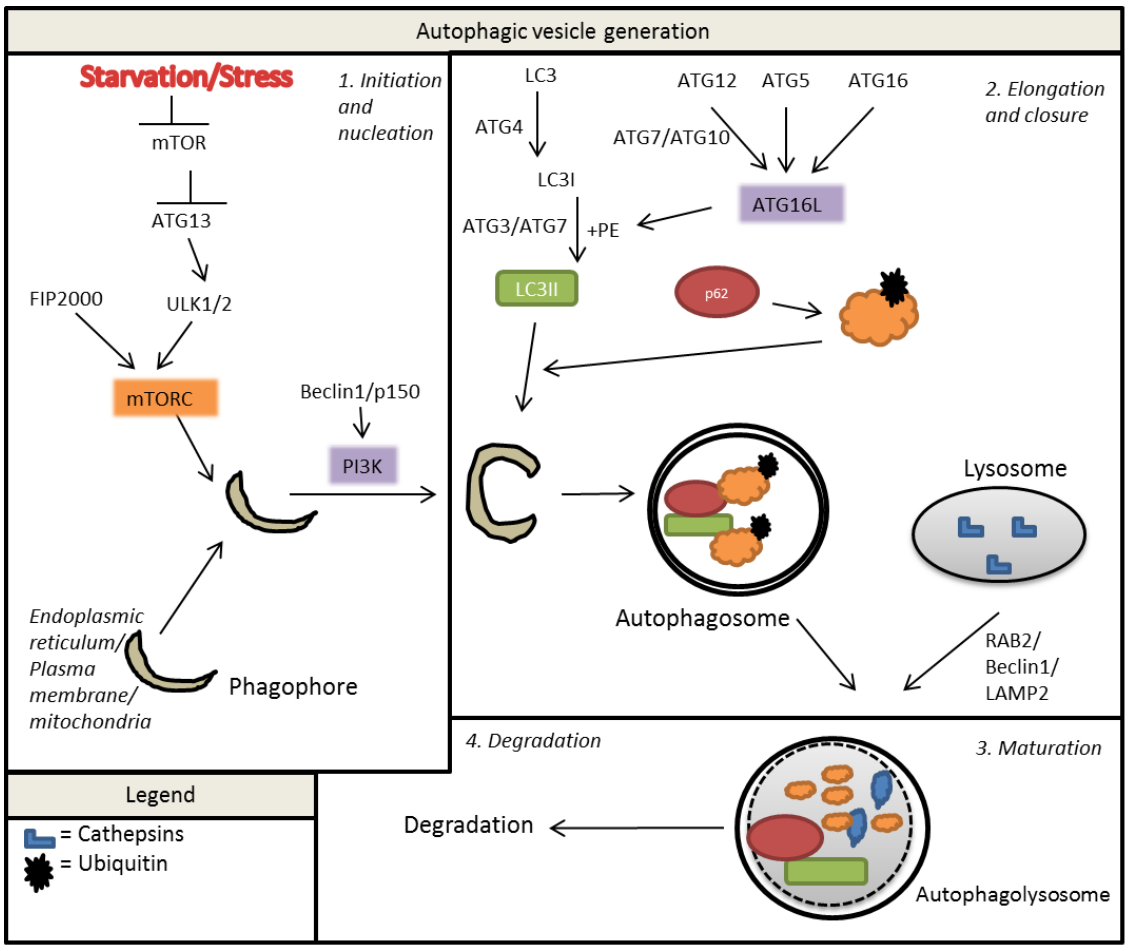

Figure 1.4. Schematic illustration of autophagic vesicle generation. Formation of the autophagic vesicle consists of four steps: 1) Initiation and nucleation, 2) elongation and closure, 3) maturation, and 4) degradation. Initiation of the developing phagophore is dependent on the formation of the complex mTORC (ATG13-ULK1/2-FIP2000). Nucleation depends on the PI3K binding to its core partners Beclin 1 and p150. Elongation and closure of the phagophore requires the formation of LC3-II through lipidation with phosphatidylethanolamine (PE). Maturation involves the fusion of the autophagosome and lysosome which is mediated by RAB2, Beclin 1 and LAMP2. Finally, degradation involves the lysing of cargo by cathepsins and subsequent release of broken down products.

1.5 Avocatin B

To identify novel anti-cancer agents, our lab screened an 800 compound natural health products library to identify novel agents with anti-leukemia activity. Avocatin B (AVO), an avocado-derived lipid, was identified as the most potent compound at reducing leukemia cell viability.

The avocado tree (*Persea americana*) originates from central America. Its fruit is highly consumed (1-2 per day) in various parts of Latin America without reports of any associated toxicity [56]. In fact, avocados are used in traditional herbal medicine for the treatment of various illnesses including hypertension, stomach ache, diarrhea and diabetes [57]. Avocado-derived phytochemicals also possess known chemopreventive characteristics [58]. These effects have been noted in malignant pleural mesothelioma, various carcinomas, various adenocarcinomas and oral cancer cell lines [58-60]. The chloroform extract (D003), prepared from the California Hass avocado, has displayed selective inhibition of pre- and malignant oral cancer cell lines [58]. D003 induced both death receptor and mitochondrial mediated apoptosis. D003's activity was mediated by increases in ROS which were blocked using the anti-oxidant N-acetyl cysteine [58].

Avocatin B, which consists of a 1:1 ratio of 1,2,4-trihydroxyheptadec-16-ene and 1,2,4-trihydroxyheptadec-16-yne (Figure 1.5), is compound derived from the peel and seed of unripe avocado fruit which has been found to be cytotoxic towards a small panel of cancer cell lines [57, 61]. Activity has been reported in lung carcinoma, mammary adenocarcinoma, kidney carcinoma, pancreatic carcinoma with cytotoxicity in human prostate adenocarcinoma cells being nearly as potent as doxorubicin [57, 59]. Avocatin B has also been reported as a natural insecticide with potent activity in yellow fever mosquito larva, epimastigotes and trypomastigotes [57, 59].

Figure 1.5. Avocatin B's chemical structure. Avocatin B is an avocado derived compound consisting of 1,2,4-trihydroxyheptadec-16-ene and 1,2,4-trihydroxyheptadec-16-yne (1:1 ratio). Image taken from ChemBankID:3198534.

Chapter 2: Objectives and Hypothesis

The objectives of this project are:

1. Characterize and evaluate avocatin B's mechanism of action in acute myeloid leukemia cells *in vitro* and;

2. Determine avocatin B's efficacy in primary and primitive AML cells.

These objectives fulfilled the hypothesis that:

Avocatin B inhibits fatty acid oxidation to induce ROS-mediated autophagy and apoptosis in AML and LSCs.

Short term goals:

The short terms goals are to demonstrate avocatin B's pre-clinical efficacy and determine avocatin B's mechanism of action to further warrant investigation for the clinical application of treating acute myeloid leukemia.

Long term goals:

Upon successful completion of the aforementioned short term goals, the next steps would be to 1) determine pharmacokinetic properties and safety in animal models and 2) submit for Phase 1 clinical trial testing.

Chapter 3: Methods

3.1 Methods

3.1.1 Cell culture

Leukemia (OCI-AML2,K562, HL60, KG1A; JURKAT, U937) cells were cultured in Iscove's Modified Dulbecco's Medium (IMDM) (Life Technologies; Grand Island, NY) or RPMI Medium (Life Technologies) supplemented with 10% Fetal Bovine Serum (FBS; Seradigm; Providence, UT) and antibiotics (100 units/ml of streptomycin and 100 µg/m of penicillin; Sigma Chemical; St. Louis, MO). TEX leukemia cells were cultured in 15% FBS, antibiotics and 2mM L-glutamine (Sigma Chemical), 20ng/ml stem cell factor and 2ng/ml IL-3 (Peprotech; Hamburg Germany). Lentiviral transduced ATG7, SQSTM1(p62), CPT1 (a gift from Dr. Aaron Schimmer, Toronto, ON) and PPARα OCI-AML2 knockdown cell lines (a gift from Dr. Aaron Schimmer, Toronto, ON) were maintained in IMDM (Life Technologies) supplemented with 10% FBS (Seradigm) and 1ug/mL puromycin (Sigma-Alrich).

Primary human samples (fresh and frozen) were obtained from the peripheral blood of AML patients who had at least 80% malignant cells among the mononuclear cells and cultured at 37°C in IMDM, 20% FBS and antibiotics (see supplementary table 1 for clinical parameters). Normal GCSF-mobilized peripheral blood mononuclear cells (PBSCs) were obtained from volunteers donating peripheral blood stem cells for allotransplant and were cultured similar to the primary AML samples. The collection and use of human tissue for this study was approved by the local ethics review board (University Health Network, Toronto, ON, Canada; University of Waterloo, Waterloo, ON, Canada). All cells were maintained in a humidified atmosphere containing 5% CO_2 at a temperature of 37°C. Cells were passaged every 3-4 days and passages 1-20 were used.

3.1.1.1 Long-term culture

Cells were cultured *ex vivo* using a mouse bone marrow stromal co-culturing system allowing for the long term expansion and culture (months instead of days) of primary CD34+ cells [62] using the

mural stromal cell line MS-5 and human cytokine supplementation. MS-5 cells were received as a gift from Dr. John Dick (Ontario Cancer Institute, Toronto, ON). Co-cultures were grown in H5100 media (StemCell Technologies) supplemented with 1% penicillin/streptomycin (Seradigm), GM-CSF 20ng/mL, IL3 10ng/mL, G-CSF 20ng/mL, TPO 50ng/mL, Flt3 10ng/mL, IL7 20ng/mL, SCF 100ng/mL, and IL6 20ng/mL (Peprotech).

MS-5 cells were grown on 0.1% gelatin (Sigma-Aldrich) coated 12 well plates. 48 hours later, primary cells were added and allowed to grow. Media was changed once a week and upon full confluency (~1 month), cells were trypsinized with 0.25% trypsin/0.1% EDTA (Sigma-Aldrich). Primary cells were then harvested and separated from MS-5 cells using a 40-micron cell strainer (BD Biosciences, Mississauga, ON.

3.1.2 CD34+ cell enrichment

TEX and KG1A cells were enriched for CD34+ population using the CD34+ EasySep Positive Selection Kit (StemCell) and EasySep Magnet (StemCell). Approximately 2-5x10^8 cells were re-suspended in a 5mL polystyrene tube in 1mL of PBS (Sigma-Aldrich) containing 2% FBS (Seradigm) and 1mM EDTA (Sigma-Aldrich) (enrichment buffer). EasySep Positive Selection Cocktail was then added at 100 µL/mL cells and allowed to incubate at room temperature for 15 minutes. EasySep Magnetic Nanoparticles were then added at 50 µL/mL cells and allowed to incubate 10 minutes at room temperature. The tube was then placed inside the EasySep Magnet and left aside for 5 minutes. Following, the supernatant fraction was poured out resulting in the magnetically labeled cells to remain in the tube. Cells were then re-suspended in enrichment buffer and magnetic separation was repeated for a total of 5 times. The positively selected cells were then verified by flow cytometry.

3.1.3 Flow cytometry

Unless otherwise noted, all flow cytometry assays were performed in 96 well plates using a Guava easyCyte 8HT (Millipore, Billerica, MA) and GuavaSoft (Millipore) flow cytometry software. All

assays performed involved an unstained control to set basal thresholds as well as single stain controls (for multi-stain assays) to set compensation.

3.1.3.1 Mitochondrial membrane potential assessment

Following drug treatments, $0.5x10^6$ cells were collected and washed in 0.5mL PBS (Sigma-Aldrich). 1µL of 30µM Rhodamine123 (R123; Enzo Life Sciences, Farmingdale, NY) was added to each sample and then allowed to incubate for 20 minutes in a humidified atmosphere containing 5% CO2 at a temperature of 37°C. Samples were then washed and measured using flow cytometry. R123 is a cationic dye is used to monitor the membrane potential of the mitochondria ($\Delta\psi m$) [63].

3.1.3.2 Mitochondrial integrity assessment

$0.5x10^6$ cells were collected from each cell line to be assessed and washed in 0.5mL PBS (Sigma-Aldrich). 1µL of 50µg/mL nonyl-acridine orange (NAO) (Enzo Life Sciences) was added to each sample and then allowed to incubate for 20 minutes in a humidified atmosphere containing 5% CO_2 at a temperature of 37°C. Following, samples were washed and measured using flow cytometry. NAO is a mitochondria specific dye that binds to the mitochondrial phospholid cardiolipin and is taken up into the mitochondria independent of $\Delta\psi$ [64].

3.1.3.3 Cell surface marker assessment

$1x10^5$ cells were collected from each cell line tested. 2µL of fluorescently-conjugated cell surface receptor antibody was added to each sample and allowed to incubate for 30 minutes in the dark at room temperature. Cells were then washed twice in PBS (Sigma-Aldrich) containing 5% FBS (Seradigm) and then read using flow cytometry. Antibodies used include FITC mouse anti-human CD38 (BD Biosciences), PE mouse anti-human CD33 (BD Biosciences), APC mouse anti-human CD19 (BD Biosciences), APC mouse anti-human CD34 (BD Biosciences) and BD CompBeads anti-mouse Ig, k particles (BD Biosciences) as a positive control.

3.1.3.4 Reactive oxygen species detection

Reactive oxygen species (ROS) were detected using 2′,7′dichlorohydrofluorescein-diacetate (DCFH-DA; Sigma Chemical) and dihyodroethidium (DHE; Sigma Chemical). DCFH-DA is hydrolyzed by intracellular esterase to produce a non-fluorescent DCFH product. It can then be oxidized by ROS to produce a highly fluorescent DCF product [65]. DHE is a superoxide indicator which upon contact with superoxide anions produces the fluorescent product 2-hydroxyethidium [66]. Following drug treatment, TEX cells (5x105) were collected and washed in PBS (Sigma-Aldrich). Cells were stained with 5μM (final concentration) DCFH-DA or 10μM DHE and allowed to incubate for 30 minutes in a humidified atmosphere containing 5% CO2 at 37°C. Samples were then washed in PBS and ROS was measured by flow cytometry.

3.1.4 Palmitate, malonyl-CoA, acetyl-CoA, and oleic acid study

To assess avocatin B's activity on fatty acid biosynthesis, TEX cells were co-incubated with the end-products of major enzymatic reactions of the fatty acid biosynthesis pathway, and assessed using MTS and annexin/PI viability assays. It was hypothesized that supplementation would rescue cells from avocatin B induced cell death. Palmitate, malonyl-CoA, acetyl-CoA and oleic acid (Sigma-Aldrich) were complexed to delipidized BSA (Sigma-Aldrich) based on the method by Luo *et al.* [67], where a 100mM stock was prepared in ethanol and then diluted to a working concentration in a 10%BSA-H_2O solution.

3.1.5 Western blotting

3.1.5.1 Whole-cell lysate preparation

Following drug treatments, cells were washed with ice-cold PBS, and then lysed with chilled RIPA buffer (Sigma-Aldrich) supplemented with protease inhibitors (Sigma-Aldrich) for 20 minutes. Next, cells were centrifuged at 13,200RPM for 20 minutes at 4°C and the supernatant was collected.

3.1.5.2 Cell fractionation

To separate cytosolic, mitochondrial and nuclear proteins, cell fractionation was performed using a protocol utilized by our collaborator Dr. Joe Quadrilatero (University of Waterloo, Department of Kinesiology). Following drug treatments, cells were washed with ice-cold PBS, and then lysed with chilled digitonin/sucrose buffer [250mM sucrose, 80mM KCl, and 50ug/mL digitonin] (Sigma-Aldrich). Next, the cytosolic fraction (supernatant) was collected through differential centrifugation at 16,000xg for 10 minutes. The remaining fraction was then lysed with chilled muscle lysis buffer [20mM HEPES, 10mM NaCl, 1.5mM MgCl, 1mM DTT, 20%, and 0.1% Triton X-100 at pH7.4] (Sigma-Aldrich). Following, the mitochondrial fraction (supernatant) was collected through differential centrifugation at 1,000xg for 10 minutes. The nuclear fraction was retrieved by re-suspending the pellet in muscle lysis buffer and sonication for 2.5 second intervals for 20 seconds.

3.1.5.3 BCA protein assay and sample preparation

Total protein content was measured using the BCA protein assay. A standard curve was generated using bovine serum albumin (BSA) (Sigma-Aldrich) diluted in distilled water at concentrations ranging from 0mg/mL-1.0mg/mL. Diluted samples (tenfold) and standards were plated on a 96 well plate where 200µL of bicinchoninic acid (BCA) working agent was added to each well (50 parts BCA:1 part copper II sulfate [Sigma-Aldrich]). The plate was then incubated for 30 minutes at 37°C. Optical density (OD) was then measured at 527nm using a spectrophotometer. Samples were prepared containing 30µg total protein, with ¼ sample buffer (240 mM Tris-HCl at pH 6.8, 6% w/v SDS, 30% v/v sucrose, 0.02% w/v bromophenol blue, and 50 mM DTT) volume and lysis buffer to a total volume of 30µl. Samples were heated at 95°C for 5 minutes and then loaded into polyacrylamide gel wells.

3.1.5.4 SDS-PAGE

Proteins were separated by SDS-PAGE in electrophoresis buffer (25 mM Tris base, 190 mM glycine, 3.5 mM sodium dodecyl sulfate) using a Mini Trans-Blot Cell (Bio-Rad, Hercules, CA),

followed by transfer of proteins onto a PVDF membrane (Bio-Rad) in transfer buffer (25 mM Tris base, 190 mM glycine, 20% v/v methanol) using a Trans-Blot semi-dry transfer cell. Membranes were then blocked with 5% bovine serum albumin (BSA) in Tris-buffered saline (20 mM Tris base (TBS) plus 0.1% Tween (TBS-T) for 1 h at room temperature, followed by incubation with primary antibody added to blocking buffer overnight at 4°C. Membranes were washed three times with TBS-T, and then incubated with appropriate secondary antibody in blocking buffer for 1 h at room temperature. Membranes were washed five additional times with TBS-T. Western enhanced chemiluminescent substrate (ECL; GE healthcare; Baie d'Urfe, Quebec) was used to visualize proteins on a Kodak 4000MM Pro Imaging Station and Kodak Molecular Imaging software.

3.1.5.5 Antibodies

Antibody	Isotype	Molecular weight (kDa)	Manufacturer
AIF	mouse	57	Santa Cruz
ANT1/2	goat	33	Santa Cruz
Atg7	rabbit	78	Cell signaling
Beclin-1	rabbit	60	Cell signaling
Cytochrome c	rabbit	14	Cell signaling
ND1	goat	36	Santa Cruz
Parkin	mouse	50	Cell signaling
PARP	rabbit	89,116	Cell signaling
SQSTM1/p62	rabbit	60	Cell signaling
a-tubulin	mouse	55	Santa Cruz
LC3B	rabbit	14,16	Cell signaling
UCP2	Goat	70	Santa Cruz

3.1.6 Cell growth and viability

Cell growth and viability was measured using the 3-(4,5-dimethylthiazol-2-yl)-5-(3-carboxymethoxyphenyl)-2-(4-sulfophenyl)-2H-tetrazolium inner salt (MTS) reduction assay (Promega; Madison, WI) according to the manufacturer's protocol and as previously described [68]. Cells were seeded in 96-well plates, treated with drug for 72 hours and optical density (OD) was measured at 490nm. Cell viability was also assessed by the trypan blue exclusion assay and by Annexin V and PI staining (Biovision; Mountainview, CA), as previously described [68]. Cell growth and viability under normoxic

(21% O_2) and hypoxic conditions (1% O_2) were measured using the sulforhodamine B assay, as previously described [69].

3.1.7 Functional stem cell assays

Clonogenic growth assays with primary AML and normal hematopoietic stem cells were performed, as previously described [68]. Briefly, $CD34^+$ bone marrow-derived normal stem cells (StemCell Technologies; Vancouver, Canada) or AML mononuclear cells from patients with >80% blasts in their peripheral blood ($4x10^5$ cells/ml) were treated with vehicle control or increasing concentrations of avocatin B and plated in duplicate by volume at 10^5 cells/ml per 35 mm dish (Nunclon; Rochester, USA) in MethoCult GF H4434 medium (StemCell Technologies) containing 1% methylcellulose in IMDM, 30% FBS, 1% bovine serum albumin, 3 U/ml recombinant human erythropoietin, 10^{-4} M 2-mercaptoethanol (2ME), 2mM L-glutamine, 50ng/ml recombinant human stem cell factor, 10ng/ml recombinant human granulocyte macrophage-colony stimulating factor and 10ng/ml recombinant human IL-3. After 7-10 days of incubation at 37°C with 5% CO_2 and 95% humidity, the numbers of colonies were counted on an inverted microscope with a cluster of 10 or more cells counted as one colony.

Mouse xenotransplant assays were performed as previously described [28, 70]. Briefly, AML patient cells were treated with 3.0μM avocatin B or dimethyl sulfoxide (DMSO) (as a control) for 48 hours in vitro. Next, these cells were transplanted into femurs of sublethally irradiated, CD122 treated NOD/SCID mice and following a 6 week engraftment period, mice were sacrificed, femurs excised and bone marrow flushed and the presence of human myeloid cells ($CD45^+/CD33^+/CD19^-$) were detected by flow cytometry. All animal studies were carried out according to the regulations of the Canadian Council on Animal Care and with the approval of the University Health Network, Animal Care Committee.

3.1.8 High-throughput screen

A high throughput screen of a natural product library (n=800; Microsource Discovery Systems Inc.; Gaylordsville, CT) was performed as previously described [28, 68]. Briefly, TEX leukemia cells ($1.5x10^4$/well) were seeded in 96-well polystyrene tissue culture plates. After seeding, cells were treated

with aliquots (10μM final concentration) of the chemical library with a final DMSO concentration no greater than 0.05%. After 72 hours, cell proliferation and viability were measured by the MTS assay.

3.1.9 Drug combination studies

The combination index (CI) was used to evaluate the interaction between avocatin B and cytarabine. TEX cells were treated with increasing concentrations of avocatin B in the presence and absence of cytarabine and after 72 hours cell viability was measured by the MTS assay. CI values, generated by the CalcuSyn median effect model, were used to evaluate whether the avocatin B/cytarabine combination was synergistic, antagonistic or additive. CI values of <1 indicate synergism, CI=1 indicate additivity and CI>1 indicate antagonism [71, 72].

3.1.10 mRNA detection

Quantitative PCR were performed as previously described [73] in triplicate using an ABI 7900 Sequence Detection System (Applied Biosystems) with 5 ng of RNA equivalent cDNA, SYBR Green PCR Master mix (Applied Biosystems, Foster City, CA, USA), and 400 nM of CPT1-specific primers (forward: 5'- TCGTCACCTCTTCTGCCTTT-3', reverse: 5'-ACACACCATAGCCGTCATCA-3',). Relative mRNA expression was determined using the ΔΔCT method as previously described [73].

3.1.11 Assessment of fatty acid oxidation and mitochondrial respiration

Measurement of oxygen consumption rates were performed using a Seahorse XF24 extracellular flux analyzer (Seahorse Bioscience; North Billerica, MA). TEX cells were cultured in α-Minimum Essential Medium (Life Technologies) containing 1% FBS and plated at 1 x 10^5 cells/well in poly-L-Lysine (Sigma Chemical) coated XF24 plates. Cells were incubated with etomoxir (100μM; Sigma Chemical) or vehicle control for 30 minutes at 37°C in a humidified atmosphere containing 5% CO_2. Next, palmitate (175μM; Seahorse Bioscience) or avocatin B (10μM) was added and immediately transferred to the XF24 analyzer. Oxidation of exogenous fatty acids was determined by measuring mitochondrial respiration through sequential injection of 5μM (final concentration) oligomycin, an ATP synthase inhibitor, (Millipore, Billerica, MA), 5μM CCCP, a hydrogen ion ionophore, (Sigma Chemical),

and 5μM rotenone (Millipore)/5μM antimycin A, which inhibit complex III activity, (Sigma Chemical). Fatty acid oxidation was determined by the change in oxygen consumption following oligomycin and CCCP treatment and prior to antimycin and rotenone treatment, according to the manufacturer's protocol and as described in Abe et al. (2013) [74]. Data were analyzed with XF software (Seahorse Bioscience).

3.1.12 NADPH detection

Nicotinamide adenine dinucleotide phosphate (NADPH) was measured by a commercially available Amplite™ Fluorimetric kit (AAT Bioquest; Sunnyvale, CA) according to the manufacturers' protocol and as previously described [75], following incubation of increasing duration with avocatin B (10μM) or palmitate (175μM) in the presence or absence of etomoxir. Data are presented as a percent NADPH compared to control treated cells ± SD.

3.1.13 Apoptosis measurements

Apoptotic phenotype of Annexin V^+ (ANN)/Propidium Iodide $(PI)^-$ was assessed using the ANN/PI assay, as previously described [76]. ANN binds to surface phosphatidylserine and PI transverses only disrupted plasma membranes to intercalate with DNA. Thus, measurements of ANN^+/PI^- indicate apoptosis whereas ANN^+/PI^+, ANN^-/PI^- indicate a dead or viable cell, respectively. Analysis of the sub G1 peak was performed by assessing cell cycle as previously described [68]. Briefly, TEX cells treated for 24 hours with 10μM avocatin B were harvested, washed with cold PBS and re-suspended in PBS and cold absolute ethanol. Cells were then treated at 37ºC for 30 min with 100 ng/mL of DNase-free RNase A (Invitrogen; Carlsbad, CA), washed with cold PBS, resuspended in PBS and incubated with 50 μg/mL of propidium iodine (PI) for 15 min at room temperature in the dark. DNA content was measured by flow cytometry and analyzed with the Guava Cell Cycle software (Millipore). Caspase activation was performed using a commercially available kit (Promega) and was performed according to the manufacturer's protocol. Z-VAD-FMK (Sigma Chemical) was used as a pan-caspase inhibitor. Cleavage of poly (ADP) ribose polymerase (PARP), a DNA repair enzyme and a common downstream target of active caspase 3 and 7 were measured as previously described [76].

3.1.14 AIF and cytochrome c detection

To determine avocatin B's effect on the release of pro-apoptotic mitochondrial proteins cytochrome c and AIF, we used a flow cytometry-based assay as previously described [77, 78]. Briefly, pre-treated TEX cells (2 $x10^5$) were collected and permeabilized in ice-cold digitonin buffer (50μg/ml, 100mM KCl, in PBS) for 3-5 minutes on ice (until >95% cells were permeabilized, as assessed by trypan blue staining). Permeabilized cells were fixed in 4% paraformaldehyde (in PBS) for 20 minutes at room temperature, washed 3 times in PBS, and then resuspended in blocking buffer (0.05% saponin, 3% BSA in PBS) for 1 hour at room temperature. Cells were incubated overnight at 4°C with 1:200 cytochrome c antibody or AIF antibody (Santa Cruz Biotechnology) diluted in blocking buffer, washed three times with PBS and then incubated for 1 hour at room temperature with 1:200 Alexa Fluor-488 donkey anti-mouse IgG secondary antibody (Life Technologies) diluted in blocking buffer. Cells were washed three times in PBS and analyzed by flow cytometry using the BD FACS Calibur.

3.1.15 Hypoxia experiments

Cells were transferred to hypoxic culture chambers (MACS VA500 microaerophilic workstation, H35 HypoxyWorkStation; Don Whitley Scientific; UK) in which the atmosphere consisted of residual N2, 5% H_2, 5% CO_2 and 1% or 21% O_2. Cell growth and viability were measured by the sulforhodamine B assay (Sigma Chemical) following 72 hours of incubation. Data are presented as the % change in viability from 21%-1% oxygen.

3.1.16 Autophagy detection

Autophagy was detected by assessing lysosome size by confocal microscopy following cathepsin B staining, which increases in activity and intensity following autophagolysosome formation [79]. Confocal microscopy of TEX cells was performed, as previously described [69]. Briefly, TEX cells (2.0 x 10^5) treated with avocatin B or vehicle control were incubated with Magic Red cathepsin B for 30 minutes at 37^{o}C, according to manufacturer's instructions (ImmunoChemistry Technologies, Bloomington, MN). Cells were then imaged on a Zeiss LSM 700 confocal microscope (Carl Zeiss,

Germany) using a 40x objective. Images were analyzed using LSM image analysis software (Carl Zeiss, Germany). Representative micrographs shown.

3.1.17 RNAi knockdown of Atg7 and p62

Lentiviral transductions were performed as described by Spagnuolo *et al.* 2013 [73]. Briefly, OCI-AML 2 cells (5 x 10^6) were centrifuged and re-suspended in 6.5 mL media containing protamine sulfate (5 μg/mL) and 1 mL of virus cocktail (containing the short hairpin RNA (shRNA) sequence and a puromycin antibiotic resistance gene) and incubated overnight at 37^{o}C. Following, the virus was removed from suspension by centrifugation and the cells were washed and resuspended in fresh media containing puromycin (1 μg/mL). After two days, puromycin resistant live cells were plated for viability and growth assays. The shRNA coding sequences were: Atg7 (Accession No. NM_006395.1-685s1c1): 5'-CCAAGGTCAAAGGACGAAGAT-3', Atg7 (Accession No. NM_006395.1-1520s1c1): 5'-GCTTTGGGATTTGACACATTT-3', SQSTM1/p62 (Accession No. NM_003900.4-783s21c1): 5'-GAGGATCCGAGTGTGAATTTC-3', SQSTM1/p62 (Accession No. NM_003900.2-325s1c1): 5'-CCGAATCTACATTAAAGAGAA-3'. *These experiments were performed by Elena Kreinin.*

3.1.18 Interrogation of chemogenomics database

The chemogenomic expression profiles of avocatin B and rapamycin were assessed in a publicly available yeast chemogenomics database (http://chemogenomics.pharmacy.ubc.ca/HIPHOP). The database identified the top 15 yeast genes sensitive to drug treatment, based on fitness defect scores ($p<0.05$), and were assessed for gene ontology biological processes associated with autophagy and/or vesicle-mediated transport using AmiGO (Gene Ontology Consortium), as previously described [80, 81].

3.1.19 Statistical analysis

Statistical analysis was conducted using GraphPad Prism 5.0 (GraphPad Software, USA) using Student's t-test for comparing two data sets, or one-way analysis of variance (ANOVA) with Tukey's post hoc test for comparing three or more data sets. Unless otherwise noted, all results are presented as

mean ± SD. For graphs, *=$p<0.05$, **=$p<0.01$, and ***=$p<0.001$ compared to control cells. Drug combination data were analyzed using Calcusyn software (Biosoft; UK).

Chapter 4 Results

**Note: Unless otherwise stated, data was generated by Eric A. Lee.*

4.1.1 A high-throughput screen for novel anti-AML compounds identifies avocatin B

To identify novel compounds with anti-AML activity we screened a commercially available natural health products specific library against TEX leukemia cells. These cells possess several LSC properties, such as marrow repopulation and self-renewal [28, 73, 82, 83]. The compound which imparted the greatest reduction in viability was avocatin B (Figure 4.1A; left panel, arrow indicates avocatin B). Avocatin B is a 1:1 mixture of two 17-carbon lipids derived from avocados and belongs to a family of structurally related lipids [84] (Figure 4.1A right panel, Avocatin B's structure [85]). We tested 4 avocatin lipid analogues and determined that avocatin B was the most cytotoxic (EC50: 1.5 ± 0.75μM; supplementary figure 4.1).

Avocatin B's selectivity toward leukemia cells was validated in primary AML samples and in peripheral blood stem cells (PBSCs) isolated from GCSF-stimulated healthy donors. Avocatin B, at concentrations as high as 20μM, had no effect on the viability of normal PBSCs (n=4). In contrast, avocatin B reduced the viability of primary AML patient cells (n=6) with an EC50 of 3.9 ± 2.5 μM, which is similar to other recently identified compounds with anti-AML activity [28, 69, 70, 86] (Figure 4.1B; see supplementary table 1 for patient sample characteristics).

Avocatin B was also tested in combination with cytarabine; the primary backbone of current clinical AML therapy. The Calcusyn median effect model was used to evaluate whether the avocatin B/cytarabine combination was synergistic, antagonistic or additive [71, 72]. The cytarabine-avocatin B combination synergistically induced cell death in TEX cells with combination index values of 0.20, 0.19, and 0.15, at EC 30, 50 and 80, respectively (Figure 4.1C).

4.1.2 Avocatin B is selectively toxic toward leukemia progenitor and stem cells

Given the selectivity toward AML patient samples over normal hematopoietic cells, we next assessed avocatin B's effects on functionally defined subsets of primitive human AML and normal cell

populations. Adding avocatin B (3μM) into the culture medium reduced clonogenic growth of AML patient cells (n=3; supplementary table 1 for patient characteristics). In contrast, there was no effect on normal cells (n=3; Figure 4.1D; left panel). In addition, treatment of primary AML cells with avocatin B (3.0μM) reduced their ability to engraft in the marrow of immune deficient mice (Figure 4.1D; right panel). Taken together, avocatin B selectively targets primitive leukemia cells.

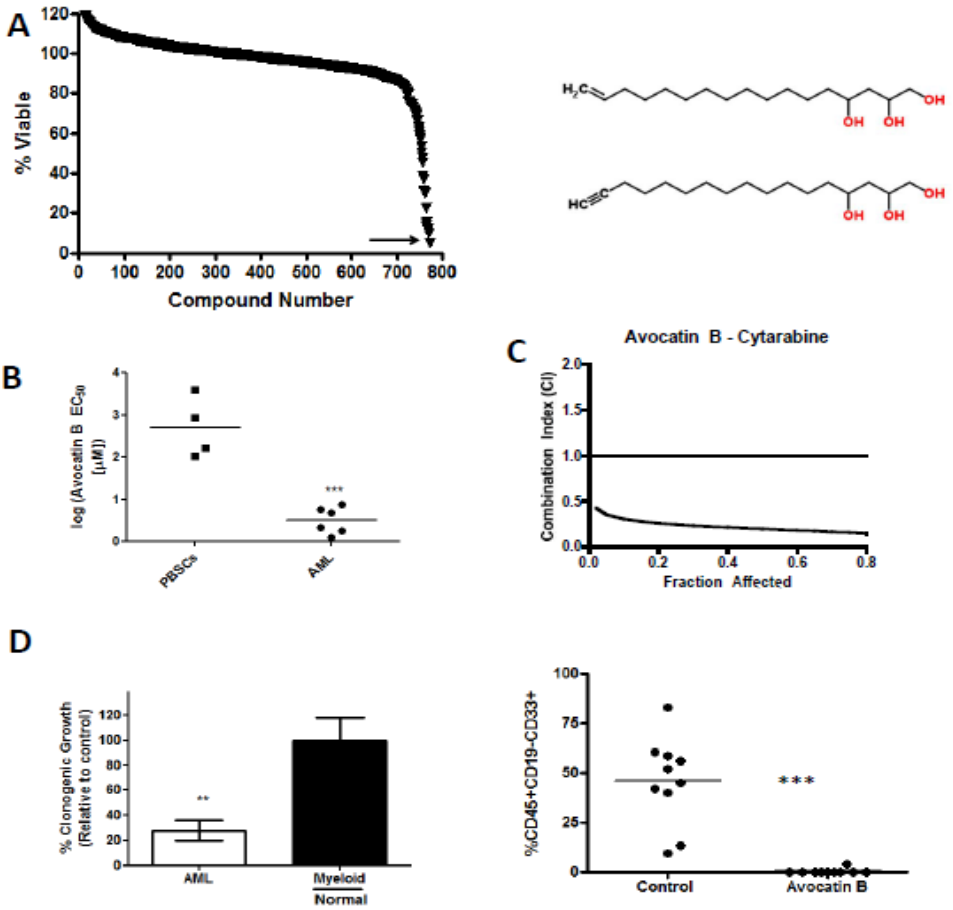

Figure 4.1. Avocatin B is selectively toxic toward AML cells. **(A)** (Left panel) A screen of a natural health product library identified avocatin B as the most potent compound at reducing TEX leukemia cell viability. Cells were incubated with compounds for 72 hours and cell growth and viability were measured by the MTS assay. Arrow indicates avocatin B. *Experiment was performed by Dr. Paul Spagnuolo.* (Right panel) Avocatin B's structure[85]. **(B)** Avocatin B's activity was tested in peripheral blood stem cells (PBSCs; n=4) isolated from GCSF stimulated donors or cells isolated from AML patients (n=6). Primary cells were treated with increasing avocatin B concentrations for 72 hours and viability was measured by the Annexin V (ANN)/Propidium Iodide (PI) assay and flow cytometry. Data are presented as log10 EC50 values. *Experiment was partially performed by Princess Margaret Cancer Centre.* **(C)** Avocatin B was tested in combination with cytarabine using Calcusyn software as detailed in the methods section. Experiments were performed twice in triplicate; representative figure shown. **(D)** (Left panel) Primary AML (n=3) and normal (n=3) cells were cultured with avocatin B (3μM) for 7-14 days and clonogenic growth was assessed by enumerating colonies (colony defined as >10 cells). Data are presented as % clonogenic growth compared to control ± SEM, similar to previously described [28, 87]. Experiments were performed twice in triplicate. *Experiment was performed by Sarah Rota.* (Right panel) AML cells from one patient were treated with avocatin B (3μM) for 48 hours or a vehicle control and then intrafemorally injected into sublethally irradiated, CD122 treated, NOD/SCID mice (n=10/group). After 6 weeks, human AML cells ($CD45^+/CD19^-/CD33^+$) in mouse bone marrow were detected by flow cytometry. *Experiment performed by Princess Margaret Cancer Centre.*$^{**}p<0.01$; $^{***}p<0.001$.

4.1.3 Avocatin B's selective cytotoxicity correlates with CD33+/CD34+ expression

In Section 4.1.1, Avocatin was tested in a number of leukemia cell lines (TEX, KG1A, OCI-AML2, JURKAT). Avocatin B was also tested in additional leukemia cell lines (HL60, U937, and K562) where avocatin B did not display potent toxicity towards these lines (Figure 4.2 left panel). Next, we performed phenotypic assessment for CD33+/CD19- (myeloid marker) and CD34+/CD38- (stem cell marker) of our tested cell lines to identify a correlation with avocatin B's activity. Here, we reported that TEX cells display both high proportions of CD33+/CD19- and CD34+/CD38- fractions whereas neither of the other AML lines displayed this phenotype (Figure 4.2 right panel). Next, we aimed to assess whether avocatin B was selectively toxic to CD34+ enriched cells. Therefore we enriched the KG1A cell line for CD34 positive cells (Figure 4.3A) and treated it with avocatin B (Figure 4.3B). These cells were still insensitive to avocatin B, suggesting that avocatin B's preferential toxicity is associated with CD33+/CD19- and CD34+/CD38- expression.

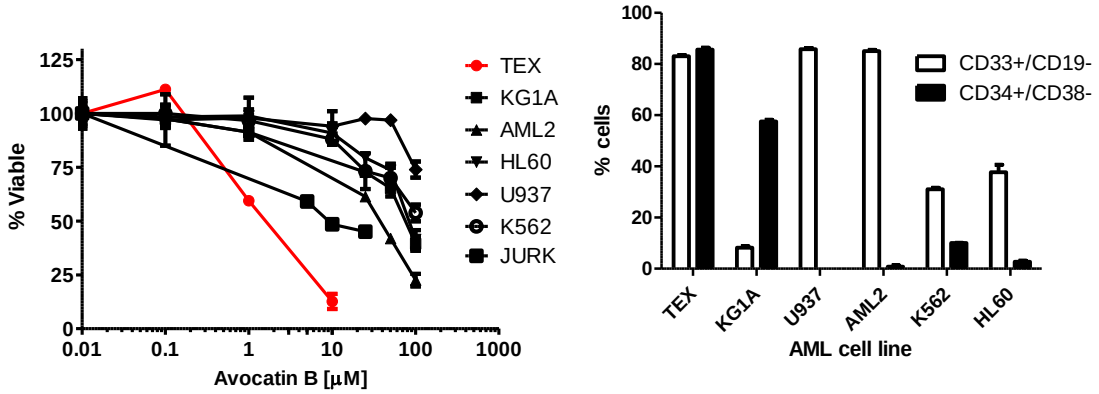

Figure 4.2. Avocatin B's preferential toxicity is associated with CD33+/CD19- and CD34+/CD38- expression. (Left panel) Avocatin B was tested in a panel of leukemia cell lines (TEX, KG1A, AML2, HL60, U937, K562 and Jurkat) over 72 hours. Viability was measured by the MTS assay and data are presented as mean percentage of live cells. (Right panel) The expression of cell surface markers for myeloid cells, CD33+/CD19-, and stem cells, CD34+/CD38-, was measured in our AML cell lines by flow cytometry. All experiments were performed three times in triplicate, representative figures are shown.

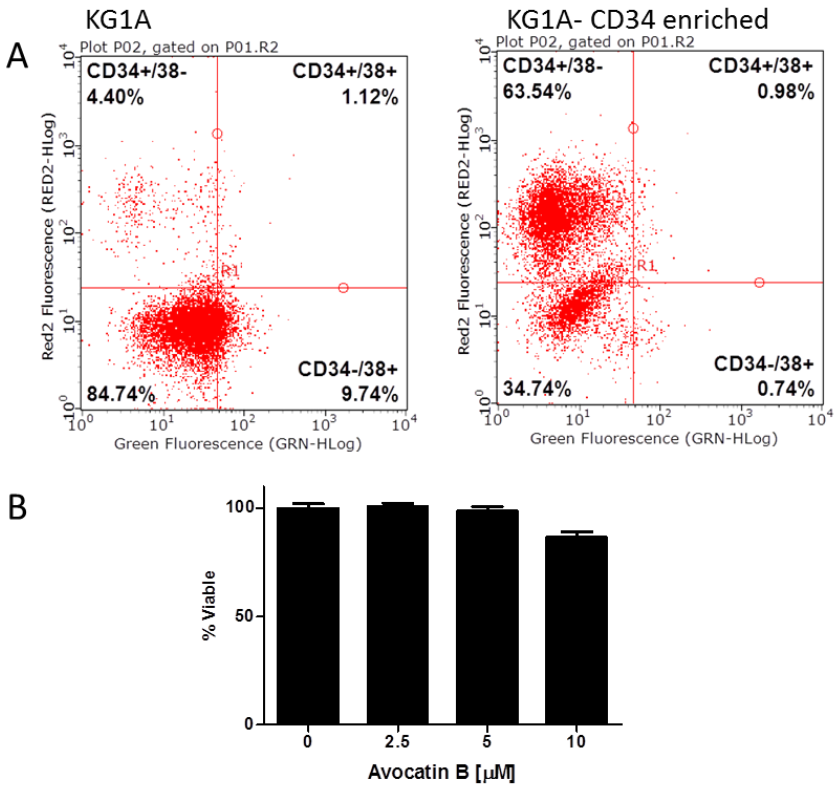

Figure 4.3. Assessing avocatin B in enriched CD34 KG1A cells. (A) KG1A cells were enriched for CD34 positive cells using the CD34+ EasySep Positive Selection Kit and EasySep Magnet. This was confirmed by flow cytometry. Representative dot plots are shown. (B) Enriched CD34 KG1A cells were incubated with avocatin B over 72 hours. Viability was measured using the MTS viability assay and data are presented as mean percentage of live cells. All experiments were performed three times in triplicate, representative figures are shown.

4.1.4 Avocatin B induces mitochondria-mediated apoptosis

We next assessed the mode of avocatin B induced leukemia cell death. Externalization of phosphatidylserine, an early marker of apoptosis detected by Annexin V, was observed in live cells (i.e., ANN^+/PI^-) treated with avocatin B and flow cytometry 48 hours post treatment (Figure 4.4A; $F_{3,7}=19.09;p<0.05$; see supplementary figure 4.2 for raw data). This coincided with the occurrence of DNA fragmentation (Figure 4.4B; $F_{4,14}=171.4;p<0.001$), caspase activation (Figure 4.4C; $F_{3,16}=69.56;p<0.001$) and PARP cleavage (Figure 4.4D), as measured by cell cycle analysis (see supplementary figure 4.3 for raw data), a caspase activation assay and Western blotting, respectively.

To test whether death was dependent on caspase enzymes we co-incubated avocatin B with the pan-caspase inhibitor Z-VAD-FMK or the caspase-3 specific inhibitor QVD for 72 hours. Both inhibitors

only slightly protected from avocatin B-induced death ($F_{4,9}$=2.714;p<0.01; Figure 4.4E). Since cell death can occur independent of caspase enzymes through the release of mitochondria localized proteins such as apoptosis inducing factor (AIF), we tested for the presence of AIF in cytosolic fractions of avocatin B treated TEX cells. However, given that AIF release involves mitochondrial outer membrane permeability and that we detected caspase activation; we also simultaneously tested for the presence of cytochrome c, which activates caspase enzymes following its release from the mitochondrial intermembrane space. Cells treated with avocatin B showed an increase in cytoplasmic concentrations of AIF ($F_{4,20}$=8.211;p<0.001; Figure 4.4F) and cytochrome c ($F_{4,20}$=13.57;p<0.001; Figure 4.4F). To further support this, Western Blotting revealed an increase in AIF protein expression in avocatin B treated cells (Figure 4.5).

Another characteristic associated with mitochondria-mediated apoptosis is the dissipation of the mitochondrial membrane potential (ΔΨm). Dissipation of ΔΨm has been associated with mitochondrial outer membrane permeabilization (MOMP) and the release of cytochrome c [88, 89]. It has also been reported that ΔΨm disruption can lead to ROS generation resulting in MOMP [88]. As such, we investigated whether avocatin B disrupted ΔΨm in TEX leukemia cells. Avocatin B treatment caused a significant reduction in ΔΨm consistent with the release of cytochrome c and AIF (Figure 4.6). Therefore, avocatin B induced apoptotic death characterized by the release of the mitochondrial proteins AIF and cytochrome c.

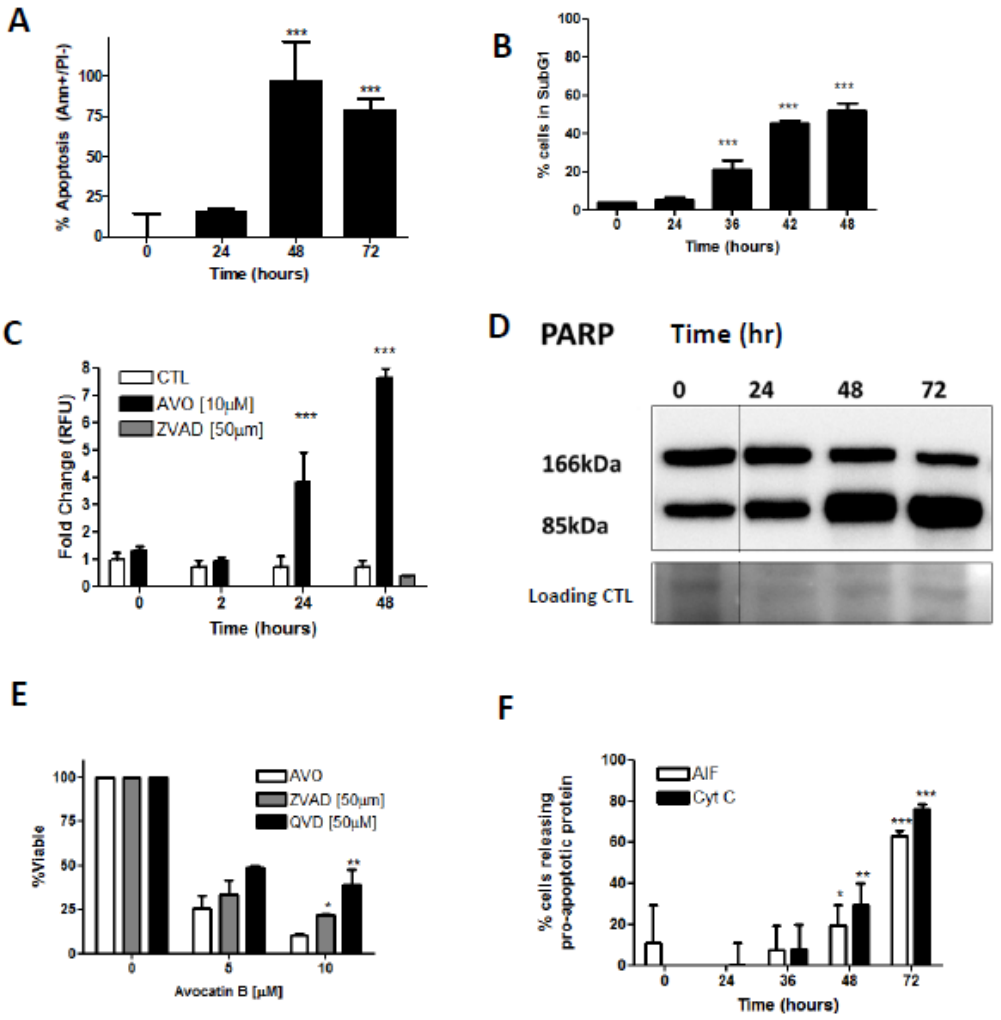

Figure 4.4. Avocatin B induces mitochondria-mediated apoptosis. **(A)** TEX cells were treated with 10μM avocatin B for increasing duration and phosphatidylserine exposure in live cells (i.e., apoptotic phenotype; ANN^{+}/PI^{-}) and **(B)** DNA fragmentation were measured by flow cytometry. Data are presented as fold change in apoptotic phenotype and percent cells in sub G1 peak, respectively. **(C)** TEX cells were treated with 10μM avocatin B for increasing duration and caspase 3 and 7 activation and (**D)** cleavage of PARP, a substrate of caspase 3, were measured by a commercially available activation assay and Western blotting, respectively. **(E)** TEX cells were treated with 10μM avocatin B in the presence and absence of the pan caspase inhibitor Z-VAD-FMK (ZVAD) or the caspase-3 specific inhibitor Q-VD-OPh (QVD). Viability was measured after a 72 hour incubation period by the MTS assay. Data are presented as percent change in viability compared to controls ± SD. **(F)** TEX cells were treated with 10μM avocatin B for increasing duration and cytochrome c and AIF release were measured in cytoplasmic fractions by flow cytometry. Data are presented as percent of cells releasing cytochrome c or AIF ± SD. All experiments were performed three times in triplicate, representative figures are shown. *p<0.05; **p<0.01;*** p<0.001.

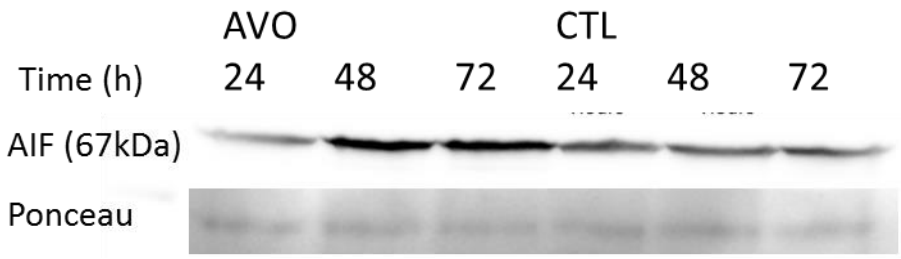

Figure 4.5. Avocatin B increases AIF protein expression. Western Blot of AIF (67kDa) protein in TEX cells treated with 10μM avocatin B or DMSO control over 24, 48 and 72 hours. Ponceau staining was used to quantify equal loading of samples.

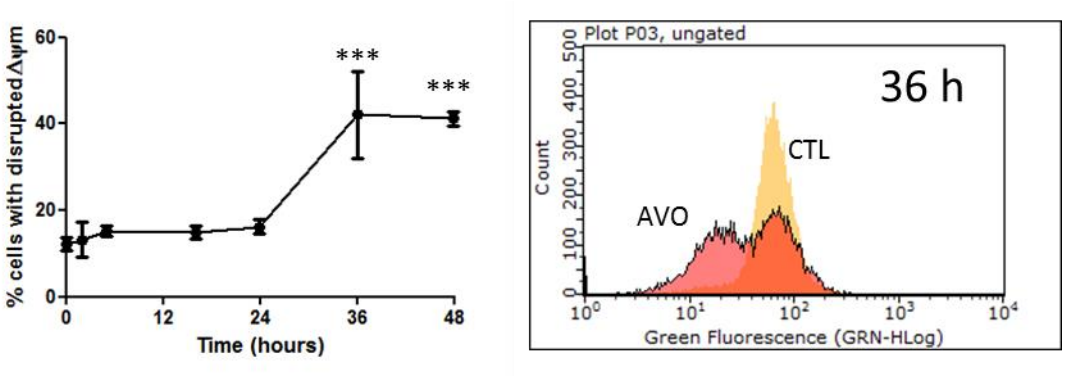

Figure 4.6. Assessing avocatin B's impact on ΔΨm. (Left panel) TEX cells were incubated with 10μM avocatin B over a 48 hour time course. ΔΨm was assessed by rhodamine 123 staining and flow cytometry. Data are represented as %cells with disrupted ΔΨm. (Right panel) Histogram plot displaying shift in rhodamine 123 fluorescence after 36 hour incubation with avocatin B. ***p<0.001.

4.1.5 Avocatin B's activity involves the fatty acid metabolism pathway

Prior to this study, little has been published on the mechanism of avocatin B with only reports of activity in various solid cancer cell lines [59]. However, similarly structured avocado-derived compounds have been shown to inhibit acetyl-CoA carboxylase, a key enzyme in fatty acid biosynthesis [90]. As such, we aimed to explore whether avocatin B also affected the fatty acid biosynthesis pathway (Figure 4.7). We co-incubated TEX cells with avocatin B and palmitate, the end product of the fatty acid biosynthesis pathway, and reported that palmitate abrogated avocatin B's cytotoxicity (Figure 4.8).

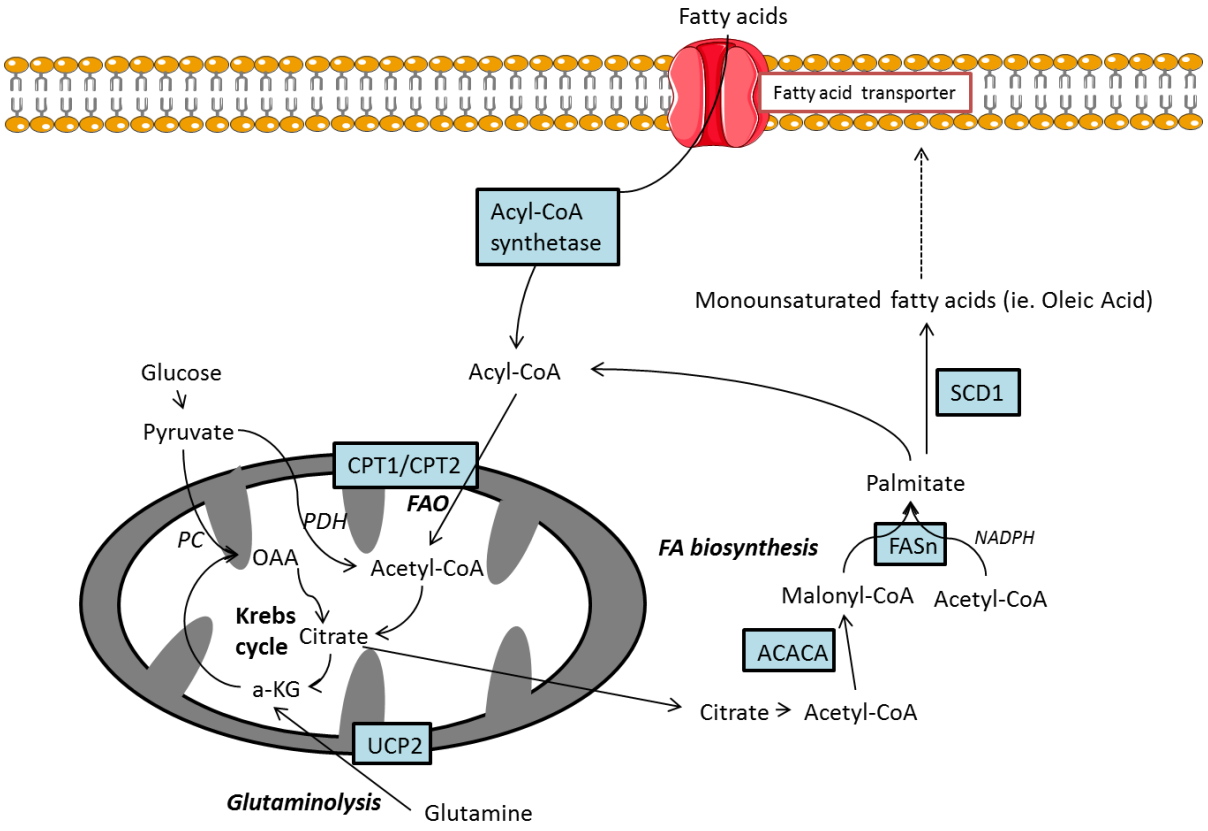

Figure 4.7. Schematic diagram of the fate of fatty acids in the cell. Fatty acids can undergo fatty acid oxidation to fuel the Kreb's cycle or can be converted to monounsaturated fatty acids to contribute towards the phospholipid bilayer. Adapted from Samudio *et al*. 2010 and Carracedo *et al*. 2013 using Servier Medical Art (Creative Commons Attribution 3.0 Unported License).

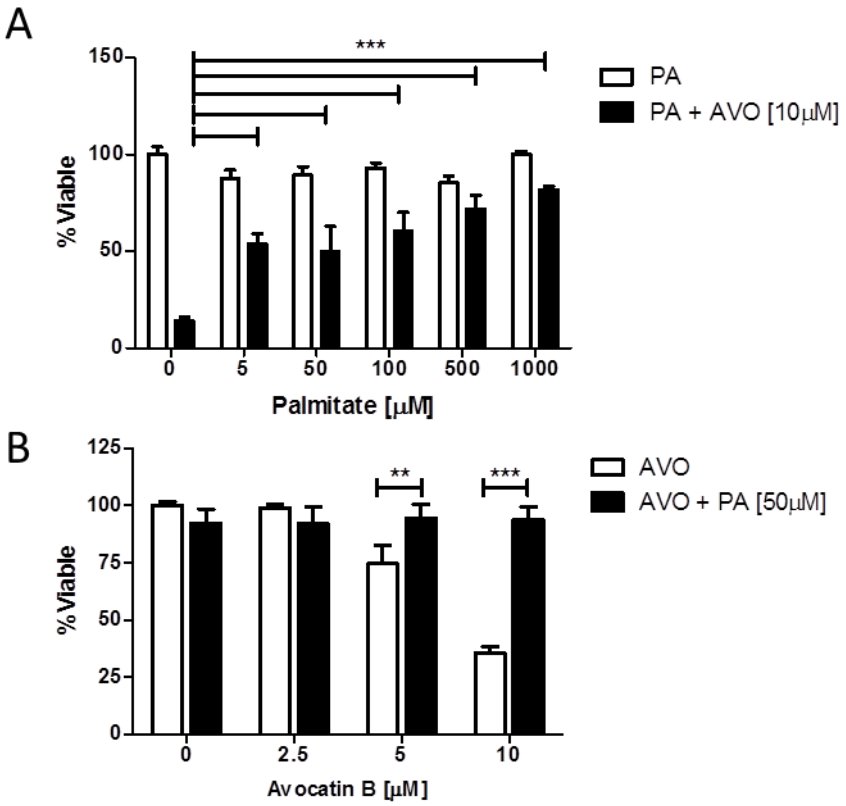

Figure 4.8. Avocatin B's activity is dependent on the fatty acid metabolism pathway. (A) TEX cells were co-incubated with 10μM avocatin B and increasing concentrations of palmitate over 72 hours. Viability was measured using the MTS viability assay and data are represented as mean percentage of live cells. (B) TEX cells were co-incubated with 50μM palmitate and increasing concentrations of avocatin B. Viability was measured using the ANN/PI flow cytometry assay and data are presented as mean percentage of live cells. All experiments were performed three times in triplicate, representative figures are shown. **p<0.01; ***p<0.001.

Fatty acids, including palmitate, are produced by fatty acid synthase (FASN), a major enzyme involved in fatty acid biosynthesis, from the substrates acetyl-CoA, malonyl-CoA and NADPH [91, 92]. Given that palmitate rescued cells from avocatin B induced cell death, we investigated if avocatin B's activity was dependent on FASN. We co-incubated TEX cells with avocatin B and orlistat, a chemical inhibitor of FASN (Figure 4.9A) [93]. Avocatin B's activity was not affected by orlistat suggesting that its activity is not dependent on FASN.

Upstream of FASN is acetyl-CoA carboxylase, an enzyme responsible for the production of the FASN substrate malonyl-CoA. Given that avocado-derived compounds with a similar structure to

avocatin B have been shown to inhibit acetyl-CoA carboxylase (ACC) [49], we investigated whether avocatin B's activity was dependent on ACC. This was done by co-incubating avocatin B with acetyl-CoA and/or malonyl-CoA (Figure 4.9B, C & D), which is produced by ACC. Unlike co-incubation with palmitate, acetyl-CoA and/or malonyl-CoA were not capable of affecting avocatin B's activity in TEX cells indicating that ACC was not essential to its activity.

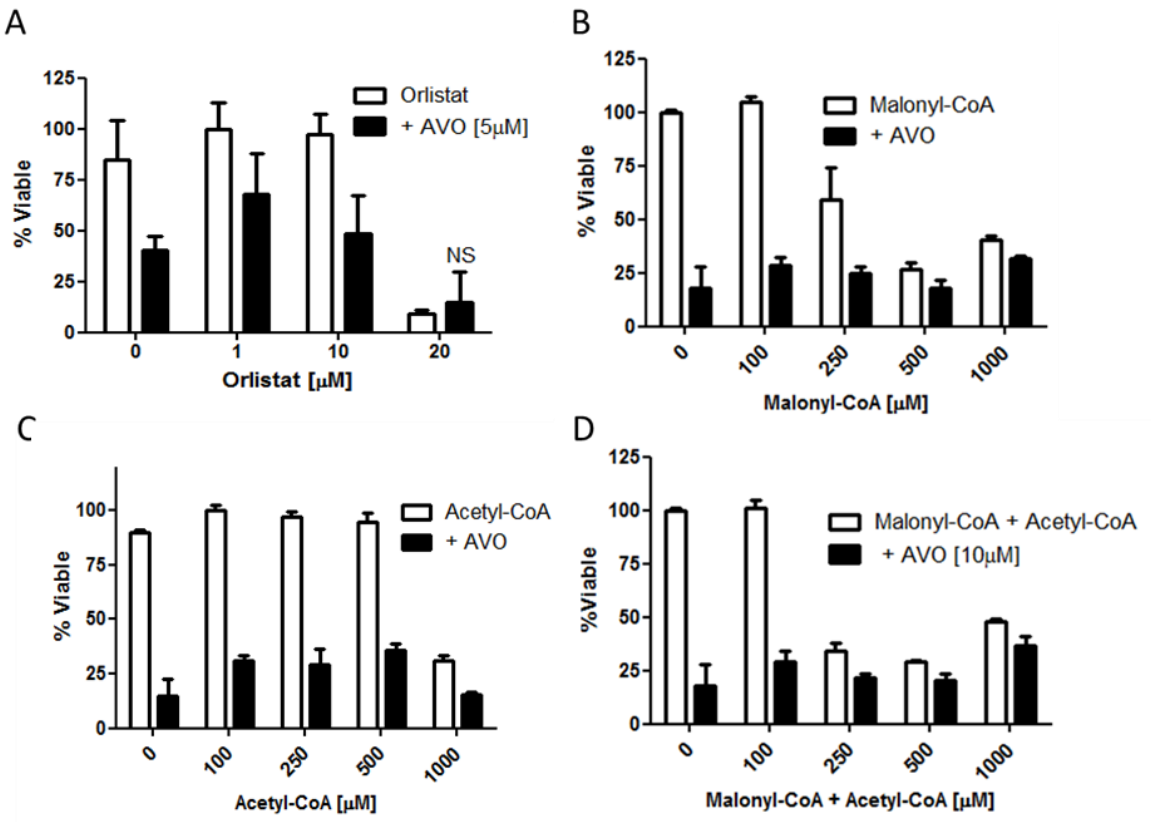

Figure 4.9. Assessing avocatin B's role in the fatty acid biosynthesis pathway. (A) TEX cells were co-incubated with 5µM avocatin B and increasing concentrations of the FASN inhibitor orlistat over 72 hours. Viability was measured using the MTS viability assay and data are represented as mean percentage of live cells. (B) TEX cells were co-incubated with 10µM avocatin B and increasing concentrations of malonyl-CoA. Viability was measured using the MTS viability assay and data are represented as mean percentage of live cells. (C) TEX cells were co-incubated with 10µM avocatin B and increasing concentrations of acetyl-CoA. Viability was measured using the MTS viability assay and data are represented as mean percentage of live cells. (D) TEX cells were co-incubated with 10µM avocatin B and increasing concentrations of malonyl-CoA and acetyl-CoA. Viability was measured using the MTS viability assay and data are represented as mean percentage of live cells. All experiments were performed three times in triplicate, representative figures are shown.

Once fatty acids have been produced by FASN, they can be used as a metabolic fuel source through fatty acid oxidation, or they can be desaturated to monounsaturated fatty acids (MUFA) to contribute towards cellular tissues [94]. Stearoyl-CoA desaturase-1(SCD1) is an enzyme responsible for the conversion of saturated fatty acids to MUFAs. Oleic acid is the primary product from SCD1 [94]. To investigate whether avocatin B inhibited SCD1, we co-incubated avocatin B with oleic acid to see if could rescue cells from avocatin B's cytotoxic effects (Figure 4.10). Treatment with oleic acid failed to abrogate avocatin B's activity indicating that its activity was unrelated to the MUFA pathway of fatty acid biosynthesis. Given that only palmitate rescued cells from avocatin B treatment, we chose to investigate downstream pathways such as fatty acid oxidation (next section). Thus, high palmitate concentrations rescue cells from death likely by outcompeting avocatin B for entry into mitochondria through CPT1.

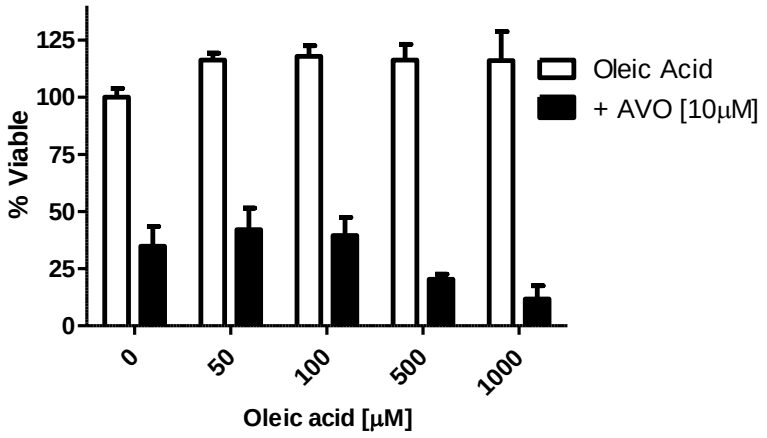

Figure 4.10. Avocatin B's activity is independent of the monounsaturated fatty acid biosynthesis pathway. (A) TEX cells were co-incubated with 10μM avocatin B and increasing concentrations of oleic acid over 72 hours. Viability was measured using the MTS viability assay and data are represented as mean percentage of live cells. All experiments were performed three times in triplicate, representative figures are shown.

4.1.6 Avocatin B inhibits fatty acid oxidation

Apoptosis was characterized by the release of mitochondrial proteins following avocatin B treatment. Since avocatin B is a 17-carbon lipid and lipids of that size can enter the mitochondria and undergo fatty acid oxidation after they have been processed by carnitine palmitoyltransferase 1 (CPT1),

we evaluated the impact of avocatin B on fatty acid oxidation. Fatty acid oxidation produces acetyl-CoA which enters the TCA cycle to produce NADH, which fuels oxidative phosphorylation, and NADPH, an important co-factor that participates in catabolic processes during cell proliferation [95] and is the precursor of reduced glutathione - an important intracellular and mitochondrial antioxidant [96, 97] (Figure 4.11A). To test the effects of avocatin B on fatty acid oxidation, we measured mitochondrial bioenergetics of TEX cells pre-incubated with avocatin B or palmitate in the absence or presence of etomoxir by measuring the change in maximum oxygen consumption following oligomycin and CCCP treatment and prior to the addition of antimycin and rotenone, as described in Abe *et al.* (2013) [74]. As expected, treatment with palmitate increased the oxygen consumption rate (OCR), consistent with oxidation of exogenous fatty acid substrates and this increase was blocked by treatment with etomoxir, a CPT1 inhibitor (Figure 4.11B&C). Similarly, avocatin B reduced palmitate oxidation demonstrating that avocatin B inhibits the oxidation of exogenous fatty acids ($F_{5,17}$=40.83;$p<0.05$; Figure 4.11B&C; arrows indicate the time when oligomycin, CCCP and antimycin/rotenone were added to the cells). Future studies are needed to further determine the nature of CPT1's preference for avocatin B over palmitate.

4.1.7 Inhibiting fatty acid oxidation results in reduced NADPH and elevated ROS

Inhibiting fatty acid oxidation can decrease NADPH and subsequently decrease antioxidant capabilities [75]. Thus, we tested the effect of avocatin B on NADPH levels in TEX leukemia cells. Avocatin B (10µM), similar to etomoxir (100µM), resulted in a 50% reduction in NADPH, an effect that was observed even in the presence of palmitate (175µM; $F_{9,19}$=5.129;$p<0.05$; Figure 4.11D).

Inhibition of fatty acid oxidation can reduce NADPH leading to reduced antioxidant capacity, elevated reactive oxygen species (ROS) and cell death [75]. ROS levels were tested in avocatin B treated cells using DCFH-DA and DHE, which measure general ROS and superoxide, respectively. TEX cells treated with avocatin B had a time-dependent increase in ROS levels as measured by DCFH-DA ($F_{5,11}$=176.7;$p<0.01$; Figure 4.11E; see supplementary figure 4.4 for histogram data) and DHE ($F_{5,11}$=36.75;$p<0.01$; Figure 4.11E; see supplementary figure 4.4 for histogram data). To test the

importance of ROS in avocatin B-induced death, we co-incubated cells with the antioxidants N-acetylcysteine (NAC) or α-tocopherol (α-Toc). NAC neutralizes ROS through glutathione generation, which is reduced following NADPH depletion [75] and α-tocopherol is a lipid-based antioxidant that accumulates in organelle membranes, particularly mitochondria; to prevent lipid peroxyl radicals formed by ROS induced membrane damage [98]. Co-incubation with NAC ($F_{3,7}$=70.55;$p<0.05$; Figure 4.11F, right panel) or α-tocopherol ($F_{3,7}$=10.23;$p<0.05$; Figure 4.11F, right panel) abolished avocatin B-induced death. Daunorubicin (DNR) was used a negative control, as antioxidants do not protect against its cytotoxicity [99, 100]. Together, these results demonstrate that avocatin B reduces NADPH and that ROS is functionally important for avocatin B-induced death.

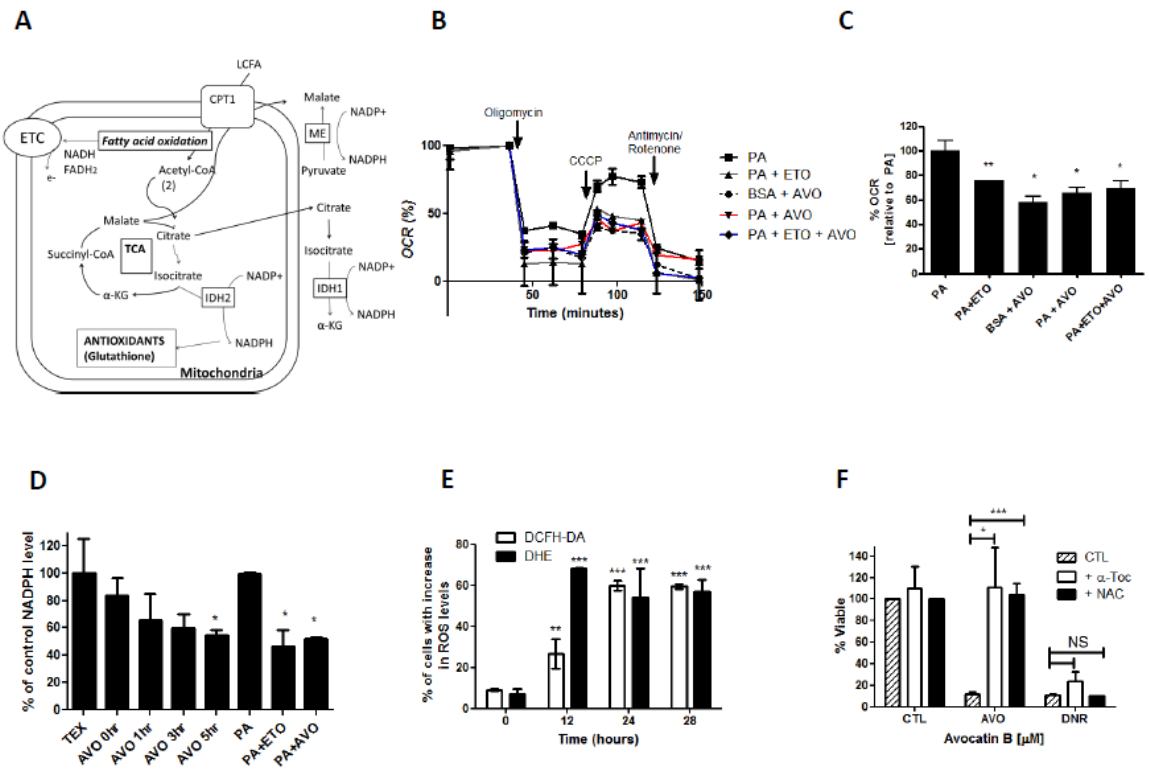

Figure 4.11. Avocatin B inhibits fatty acid oxidation resulting in reduced NADPH and elevated ROS**. (A)** Illustration of fatty acid oxidation in mitochondria. Long chain fatty acids (LCFA) enter the mitochondria via CPT1 for fatty acid oxidation to yield acetyl-CoA. Acetyl-CoA enters the TCA cycle to generate NADPH, an enzymatic co-factor and antioxidant. (ME: malic enzyme; IDH: isocitrate dehydrogenase; α-KG: α-ketoglutarate). **(B)** Oxidation of exogenous fatty acids was assessed by measuring the oxygen consumption rate (OCR) in TEX cells treated with palmitate (175μM), avocatin B (10μM), avocatin B and palmitate or palmitate and etomoxir (100μM). Arrows indicate the time when oligomycin, CCCP and antimycin/rotenone were added to the cells. Effects on fatty acid oxidation were measured with the Seahorse Bioanalyzer, as detailed in the methods section, and **(C)** quantified by peak area after oligomycin and CCCP treatment, as described by the manufacturer's protocol and detailed in the methods. Data are presented as percent OCR compared to palmitate treated cells ± SD. **(D)** NADPH was measured using the commercially available Amplite™ Fluorimetric Assay following treatment with avocatin B (10μM), palmitate (175μM) or etomoxir (100μM), according to the manufacturer's protocol. Data are presented as a percent NADPH compared to vehicle control treated cells ± SD. **(E)** Reactive oxygen species (ROS) were measured in TEX cells treated with 10μM avocatin B for increasing time by DHE and DCFH-DA by flow cytometry. Data are presented as fold change in fluorescence, compared to vehicle control, ± SD from representative experiments. **(F)** TEX cells were treated with 10μM avocatin B in the presence or absence of the anti-oxidants, N-acetyl cysteine (NAC) or α-tocopherol (α-Toc). Daunorubicin (DNR) was used as a negative control. Viability was measured by the ANN/PI assay and data are presented as mean percentage of viable cells (i.e., ANN^-/PI^-) ± SD from representative experiments. All experiments were performed three times in triplicate, representative figures are shown. *p<0.05; **p<0.01; ***p<0.001.

4.1.8 Assessing PPARα's role in avocatin B mediated leukemia cell death

Peroxisome proliferator-activated receptor (PPAR)α is a nuclear receptor protein that regulates FA oxidation and UCP expression, however its role in cancer cell proliferation remains unclear [20, 101, 102]. In several cancer cell models however, activation of PPARα inhibited tumor growth [20]. To determine a possible role of PPARα, we tested avocatin B's activity in PPARα knockdown cells. Cells lacking PPARα were equally sensitive to avocatin B as wild-type cells (Figure 4.12), suggesting that avocatin B's effect on fatty acid oxidation is independent of PPARα. Although PPARα is central to FAO, PPAR transcription factors have multiple isoforms including PPAR delta and PPAR gamma. In fact, evidence suggests that a related family member PPAR delta is in fact required for the maintenance of HSCs and LSCs through FAO [21]. This result suggests that PPAR delta and PPAR gamma are related to avocatin B's activity. Future studies should explore if PPAR delta and gamma play a role in regulating avocatin B's activity.

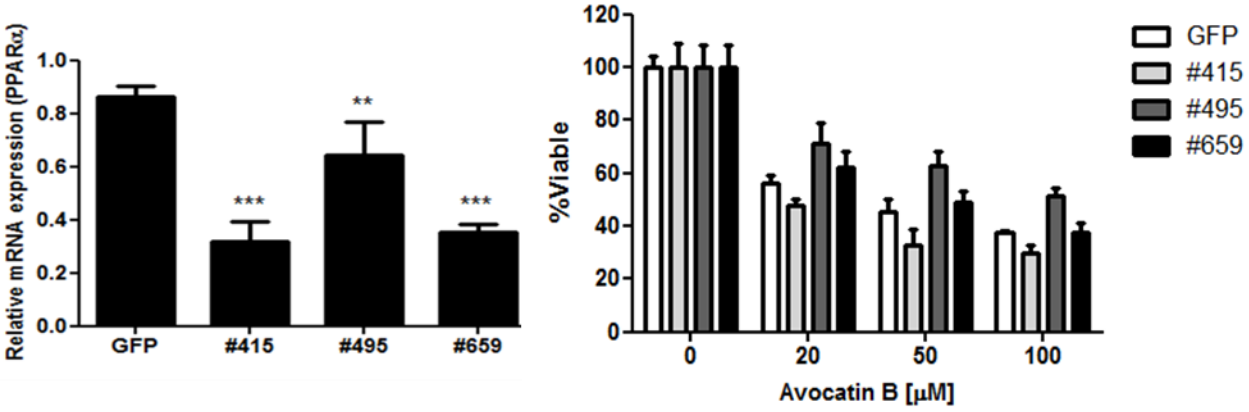

Figure 4.12. Avocatin B's activity is independent of PPARα. (Left panel) mRNA expression demonstrating knockdown of PPARα in AML2 cells. *Experiment performed by Princess Margaret Hospital*. (Right panel) AML2 cells lacking PPARα were co-incubated with increasing concentrations of avocatin B 72 hours. Viability was measured using the ANN/PI viability assay and data are represented as mean percentage of live cells. All experiments were performed three times in triplicate, representative figures are shown.

4.1.9 Mitochondria and CPT1 are functionally important for avocatin B-induced death

We demonstrated that avocatin B inhibits fatty acid oxidation and induces apoptosis characterized by the release of mitochondrial proteins cytochrome c and AIF. Since avocatin B is a lipid and leukemia cells possess mitochondrial and metabolic alterations that increase their demand for fatty acid substrates [24], we hypothesized that avocatin B's toxicity was related to its localization in mitochondria. To first test avocatin B's reliance on mitochondria for cytotoxicity, we generated leukemia cells lacking functional mitochondria by culturing Jurkat-T cells in media supplemented with 50ng/ml of ethidium bromide (EtBr), 100mg/ml sodium pyruvate and 50µg/ml uridine, as previously described [103, 104]. Following 60 days of passaging only live cells, the presence of mitochondria were tested by flow cytometry following 10-nonyl acridine orange (NAO) staining and by Western blotting for mitochondrial specific proteins ND1 (i.e., complex 1) and adenine nucleotide translocator (ANT). The significant reduction of mitochondria was confirmed, as cells co-cultured in EtBr containing media demonstrated a drastic reduction in NAO staining (supplementary figure 4.5) and a near absence of ND1 and ANT (Figure 4.13A). Avocatin B's toxicity was abolished in cells lacking functional mitochondria, as measured by the ANN/PI assay ($F_{2,12}$=6.509; $p<0.001$; Figure 4.13B). Highlighting the utility of these cells in assessing mitochondrial participation in drug activity, we previously showed that cells lacking mitochondria were equally sensitive to their mitochondria containing controls when subjected to a compound that activates mitochondria-independent, calpain-mediated apoptosis [76].

In hypoxic conditions (i.e., reducing oxygen concentrations), ATP production is shifted away from the mitochondrial pathways of oxidative phosphorylation and fatty acid oxidation toward glycolysis [105-107]. Thus, we compared avocatin B's cytotoxicity in normoxic (21% oxygen) and hypoxic (1% oxygen) conditions. As controls, we tested drugs that directly target mitochondria such as antimycin and rotenone and drugs that do not directly target mitochondria such as cytarabine and daunorubicin. These controls demonstrated that the activity of mitochondria target drugs are reduced in hypoxic conditions whereas non-mitochondria target drugs are unaffected by these conditions. As expected, avocatin B's activity was significantly reduced in conditions in which cellular metabolism is shifted away from

mitochondrial pathways ($F_{4,24}$=98.51; p<0.0001; Figure 4.13C). However, it is important to note that although avocatin B's activity was decreased in reduced oxygen; it did remain active at oxygen concentrations (i.e., 6.1% ± 1.7%[108]) found in bone marrow (supplementary figure 4.6).

Excessive accumulation of fatty acids within the mitochondria increases the expression of uncoupling proteins (UCP) [109]. Thus, we measured expression of UCP2, the leukemia specific UCP [30], as an indirect measure of mitochondrial fatty acid accumulation by Western blotting. Treatment with avocatin B increased UCP2 protein expression in leukemia cells (Figure 4.13D).

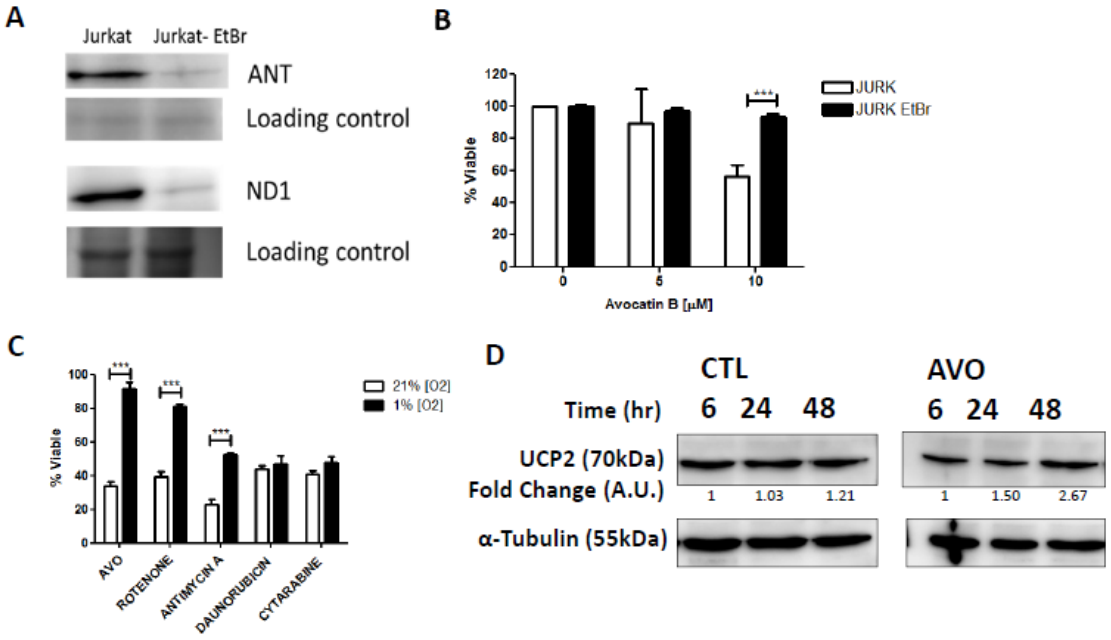

Figure 4.13. Mitochondria are functionally important for avocatin B-induced death. **(A)** Jurkat T cells were cultured in 50ng/ml of ethidium bromide, 100mg/ml sodium pyruvate and 50µg/ml uridine for 60 days to create Jurkat-EtBr cells which lack functional mitochondrial. To confirm that Jukat-EtBr cells lack mitochondria, we measured the mitochondria specific markers adenine nucleotide translocator (ANT) and complex I (ND1) by Western blotting. **(B)** Avocatin B's activity was tested in cells with (JURK) and with reduced (JURK-EtBr) mitochondria. Viability was measured by the ANN/PI assay and flow cytometry and data are presented as mean percentage of live cells (i.e., ANN^-/PI^-) ± SD from representative experiments. **(C)** TEX cells were grown in normoxic ($21\%O_2$) or hypoxic ($1\%O_2$) conditions and treated with avocatin B (2µM), antimycin A (1µM), rotenone (3µM), daunorubicin (5nM) or cytarabine (4nM). Cell viability was measured by the sulforhodamine B assay, as described in the methods, following a 72 hour incubation period. Data are presented as percent viable. *Experiment performed by Princess Margaret Cancer Centre.* **(D)** Uncoupling protein 2 (UCP2) was measured in whole cell lysates of avocatin B (10µM) or DMSO-control treated TEX cells by Western blotting. Arbitrary units (AU) are presented as fold change (compared to the 6 hour time point) and were calculated by dividing each treatment lane by the densitometry of its loading control. Densitometry was calculated as outlined in the methods. All experiments were performed three times in triplicate, representative figures are shown. *p<0.05; **p<0.01***; p<0.001.

Lipids of 16-20 carbon length enter mitochondria by the activity of CPT1 [110]. To determine the role of CPT1 in avocatin B-induced death we blocked CPT1 activity chemically with etomoxir and genetically using RNA interference. Etomoxir concentrations that did not reduce viability (100µM; $F_{3,11}$=19.81;p<0.001; Figure 4.14A), abrogated avocatin B-induced cell death ($F_{5,17}$=94.45;p<0.001; Figure 4.14B). As a genetic approach, we generated cells with reduced CPT1A gene expression (Figure 4.14C, left panel). CPT1A knockdown cells were significantly less sensitive to avocatin B ($F_{9,32}$=23.73;p<0.001; Figure 4.14C, right panel). Together, these results suggest that avocatin B is a lipid that localizes to the mitochondria and impairs fatty acid oxidation.

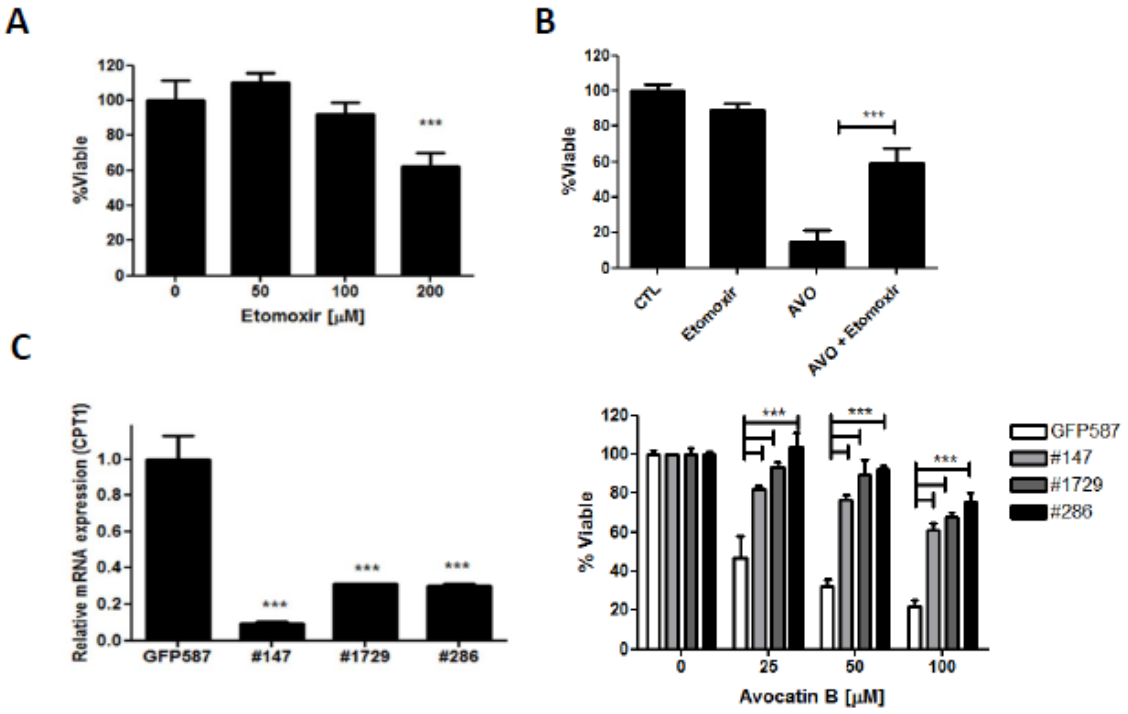

Figure 4.14. CPT1 is functionally important for avocatin B induced death. **(A)** TEX cells were incubated with increasing concentrations of the CPT1 inhibitor etomoxir for 72 hours. **(B)** Avocatin B's (10µM) activity was tested in the presence of etomoxir (100µM; which does not impart toxicity) or **(C)** (right panel) in cells lacking CPT1A. (left panel) mRNA expression demonstrating knockdown of CPT1A. *Experiment performed by Princess Margaret Cancer Centre.*. Unless otherwise noted, viability was measured by the ANN/PI assay and flow cytometry and data are presented as mean percentage of live cells (i.e., ANN^-/PI^-) ± SD from representative experiments. All experiments were performed three times in triplicate, representative figures are shown. *p<0.05; **p<0.01***; p<0.001.

4.1.10 Avocatin B activates autophagy

Treatment with avocatin B resulted in a delayed onset of death (i.e., after 24-48h), which was ROS-dependent (ROS increased after 18h of incubation) [111]. ROS-induced cell death can occur via apoptosis (type I programmed cell death) or autophagy (type II programmed cell death). Autophagy is classically activated by nutrient starvation [112] and autophagic cell death can occur following prolonged autophagic signaling [113]. Given the delayed onset of death that was characterized by increased levels of ROS [111] and that death follows inhibiting leukemia cells of an essential metabolic substrate (i.e., fatty acids), we assessed whether avocatin B activated autophagy.

First, we interrogated databases derived from haploinsufficiency profiling (HIP) in yeast, a validated chemical genomics platform used to identify cellular response patterns [28, 80, 114, 115]. Briefly, HIP in *Saccharomyces cerevisiae* allows for the quantitative measurement of the relative drug sensitivity of 6000 yeast genes [115]. Avocatin B was tested in a yeast chemogenomic screen consisting of >3250 small molecules [116] and its chemogenomic profile was retrieved from the HIPHOP yeast chemogenomics database and interrogated for mechanistic sensitivities. Of the top 15 genes sensitive to avocatin B ($p<0.05$), 4 have known biological associations with autophagy and/or vesicle-mediated transport (Figure 4.15A). Notably, 3 out of the 4 identified genes belong to the SEC protein family, which are essential for autophagosome formation [117, 118]. We also compared avocatin B's chemogenomic profile to rapamycin, a known autophagy inducer in mammalian cells. Similarly, 3 out of the top 15 genes sensitive to rapamycin have known biological associations with autophagy and/or vesicle-mediated transport (Figure 4.15A). Together, these findings suggest autophagy is mechanistically involved in avocatin B's activity.

To assess whether avocatin B activates autophagy in leukemia cells, we examined changes in lysosome size following cathepsin B staining by confocal microscopy. Lysosome size was increased in avocatin B treated TEX cells consistent with the creation of autophagolysosomes (Figure 4.15B) [79, 119]. A panel of autophagy markers was also tested by immunoblotting. Consistent with an autophagy response, avocatin B increased protein levels of Atg7, critical in autophagosome formation [42], and

mediated the conversion of LC3I to LC3II, a gold standard autophagy marker involved in autophagosome formation [42]. Moreover, avocatin B decreased protein levels of p62, an adaptor molecule that facilitates the interaction between ubiquitinated targets and LC3II [33] and Nix/BNIP3, a mitochondrial specific protein that is ubiquitinated prior to mitochondrial degradation [33, 120] (Figure 4.15C). Taken together, avocatin B activates autophagy in leukemia cells.

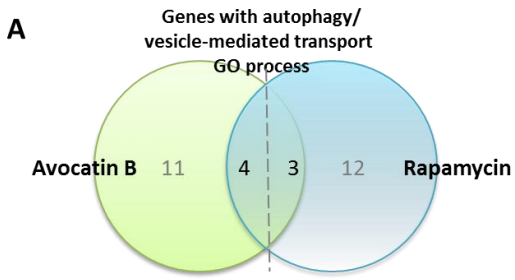

Drug	# of autophagy/vesicle-mediated transport genes in top 15 HET fitness defect scores (HIP)	Gene	FD score	P-value
Avocatin B	4	SEC2	2.93	0.00168
		SEC8	2.65	0.00398
		YIP1	2.26	0.012
		SEC17	2.22	0.0132
Rapamycin	3	TOR2	17.9	6.33E-72
		KOG1	16.9	4.41E-64
		NEO1	11.6	3.55E-31

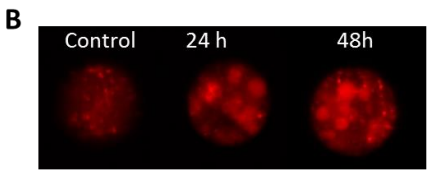

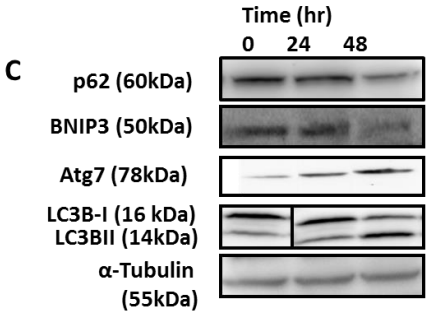

Figure 4.15. Avocatin B induces autophagy. **(A)** Interrogation of avocatin B's chemogenomic profile from a publicly available yeast chemogenomics database. (Left panel) Identification of genes related to autophagy and/or vesicle-mediated transport that are sensitive to avocatin B or rapamycin treatment. (Right panel) List of genes found in top 15 HET fitness scores related to autophagy and/or vesicle-mediated transport that sensitive yeast to avocatin B or rapamycin treatment. **(B)** Avocatin B increases lysosome size as measured by confocal microscopy. Following a 24 and 48 hour incubation period with 1.5μM avocatin B, TEX leukemia cells were stained with cathepsin B, a lysosomal protease, and lysosomes were observed by confocal microscopy. At 24 and 48 hours, the presence of larger vesicles is consistent with the formation of autophagolysosomes (representative figures shown). *Experiment was performed by Dr. Paul Spagnuolo.* **(C)** Avocatin B (1.5μM) increases protein levels of Atg7 and LC3B-II, and decreases protein levels of p62 and BNIP3L in TEX leukemia cells treated for 24 and 48 hours. Proteins were measured by Western blotting and α-tubulin was used as a loading control. *Experiment was partially performed by Elliott McMillan.*

4.1.11 Autophagy is functionally important for avocatin B-induced death

We previously demonstrated that avocatin B induces selective leukemia cell death following the release of mitochondrial pro-apoptotic proteins cytochrome c and AIF [111]. Next, we aimed to evaluate whether autophagy was critical to avocatin B's cytotoxicity. Thus, we generated Atg7 and SQSTM1/p62 knockdown cell lines (Figures 4.16A &B). Consistent with previous reports demonstrating the importance of Atg7 in autophagy induction [121], Atg7 knockdown cells were significantly less sensitive to avocatin B ($F_{6,24}$=53.07;$p<0.001$; Figure 4.16A, right panel). In contract, but similar to reports highlighting that genetic knockdown of SQSTM1/p62 increased autophagy signaling [122] and ROS levels leading to reduced viability of Ras transformed lung cancer cells [123], knockdown of SQSTM1/p62 renders leukemia cells more sensitive to avocatin B (Figure 4.16B, right panel). Indeed, basal ROS levels were elevated in SQSTM1/p62 knockdown cells compared to GFP controls (Figure 4.16C). Collectively, these results suggest that autophagy is functionally important in avocatin B-induced death.

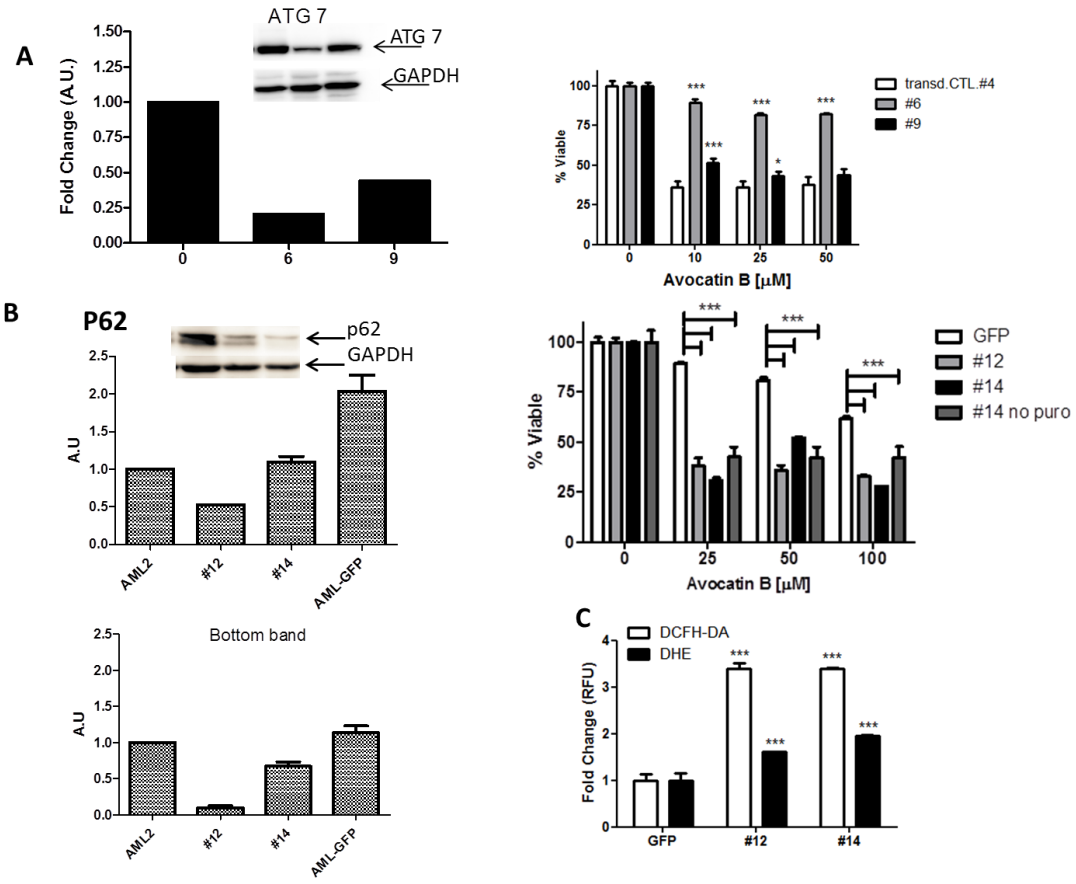

Figure 4.16. Autophagy is functionally important for avocatin B-induced death. **(A)** (Left panel) Immunoblots and densitometry showing protein levels of Atg7 in OCI-AML2 cells treated with scramble or 2 independent Atg7 vectors. Arbitrary units were normalized to loading controls (GAPDH) and standardization to GFP controls. *Experiment was performed by Leonard Angka.* (Right panel) Avocatin B was tested in cells lacking Atg7. Viability was measured by the ANN/PI assay and flow cytometry and data are presented as mean percentage of live cells (i.e., ANN^-/PI^-) ± SD from representative experiments. **(B)** (Left panel) Immunoblots and densitometry showing protein levels of p62 in OCI-AML2 cells treated with GFP or 2 independent p62 vectors. Arbitrary units were calculated as above. Both bands of p62 were quantified, the top band represents the UBA-conjugated p62 protein. *Experiment was performed by Leonard Angka.* (Right panel) Avocatin B was tested in cells lacking SQSTM1 (p62). Viability was measured by the ANN/PI assay and flow cytometry and data are presented as mean percentage of live cells (i.e., ANN^-/PI^-) ± SD from representative experiments. **(C)** Basal ROS levels were detected in GFP and SQSTM1 knockdown cells using DCF-DA and DHE, as outlined in the methods. All experiments were performed three times in triplicate, representative figures are shown. *p<0.05; **p<0.01***; p<0.001.

4.1.12 Establishing a methodology for the long-term culture of primary AML samples

In our studies, we assessed avocatin B`s anti-leukemia activity in primary AML and normal CD34+ hematopoietic cells. In order to facilitate the long-term use of these cells, we used a mouse bone marrow stromal co-culturing system (Chapter 3: Methods) allowing for the long term expansion and

culture of primary AML and CD34+ normal cells [62]. Through co-culturing with stromal cells, we were able to create a simulated bone marrow microenvironment, which is essential in preventing cell differentiation and preventing apoptosis through the up regulation of anti-apoptotic proteins [124]. Using this co-culturing system, we were able to expand and grow primary cells for an extended period of time (Figure 4.17).

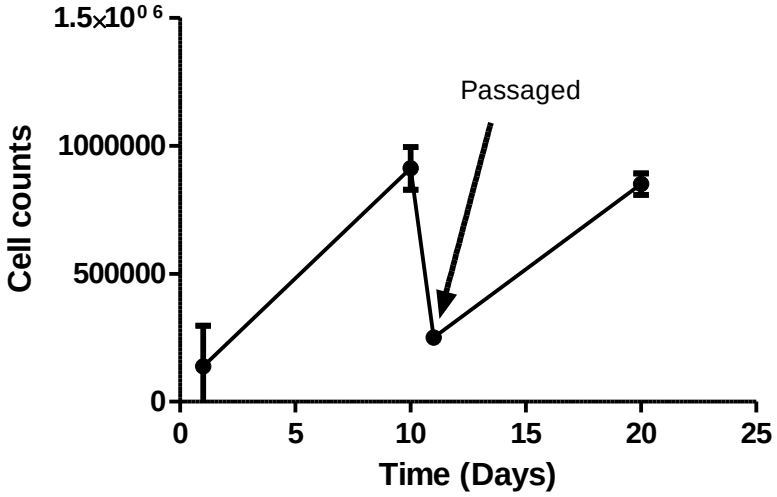

Figure 4.17. Bone marrow stromal co-culuring allows for the long term culture of primary cells. Cell counts of normal CD34+ hematopoietic cells co-cultured with mouse bone marrow stromal cells over a period of 25 days. Cells were counted using the trypan blue exclusion assay and a hemocytometer.

4.2 Supplemental figures

Table S4.1a. AML patient sample details used for annexin/PI

Label #	CD34 (%)	Interpretation
AML1	77	43~44,XX,dic(3;12)(p13;p11.2),-5,-7,+del(11)(q13),?dup(18)(q21q22),del(20)(q13.1),-22,+mar[cp10]
AML2	88	44~48,XX,del(5)(q13q33),i(9)(p10),-18,add(20)(q13.3),+mar[cp17]/46,XX[3]
AML3	87	46,XX,t(2;8)(p13;q22)[20].ish t(2;8)(MYC+;MYC-)
AML4	1	NPM, Flt3-TKD
AML5	60	**
AML5	77	Del 5q

** Denotes unknown/not tested

Table S4.1b. AML patient sample details used for colony formation assays

Label #	CD34 (%)	Interpretation
AML6	**	43,XY,del(5)(q13q33),-7,t(9;12)(q12;q12),der(16)t(16;17)(q12.1;q21), -17,-18[4]/44,idem,+8[2]/46,XY[3]
AML7	**	46,XX,t(9;11)(p22;q23)[20]
AML8	**	46,XY,del(5)(q22q31)[20]

** Denotes unknown/not tested

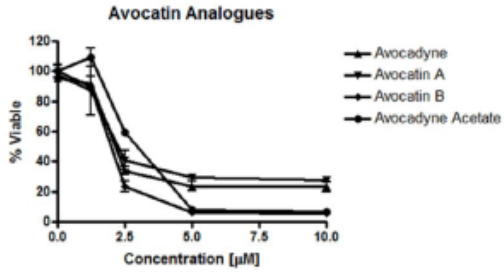

Cell line	EC_{50} (μM)	95% CI
TEX	1.271	0.5100 to 2.032
KG1A	25.43	23.49 to 27.36
OCI-AML2	25.20	24.18 to 26.22
JURKAT	9.974	8.028 to 11.92

Supplementary figure 4.1. Avocatin B is the most active avocado lipid analogue. **(A)** TEX cells were treated with increasing concentrations of avocado lipid analogues. Avocatin B imparted the greatest reducing in TEX cell viability. Data are presented as mean percentage of live cells (MTS assay) ± SD from representative experiments. Experiments were performed three times in triplicate.

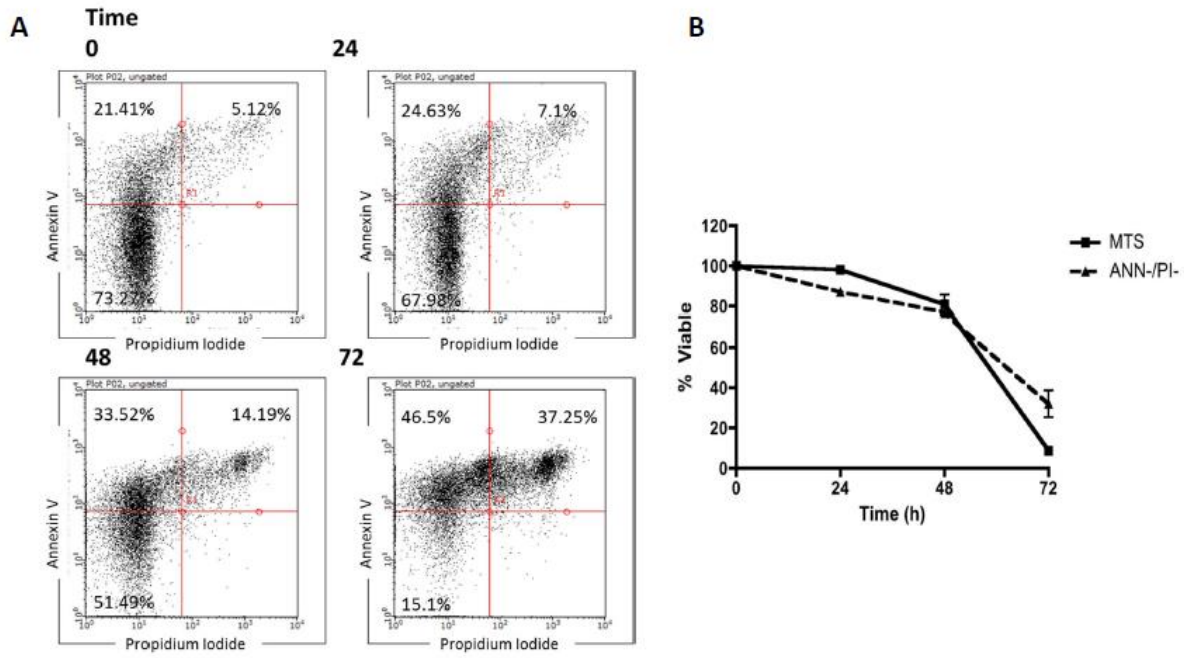

Supplementary figure 4.2. Kinetics of avocatin B-induced death. TEX cells were treated with 10µM avocatin B and **(A)** apoptotic cells (ANN+/PI-) and **(B)** cell viability (ANN-/PI-) were measured by flow cytometry. Data are presented as mean percentage of apoptotic or live cells ± SD. All experiments were performed three times in triplicate.

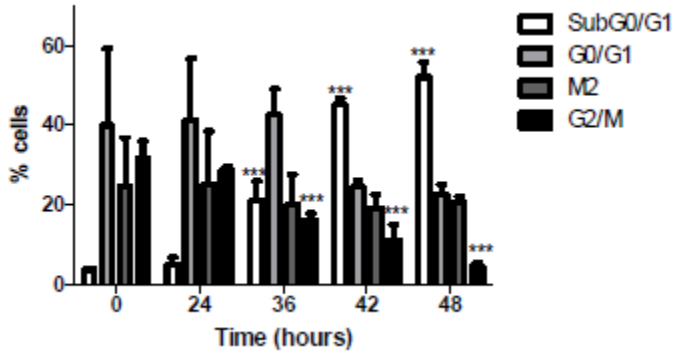

Supplementary figure 4.3. Cell cycle analysis of avocatin B treated TEX cells. TEX cells were incubated with avocatin B (10µM) over a 48 hour time course and cell cycle analysis was performed by propidium iodide staining and flow cytometry. Data are presented as percentage of cells per cell cycle phase ± SD from representative experiments. All experiments were performed three times in triplicate. ***; $p<0.001$.

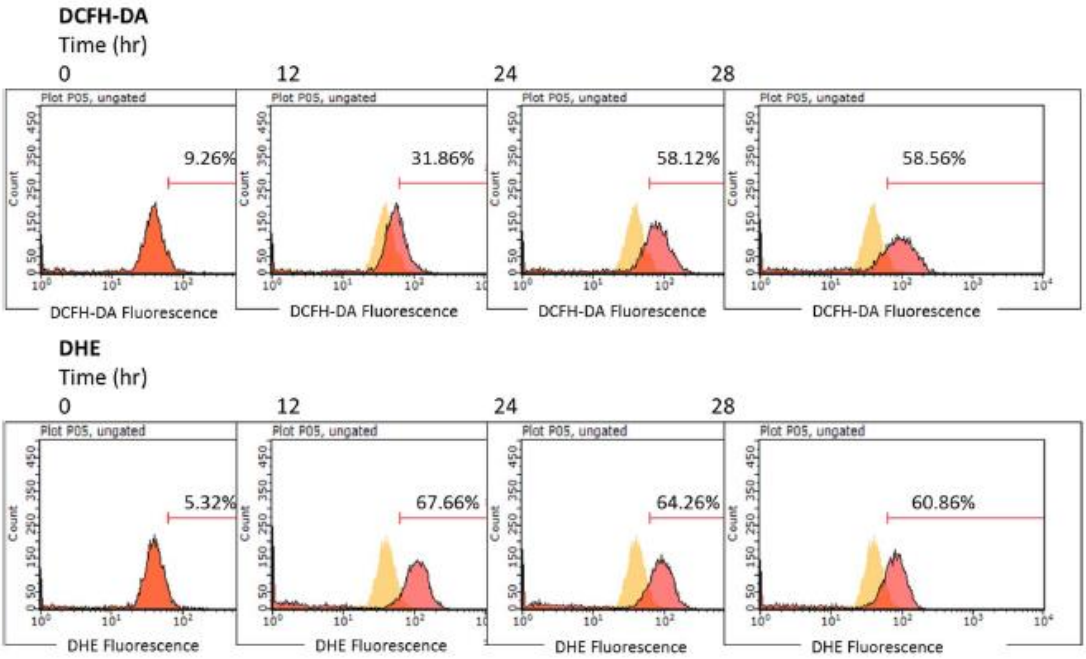

Supplementary figure 4.4. Avocatin B increases ROS. TEX cells were treated with 10µM avocatin B and DCFH-DA and DHE were measured at increasing time points by flow cytometry. Raw data showing the homogenous cell shift in DCFH-DA or DHE are shown.

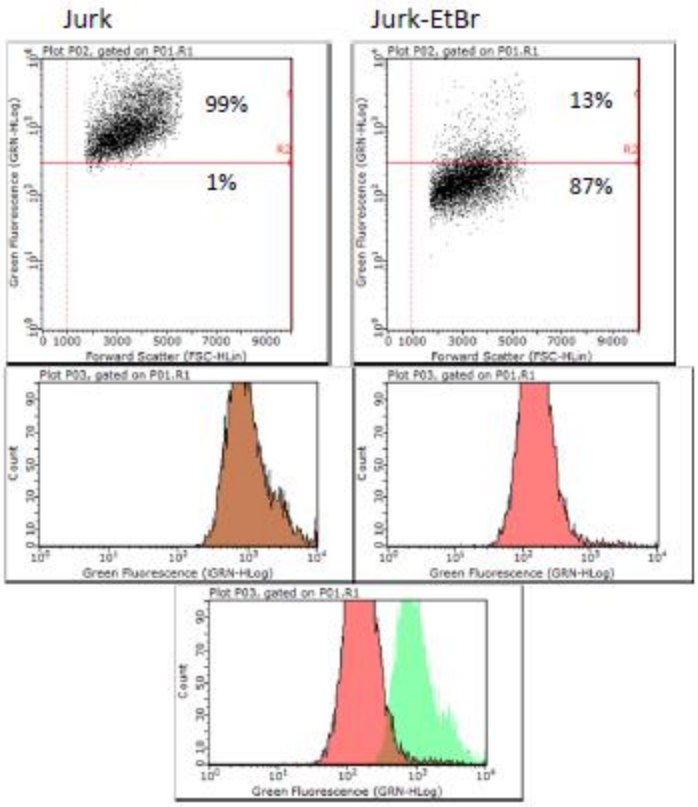

Supplementary figure 4.5. Jurkat T cells cultured in ethidium bromide medium have reduced mitochondria. **(A)** Jurkat T cells were cultured in ethidium bromide media for 60 days and mitochondria were detected by nonyl acridine orange (NAO) staining, which binds to the mitochondria specific lipid, cardiolipin. (Left panel) Jurkat T cells demonstrate positive NAO staining whereas (right panel) Jurkat-EtBr cells demonstrate a drastic reduction in NAO staining (~87%).

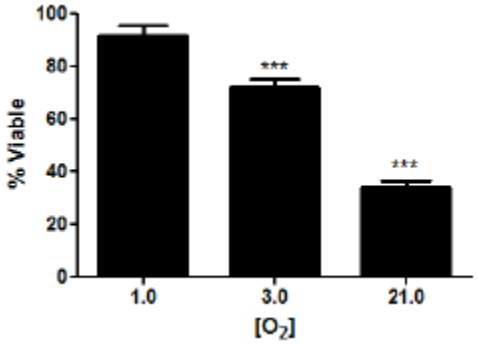

Supplementary figure 4.6. Avocatin B's cytotoxicity is dependent on [O_2]. **(A)** TEX cells were grown in normoxic (21%O_2) or hypoxic (3% and 1%O_2) conditions and incubated with avocatin B (2μM) for 72 hours. Cell viability was measured by the sulforhodamine B assay, as described in the methods. Data are presented as mean percentage of live cells ± SD. All experiments were performed three times in triplicate. ***; p<0.001. *Experiment performed by Princess Margaret Cancer Centre.*

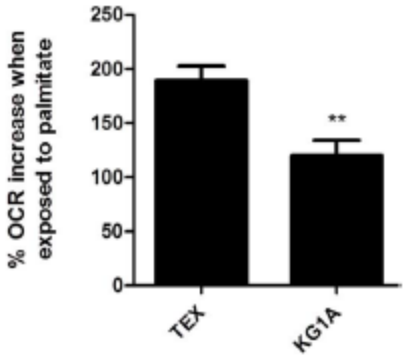

Supplementary figure 4.7. Avocatin B's toxicity is dependent on basal levels of fatty acid oxidation. Basal levels of fatty acid oxidation were tested in TEX (avocatin B sensitive) and KG1a (avocatin B insensitive) cells were treated, as described in the methods sections.

Chapter 5: Discussion

A screen of a natural health product library identified avocatin B as a novel anti-AML agent. *In vitro* and pre-clinical functional studies demonstrated that it induced selective toxicity toward leukemia and leukemia stem cells with no toxicity toward normal cells. Mechanistically, we highlight a novel strategy to induce selective leukemia cell death where mitochondrial localization of avocatin B inhibits fatty acid oxidation leading to reduced levels of NADPH and ROS-dependent, caspase and AIF-mediated apoptosis.

5.1 Avocatin B's selectivity

Avocatin B targets leukemia over normal cells. We propose this specificity is related to the leukemia cell's altered mitochondrial characteristics, as a number of observations suggest avocatin B localizes in mitochondria. For example, (1) cells with significantly reduced mitochondria or (2) lacking the enzyme that facilitates mitochondrial lipid transport, CPT1, are insensitive to avocatin B; (3) chemical treatment with etomoxir, a CPT1 inhibitor, blocked avocatin B's activity; (4) CPT1 only facilitates entry of lipids of avocatin B's size into mitochondria (e.g., 16-20 carbons [110]; avocatin B:17 carbons [85]); and (5) UCP2 levels are increased following avocatin B treatment. Leukemia cells contain higher mitochondrial mass [28] and greater demand for fatty acid substrates for metabolic activity [24] compared to normal hematopoietic cells [24]. Thus, given the leukemia cell's mitochondrial phenotype, we propose that avocatin B accumulates with greater concentration in leukemia over normal cells, thus conferring its increased toxicity toward leukemia cells.

In both normal CD34+ hematopoietic cells and peripheral blood stem cells, we reported that avocatin B imparted no toxicities at concentrations as high as 20μM whereas in primary AML cells, avocatin B had an EC50: 3.9 ± 2.5μM (chapter 4). These results suggest indeed that avocatin B's selectivity resides in these differences between AML and normal hematopoietic cells.

To confirm avocatin B's selectivity towards AML cells, Dr. Spagnuolo conducted a preliminary screen of avocatin B in other cell lines consisting of both cancer and normal models (Figure 5.1). Here, it was reported that avocatin B only reduced the viability of leukemia cells tested, whilst normal cells, including kidney and lung, and other cancers, including myeloma and solid tumours, were unaffected by avocatin B treatment. This serves as a preliminary indicator that used as a chemotherapeutic, avocatin B will not impart toxicities into other body tissues.

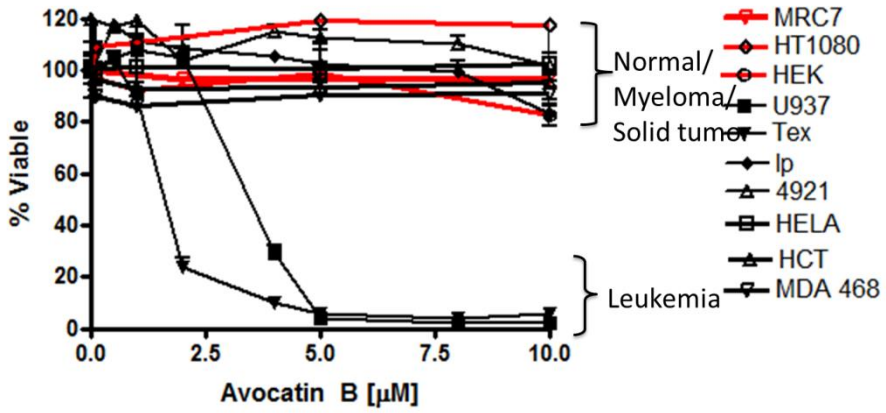

Figure 5.1. Avocatin B is sensitive towards leukemia cells. Various cancer and normal cell lines were incubated with increasing dose of avocatin B and incubated over 72 hours. Viability was assessed using the MTS assay and data are represented as mean percentage of live cells. *This work was performed by Dr. Paul Spagnuolo at the Princess Margaret Cancer Hospital (Toronto, ON)*. Cell lines: HEK293 human embryonic kidney; MRC-7 human foetal lung; HT-1080 fibrosarcoma/connective tissue; Lp1 myeloma; 4921 myeloma; Hela cervical cancer; HCT-116 colon carcinoma; MDA-468 Breast cancer; U937 leukemia; TEX leukemia.

In chapter 4, we established that avocatin B's mechanism of action involves the inhibition of fatty acid oxidation. This is mechanism takes advantage of the altered metabolic preference for fatty acids present in leukemia cells over hematopoietic cells. Of concern however, is that fatty acid oxidation is important for energy homeostasis in cardiac muscles, skeletal muscles, liver and to some degree kidney, small intestines and adipose tissue [22, 23]. Patients with fatty acid oxidation defects have been reported with hypoketonic hypoglycemia, cardiomyopathy and/or rhabdomyolysis [23]. As such, future animal studies should carefully monitor for any associated toxicities.

In chapter 4, we report that avocatin B inhibits fatty acid oxidation in leukemia cells at a 10-fold less concentration than the gold standard pharmacological inhibitor, etomoxir [24, 75, 125]. Etomoxir inhibits the CPT1 enzyme, which exerts about 80% control over the fatty acid oxidation pathway [23, 125]. Notably, etomoxir inhibits avocatin B induced cell death indicating that avocatin B's uptake into the mitochondria (chapter 4) is mediated by CPT1. CPT1 exists in 3 isoforms: CPT1A (expressed in the liver, kidney, lung, spleen, intestine, pancreas, ovary and fibroblasts), B (expressed in the heart, skeletal muscle, testis and brown adipocytes) and C (expressed only in the brain, however its function remains to be unknown) [22, 23]. In our studies, CPT1A knockout cells were insensitive to avocatin B treatment indicating that CPT1A is essential for leukemia mitochondrial import of avocatin B. In both normal lung and kidney cells (Figure 5.1), avocatin B did not cause any reduction in viability further suggesting that it may be selective only towards leukemia cells.

In order for etomoxir to inhibit CPT1, it must first be converted to a CoA ester [126]. This mechanism is similar to the entry of fatty acids, which are CoA-esterified by acyl-CoA synthetase [127]. Although not formally tested, it is presumed that avocatin B, given its dependence on CPT1 for cytotoxicity, is also CoA-esterified by acyl-CoA synthetase prior to entry into mitochondria. As such, future studies should examine the role of acyl-CoA synthetase in avocatin B's mechanistic activity.

Given that avocatin B inhibits fatty acid oxidation, understanding the *in vivo* effects of clinically used fatty acid oxidation inhibitors may shed light onto avocatin B's *in vivo* profile. To date, perhexiline, a CPT1 inhibitor, trimetazidine, a 3-ketoacyl-CoA thiolase inhibitor, and ranolazine, a 3-ketoacyl-CoA thiolase inhibitor, are approved for human use for the treatment of angina [21]. Inhibition of fatty acid oxidation shifts cardiac muscle metabolism towards glucose oxidation to increase myocardial efficiency in ischemic conditions [128]. Given these *in vivo* profiles, it is possible that avocatin B may exert a similar profile.

In chapter 4, we report that avocatin B targets the mitochondria. This is demonstrated through cells lacking functional mitochondria displaying insensitivity to avocatin B treatment, through genetic and

pharmacological inhibition of CPT1, which facilitates fatty acid transport into the mitochondria, and through increased UCP2 expression (chapter 4). Given that the mitochondria is essential for energy production and exerts control over cell death, the mitochondria is a feasible target in cancer therapy [129]. Mitochondria are implicated in tumorigenesis and tumour progression as cancer cells possess mutations in mitochondrial respiratory chain resulting in inefficient ATP production and chromosomal instability [130]. In fact, mitochondria in cancer cells are structurally and functionally different from those found in normal cells [130, 131]. Cancer cell mitochondria have been reported with a different phospholipid mitochondrial membrane composition compared to normal cells [132] as well as metabolic reprogramming (such as fatty acid oxidation in leukemia; chapter 1). The metabolic reprogramming observed in cancer cell mitochondria renders them more susceptible to mitochondrial disruption over non-cancerous cells [133, 134]. Additionally, we report that avocatin B targets leukemia and leukemia stem cells through decreases in NADPH resulting in increased levels of ROS (chapter 4). Both breast cancer stem cells and leukemia stem cells have been found to express low levels of ROS and higher levels of antioxidants compared to blast cells [32, 135]. Given the numerous structural, physiological and functional differences in cancer cell mitochondria, targeting the mitochondria is a promising therapeutic approach.

5.2 Mechanism of action

Inhibition of fatty acid oxidation by avocatin B resulted in ROS-induced apoptosis. Apoptosis was mediated by the mitochondrial proteins cytochrome c and AIF, which are commonly released following ROS-induced increases in mitochondrial outer membrane permeability [136, 137]. Inhibiting fatty acid oxidation by blocking CPT1 with etomoxir resulted in ROS-dependent death of glioma cells caused by reduced concentrations of intracellular antioxidants attributed to decreased NADPH [75]. Similarly, we demonstrated that avocatin B-induced inhibition of fatty acid oxidation reduced NADPH levels and that antioxidant supplementation rescued cells from death. NADPH is utilized for catabolic processes in proliferating cells and is the precursor of reduced glutathione, which counteracts the

detrimental effects of ROS [95, 138]. Our observed NADPH decrease (t=5h; Figure 4.11D) preceded ROS elevation (t=12h; Figure 4.11E), further confirming the relationship between inhibition of fatty acid oxidation, NADPH and ROS-dependent leukemia cell death. Of note, in our experiments avocatin B accumulated in mitochondria and inhibited fatty acid oxidation and reduced NADPH at 10μM whereas other studies used etomoxir, which blocks fatty acid entry into mitochondria and reduces NADPH, at 100μM [24] or 1000μM [75]. Together, these results point to a mechanism where avocatin B enters the mitochondria and potently inhibits fatty acid oxidation resulting in reduced NADPH and ROS-induced apoptosis.

5.2.1 Decreased levels of NADPH cause increases in ROS

Our studies report that the avocado-derived lipid avocatin B was selectively cytotoxic towards AML and AML progenitor cells. In contrast, it was not cytotoxic to normal hematopoietic cells (CD34+). Mechanistically, avocatin B inhibited fatty acid oxidation resulting in decreased levels of NADPH resulting in increased levels of ROS. NADPH is utilized for catabolic processes in proliferating cells and is necessary to regenerate reduced glutathione, which counteracts the detrimental effects of ROS [95, 138]. Notably, Pike *et al*. (2011) reported that even in the presence of glutamine and glucose, which generates NADPH through the pentose phosphate pathway, inhibition of fatty acid oxidation displayed a decrease in NADPH [75]. This suggests that NADPH generated from fatty acid oxidation is critical for defense against oxidative stress. Coupled with the fact that NADPH cannot pass through the inner mitochondrial membrane, NADPH generated from fatty acid oxidation serves as an essential source of antioxidants to combat mitochondria specific ROS [26]. Indeed, studies have shown that the mitochondrial enzyme IDH2, which regenerates NADPH, is critical towards defending cancer cells against oxidative stress and promoting cell survival [75, 139]. Mutations in IDH1 and IDH2 have been observed in AML, with reports of low levels of ROS in mice with mutated IDH1 [26, 140]. As such, it is speculated that inhibition of IDH1 or IDH2 will cause increases in ROS leading to cell death. In fact, decreased expression of IDH2 in fibroblast cell lines resulted in increased ROS levels, mitochondrial

damage and DNA fragmentation [141]. Based on these reports, I believe that our observed reports of decreased NADPH, directly contribute towards the observed increased levels of ROS in avocatin B treated leukemia cells.

5.2.2 Decreased NADPH and increased levels of ROS cause mitochondria-mediated apoptosis

In our studies, we report that avocatin B induces mitochondria-mediated apoptosis through the release of pro-apoptotic proteins cytochrome c and AIF. These reports are supported by disruption of the $\Delta\Psi m$ (chapter 4), and subsequent activation of caspases 3 and 7 (chapter 4). Cytochrome c and AIF reside in the intermembrane space of the mitochondria, requiring mitochondrial outer membrane permeabilization (MOMP) in order to be released [36]. In chapter 4, we report that avocatin B treatment increases ROS levels while decreasing NADPH levels. Excessive ROS can induce apoptosis by modifying mitochondrial proteins such as mitochondrial permeability transition pore proteins, voltage-dependent anion channel (VDAC) and adenine nucleotide translocase (ANT), resulting in cytochrome c and AIF release [142]. Further, NADPH is required for the regeneration of GSH. Studies have reported that mitochondrial GSH redox status is a key modulator of MOMP, and that decreases in GSH result in the redox modulation of ANT resulting in the release of cytochrome c and AIF [143, 144]. This coincides with our reports that avocatin B decreases both NADPH and GSH (chapter 4) resulting in mitochondria-mediated apoptosis.

5.2.3 Avocatin B's effect on the fatty acid biosynthesis pathway

Leukemia cells display a metabolic shift from the oxidation of glucose derived carbon sources to the oxidation of fatty acids [24]. As such, fatty acids play a pivotal role in providing carbon building blocks and growth factors to leukemia cells. In our studies, we report that avocatin B inhibits fatty acid oxidation resulting in autophagy and apoptosis activation. In chapter 4, we highlight how autophagy is activated as a result of deficiency in cellular building blocks and growth factors.

Given that leukemia cells rely on *de novo* fatty acid synthesis [20, 26], coupled with fact that avocatin B related compounds inhibit this pathway, we also explored avocatin B's effect on the fatty acid biosynthesis pathway. We reported, that supplementation with exogenous palmitate (chapter 4) can rescue leukemia cells from avocatin B induced death. Palmitate is the end product of the fatty acid biosynthesis pathway and is produced by FASN. FASN has been reported to be upregulated in many cancer types, while being expressed at very low levels in most normal human tissues [93]. Therefore, we co-incubated avocatin B with the FASN inhibitor orlistat, where it displayed no effect on avocatin B's activity suggesting that its activity is independent of FASN. This indicates that avocatin B and palmitate may compete for entry into the mitochondria via CPT1 (Discussed in next section). Next, we further excluded the fatty acid biosynthesis pathway through co-incubation with malonyl-CoA, acetyl-CoA (acetyl-CoA carboxylase end products) and oleic acid (SCD1 end product), and showed that neither treatments could rescue cells from avocatin B induced cell death. These results suggest that avocatin B's activity is independent of the fatty acid biosynthesis pathway, and is only reliant on the uptake and oxidation of fatty acids in the mitochondria.

Interestingly, accumulation of malonyl-CoA, an intermediary fatty acid metabolite, can be cytotoxic to cells. Indeed, treatment of TEX cells with high concentration of malonyl-CoA reduced cell viability (chapter 5). Malonyl-CoA is a cytotoxic reversible inhibitor of CPT1 which prevents newly synthesized fatty acids from undergoing oxidation [92, 93]. Accumulation of malonyl-CoA, results in apoptosis onset as a result of the activation of pro-apoptotic proteins BNIP3, TRAIL and DAPK2 [93]. Similarly, we report that avocatin B induces autophagy activation through BNIP3 expression (chapter 4), which is involved in both autophagy and apoptosis onset. Future studies will need to explore the link between fatty acid oxidation, autophagy and apoptosis onset.

5.2.4 Palmitate supplementation rescues TEX cells from avocatin B induced cell death

In chapter 4, we report that palmitate supplementation rescues TEX cells from avocatin B treatment. These results present a number of associated questions. We reported that co-incubation with

avocatin B and palmitate display a reduction in fatty acid oxidation and reduced NADPH levels. Given that long-term palmitate supplementation rescues TEX cells, avocatin B may in fact compete with palmitate for entry into the mitochondria via CPT1. This mode of action would be similar to that of other drugs that compete with endogenous ligands to alter cellular responses, as is the case with tamoxifen that competes with estrogen to block proliferation [145] or anastrozole that competes for the aromatase inhibitor in breast and ovarian cancer treatments [146]. Studies exploring this potential competitive mechanism have yet to be performed, as such should be explored in future studies.

5.2.5 Oxidation of odd-numbered lipids

Avocatin B is a 1:1 ratio of two 17-carbon lipids derived from methanol extracted avocado pear seeds (*Persea gratissima*) [84]. Odd-numbered carbons are rare, not produced endogenously and obtained only from dietary sources [147, 148]. Moreover, they are not efficiently or preferentially oxidized. For example, mice fed diets containing radiolabelled odd and even-numbered fatty acids only accumulate odd-numbered fatty acids in adipose tissue (i.e., C15 and 17) [149]; odd-numbered fatty acids show consistent adipose accumulation [147, 150, 151]. In humans, lipids of 13, 15 and 17 carbon lengths are used as serum and adipose tissue biomarkers of dietary fat intake, as these fatty acids are more slowly catabolized compared to even-numbered fatty acids [148, 152]. Although they undergo the same pathway of oxidation, the terminal step of odd-numbered fatty acid oxidation produces 1 acetyl-coA and 1 propionyl-CoA molecule whereas even-numbered fatty acids produce 2 acetyl-coA molecules [153]. Propionyl-CoA can then be converted to methylmalonyl-CoA by propinyl-CoA carboxylase and vitamin B12, at the expense of 1 ATP, which is in turn converted to succinyl-CoA that can enter the TCA cycle [151]. Since this alternate pathway requires energy and delays overall ATP production, the decreased metabolic activity (i.e., reduced acetyl-CoA production and/or decreased entry of fatty acid byproducts into the TCA cycle) likely explains our observed decrease in NADPH. As such, reduced NADPH not only results in elevated ROS but also indicates a decrease in overall metabolic activity. Thus, a novel pathway by which fatty acid oxidation can be inhibited in leukemia cells is by the odd-numbered carbon

lipid, avocatin B stalling or rendering less efficient the fatty acid oxidation pathway. This highlights a novel strategy to induce selective leukemia cell death by which preferential mitochondrial localization of avocatin B reduces leukemia cell metabolism and NADPH to increase ROS resulting in cell death.

5.2.6 Lipotoxicity

Alternatively, mitochondrial accumulation of fatty acids could have lipotoxic effects. When in excess, fatty acids can accumulate inside the mitochondrial matrix where they are deprotonated, as a result of the proton gradient, creating fatty acid anions. These are converted by ROS into lipid peroxides that in turn cause damage to mitochondrial DNA, lipids and proteins within the mitochondrial matrix [154]. However, the generation of lipotoxic products requires ROS [155], therefore; avocatin B accumulation by itself would be insufficient to impart lipotoxicity. Thus once inside the mitochondria, avocatin B or avocatin B derivatives may be converted to lipotoxic byproducts and contribute to death but only after sufficient ROS production (i.e., following avocatin B-induced inhibition of fatty acid oxidation). In further support of this explanation, avocatin B increased UCP2 levels, consistent with mitochondrial accumulation [109], but this was observed only after 48 hours of treatment (i.e., UCP2 expression follows our observed ROS elevation). In fact, a prevailing hypothesis is that the function of UCP upregulation is to drive fatty acid anions outside the mitochondrial matrix to reduce lipotoxicity [109, 156]. Thus, mitochondrial accumulation may contribute to death through lipotoxicity but this is not the underlying mechanism of avocatin B's activity.

5.3 Avocatin B induces autophagy

We reported that the avocado-derived lipid avocatin B inhibits fatty acid oxidation that was followed by ROS-mediated leukemia and leukemia stem cell apoptosis [111]. Here, we report new evidence highlighting autophagy as an essential intermediate step in avocatin B-induced selective leukemia cell apoptosis.

In this study, we show that autophagy was critical to avocatin B's toxicity. We demonstrated that autophagy was activated and that autophagy proteins were functionally important to avocatin B-induced

death. Given these findings, it seems likely that autophagy activation is due to prolonged deprivation of essential growth factors (e.g. fatty acid-derived metabolites and NADPH) that leads to the generation of ROS. Starvation is one of the most well-studied conditions that results in autophagy activation [46, 157]. Most autophagy stimuli converge at the protein complex mTORC1 which serves as a stimuli sensor, detecting nutrient and growth factor availability [45, 46]. Given that leukemia cells possess an abnormal mitochondrial phenotype characterized by a greater demand for fatty acid substrates [29, 31], we propose that inhibiting fatty acid oxidation activates autophagy by causing a significant deficiency in essential cellular building blocks. Similar to our previous study demonstrating that avocatin B-induced apoptotic cell death characterized by caspase activation and AIF release [111], serum deprivation in hippocampal HT22 neurons activated autophagy that resulted in caspase 3 and AIF-mediated apoptosis [39]. Moreover, we previously showed that avocatin B's activity was ROS-dependent (as measured by DHE and DCF-DA), as leukemia cells co-incubated with anti-oxidants block its activity[111]. Thus, it is likely that avocatin B-induced autophagy is activated by ROS following serum starvation. Indeed, accumulating evidence indicates that ROS plays an essential role in the activation of autophagy and that the mitochondria is the main source of ROS [120, 157, 158].

We have shown that avocatin B-induced apoptosis was characterized by release of the mitochondrial proteins cytochrome c and AIF [111]. In this study, we show that AML cells with significantly reduced autophagy proteins Atg7 and p62 are insensitive or increasingly sensitive to avocatin B's cytotoxicity, respectively. This indicates that autophagy plays a functional role in avocatin B's death inducing mechanism. As such, avocatin B's activation of autophagy must be involved in the induction of mitochondrial apoptosis. Similar to avocatin B, mitochondrial target drugs induce both autophagic and apoptotic responses. Arsenic trioxide and obatoclax induces both autophagy and apoptosis in leukemia cells [159, 160]; rottlerin induces both processes in prostate cancer cells [161]. Finally, APO866 and FK866 induce both autophagy and apoptosis as a result of NAD depletion in cells from various hematological malignancies, including AML [162]. Avocatin B reduced NADPH and NAD and

similar to APO866 and FK866's activity, autophagy is activated following an induced deficiency of an essential cellular growth factor.

Avocatin B-mediated leukemia cell death is dependent on the induction of autophagy. As such, there is cross-talk between autophagy and apoptosis signaling pathways. Additional studies are needed to further elucidate the mechanism of this crosstalk following avocatin B treatment. In cancer cells, the combined activation of autophagy and apoptosis has been observed through DRAM1 (damage –regulated autophagy modulator 1), which is activated by p53 [42, 44]; Beclin 1 has been linked to p53 stability and function [50]. p53 is also linked to autophagy induction through the pro-apoptotic PUMA, which induces cytochrome c release [44]. In addition, Atg12 promotes intrinsic apoptosis through inactivation of the anti-apoptotic Bcl-2 family members Bcl-2 and Mcl-1 [51]. Future studies will evaluate the role of Beclin and p53 in avocatin B's activity to further elucidate the means by which inhibition of fatty acid oxidation activates autophagy to induce apoptosis in leukemia.

In conclusion, avocatin B activates autophagy in response to increased levels of ROS as a result of fatty acid oxidation impairment. Autophagy is essential for avocatin B's anti-leukemia activity which acts through the release of mitochondrial pro-apoptotic proteins cytochrome c and AIF. Given the observed findings, we highlight a novel mechanistic link between inhibition of fatty acid oxidation, autophagy and apoptosis.

5.4 Avocatin B as a novel therapy for AML

A major long-term goal of this project involves assessing avocatin B's pre-clinical efficacy for its potential as a novel AML chemotherapeutic. Currently, avocatin B is not marketed for any indications, however our findings suggest that it can have anti-cancer effects.

Few compounds that inhibit fatty acid oxidation are currently approved for clinical use [95]. CPT1 inhibitors such as etomoxir and perhexiline are associated with hepatoxicity [163] and neurotoxicity [164], respectively, and are not approved for clinical use in North America. Other inhibitors such as trimetazidine, which inhibits 3-ketoacyl-CoA thiolase, an enzyme involved in fatty acid

catabolism and ranolazine, which blocks late sodium currents, have had clinical success for the treatment of angina [165, 166]. None of these compounds are approved for use in AML or other hematological malignancies. Future studies are needed to asses avocatin B's pharmacology and pharmacokinetics; however, initial assessment of avocatin B's physicochemical properties suggests favorable tissue distribution. In particular, it possesses a high estimated partition coefficient (LogP = 8.9 [85]) indicating that it will accumulate in lipid-rich tissues such as adipose tissue and bone marrow. Given that LSCs reside in bone marrow, this could significantly enhance avocatin B's therapeutic efficacy.

If avocatin B were to become a chemotherapeutic, we must first consider routes of administration. Based on Lipinski's rule of five, avocatin B would be unsuitable for oral formulation due to its 6 hydrogen bond donors, its LogP of 8.9, and its molecular weight of 570.88g/mol [85]. As such, avocatin B would need to be administered intravenously (IV). IV administration is not uncommon for the treatment of AML as current therapy consisting of cytarabine and daunorubicin are administered IV [1].

Although no specific pharmacokinetic data is available, mice treated with an ethanol avocado pear seed extract (*Persea Americana*) had an LD50 of 1200.75mg/kg body weight [167]. Nonetheless, future studies are needed to test the pharmacokinetics and safety of avocatin B prior to entering human trials.

5.5 Limitations

Avocatin B was initially identified in an 800 compound drug screen of the TEX leukemia cell line. A limitation of our study was the number of cell lines used to test and validate our reported results. When the US National Cancer Institute screens for novel anticancer drugs, it involves 60 different cells lines from 9 different types of tumours [168]. Unfortunately, we do not have access to that many different cell lines. Additionally, our drug displays activity in TEX, an AML cell line with LSC properties. To date, cell lines with similar properties are publicly unavailable through outlets such as ATCC. To compensate for this, we used avocatin B at higher concentrations in less sensitive cell lines to observe an effect (ie. OCI-AML2 cells). This was performed to validate avocatin B's mechanistic effects. Given that

we reported avocatin B's efficacy in primary AML patient samples as well as in mouse xenotransplantation models, we do not feel that the lack of cell line data mitigate the significance of our findings.

Another limitation is the number of primary AML patient samples tested. In our studies, we report avocatin B's efficacy in 9 patient samples through the annexin V/PI viability assay and colony formation assays. Similar drug discovery studies have reported the use of ~20 primary AML patient samples [28, 114]. Unfortunately, our lab does not have direct access to patient samples. Through collaboration with Princess Margaret Cancer Hospital, we have been fortunate to obtain frozen aliquots of the primary AML samples that were tested in this study.

5.6 Conclusions

Given the need for the discovery of novel anti-leukemia and anti- leukemia stem cell drug candidates, the findings in this thesis have provided new insight for treatment strategies. Here, we report the discovery of avocatin B, an avocado-derived lipid, which selectively targets AML and leukemia stem cells through the inhibition of fatty acid oxidation. Avocatin B's mechanism of action is unique to current AML treatment strategies, making it an ideal target for future AML therapy. Future studies will need to further elucidate avocatin B's molecular target to characterize the cross talk that is observed between autophagy, apoptosis and fatty acid oxidation. Additionally, avocatin B's safety and pharmacokinetic properties will need to be assessed in mouse models in order to validate its pre-clinical efficacy and safety. In conclusion, the findings of this thesis, has provided the groundwork to establishing avocatin B's pre-clinical efficacy as a potential AML therapeutic and have elucidated a novel therapeutic strategy for the treatment of AML.

Appendix A: Research activity resulting from this program

PUBLICATIONS AND MANUSCRIPTS

Provisional patent application. Filed Oct 2014. Inventors: Spagnuolo PA, Schimmer AD, **Lee EA**

Lee EA, Angka L, Kreinin, E, McMillan EM, Giaever G, Quadrilatero J, Schimmer AD, Spagnuolo PA. Autophagy is required for the activation of apoptosis following inhibition of fatty acid oxidation. *In preparation.*

Lee EA, Angka L, Rota SG, Hurren R, Wang XM, Gronda M, Bernard D, Minden M, Mitchell A, Joseph JW, Datti A, Wrana J, Quadrilatero J, Schimmer AD, Spagnuolo PA. Targeting mitochondria with avocatin B induces selective leukemia cell death. *Cancer Research*. CAN-14-2676. *Revisions Pending*. 2014.

Nafissi N, Alqawlaq S, **Lee EA**, Foldvari M, Spagnuolo PA, Slavcev RA. DNA ministrings: highly safe and effective gene delivery vectors. *Mol Ther Nucleic Acids*. May 27 2014.

Angka L, **Lee EA,** Rota SG, et al. Glucopsychosine increases cytosolic calcium to induce calpain-mediated apoptosis of acute myeloid leukemia cells. *Cancer letters.* Mar 12 2014.

PRESENTATIONS

Oral presentation. Inhibition of fatty acid oxidation with avocatin B selectively targets AML cells and leukemia stem cells. American Society of Hematology Meeting 2014. San Francisco, CA. Dec 2014

Guest lecture: Nutrition, metabolism and body temperature regulation. PHARM111 - Systems Approach to the Study of the Human Body 2. University of Waterloo, Waterloo, ON. July 2014

Oral presentation. AVO: a novel inhibitor of fatty acid oxidation that induces selective leukemia cell death. 3-Minute Thesis Competition. University of Waterloo, Waterloo, ON. Mar 2014

Poster. 45 - Avocatin B is a novel inhibitor of fatty acid oxidation that induces selective leukemia cell death**.** Till and McCulloch Meetings 2014. Ottawa, ON. Oct 2014

Poster. AVO: a novel inhibitor of fatty acid oxidation that induces selective leukemia cell death Institute for comparative cancer investigation 2014. Guelph, ON. May 2014

Bibliography

1. Robak, T. and A. Wierzbowska, *Current and emerging therapies for acute myeloid leukemia.* Clin Ther, 2009. **31 Pt 2**: p. 2349-70.
2. Löwenberg, B., *Acute myeloid leukemia: the challenge of capturing disease variety.* Hematology Am Soc Hematol Educ Program, 2008: p. 1-11.
3. Ferrara, F. and C.A. Schiffer, *Acute myeloid leukaemia in adults.* The Lancet, 2013. **381**(9865): p. 484-495.
4. Lane, S.W. and D.G. Gilliland, *Leukemia stem cells.* Semin Cancer Biol, 2010. **20**(2): p. 71-6.
5. Snauwaert, S., B. Vandekerckhove, and T. Kerre, *Can immunotherapy specifically target acute myeloid leukemic stem cells?* OncoImmunology, 2013. **2**(2): p. e22943.
6. van Rhenen, A., et al., *High stem cell frequency in acute myeloid leukemia at diagnosis predicts high minimal residual disease and poor survival.* Clin Cancer Res, 2005. **11**(18): p. 6520-7.
7. Jan, M. and R. Majeti, *Clonal evolution of acute leukemia genomes.* Oncogene, 2013. **32**(2): p. 135-40.
8. Watson, A.S., M. Mortensen, and A.K. Simon, *Autophagy in the pathogenesis of myelodysplastic syndrome and acute myeloid leukemia.* Cell Cycle, 2011. **10**(11): p. 1719-1725.
9. Stein, E.M. and M.S. Tallman, *Novel and emerging drugs for acute myeloid leukemia.* Curr Cancer Drug Targets, 2012. **12**(5): p. 522-30.
10. Roboz, G.J., *Novel approaches to the treatment of acute myeloid leukemia.* Hematology Am Soc Hematol Educ Program, 2011. **2011**: p. 43-50.
11. Löwenberg, B., J.R. Downing, and A. Burnett, *Acute myeloid leukemia.* N Engl J Med, 1999. **341**(14): p. 1051-1062.
12. Craig, C.M. and G.J. Schiller, *Acute myeloid leukemia in the elderly: Conventional and novel treatment approaches.* Blood Reviews, 2008. **22**(4): p. 221-234.
13. Eleni, L.D., Z.C. Nicholas, and S. Alexandros, *Challenges in treating older patients with acute myeloid leukemia.* J Oncol, 2010. **2010**: p. 943823.
14. Estey, E., *What is the optimal induction strategy for older patients?* 2011(1532-1924 (Electronic)).
15. Pollyea, D.A., et al., *Targeting acute myeloid leukemia stem cells: a review and principles for the development of clinical trials.* Haematologica, 2014. **99**(8): p. 1277-1284.
16. Dick, J.E., *Stem cell concepts renew cancer research.* Blood, 2008. **112**(13): p. 4793-4807.
17. Bonnet, D.D., J.E., *Human acute myeloid leukemia is organized as a hierarchy that originates from a primitive hematopoietic cell.* Nat Med, 1997. **3**(7): p. 730-737.
18. Snauwaert, S.V., B.; Kerre, T., *Can immunotherapy specifically target acute myeloid leukemic stem cells?* OncoImmunology, 2013. **2**(2): p. e22943-1-10.
19. Horton, S.J. and B.J. Huntly, *Recent advances in acute myeloid leukemia stem cell biology.* Haematologica, 2012. **97**(7): p. 966-74.
20. Currie, E., et al., *Cellular fatty acid metabolism and cancer.* Cell Metab, 2013. **18**(2): p. 153-61.
21. Carracedo, A., L.C. Cantley, and P.P. Pandolfi, *Cancer metabolism: fatty acid oxidation in the limelight.* Nature Reviews Cancer, 2013. **13**(4): p. 227-232.
22. Houten, S.M. and R.J. Wanders, *A general introduction to the biochemistry of mitochondrial fatty acid beta-oxidation.* J Inherit Metab Dis, 2010. **33**(5): p. 469-77.
23. Bartlett, K. and S. Eaton, *Mitochondrial beta-oxidation.* Eur J Biochem, 2004. **271**(3): p. 462-9.
24. Samudio, I., et al., *Pharmacologic inhibition of fatty acid oxidation sensitizes human leukemia cells to apoptosis induction.* J Clin Invest, 2010. **120**(1): p. 142-56.
25. Schafer, Z.T., et al., *Antioxidant and oncogene rescue of metabolic defects caused by loss of matrix attachment.* Nature, 2009. **461**(7260): p. 109-13.

26. Reitman, Z.J. and H. Yan, *Isocitrate dehydrogenase 1 and 2 mutations in cancer: alterations at a crossroads of cellular metabolism.* J Natl Cancer Inst, 2010. **102**(13): p. 932-41.
27. Lee, S.M., et al., *Cytosolic NADP(+)-dependent isocitrate dehydrogenase status modulates oxidative damage to cells.* Free Radic Biol Med, 2002. **32**(11): p. 1185-96.
28. Skrtic, M., et al., *Inhibition of mitochondrial translation as a therapeutic strategy for human acute myeloid leukemia.* Cancer Cell, 2011. **20**(5): p. 674-88.
29. Samudio, I., M. Fiegl, and M. Andreeff, *Mitochondrial Uncoupling and the Warburg Effect: Molecular Basis for the Reprogramming of Cancer Cell Metabolism.* Cancer Res, 2009. **69**(6): p. 2163-2166.
30. Samudio, I., et al., *The warburg effect in leukemia-stroma cocultures is mediated by mitochondrial uncoupling associated with uncoupling protein 2 activation.* Cancer Res, 2008. **68**(13): p. 5198-205.
31. Velez, J., et al., *Mitochondrial uncoupling and the reprograming of intermediary metabolism in leukemia cells.* Front Oncol, 2013. **3**: p. 67.
32. Lagadinou, E.D., et al., *BCL-2 inhibition targets oxidative phosphorylation and selectively eradicates quiescent human leukemia stem cells.* Cell Stem Cell, 2013. **12**(3): p. 329-41.
33. Puissant, A., G. Robert, and P. Auberger, *Targeting autophagy to fight hematopoietic malignancies.* Cell Cycle, 2010. **9**(17): p. 3470-8.
34. Hotchkiss, R.S.S., A.; McDunn, J.E.; Swanson, P.E., *Cell death.* N Engl J Med, 2009 **361**(16): p. 1570-1583.
35. Vermes, I., et al., *A novel assay for apoptosis Flow cytometric detection of phosphatidylserine expression on early apoptotic cells using fluorescein labelled Annexin V.* Journal of Immunological Methods, 1995. **184**(1): p. 39-51.
36. Samudio, I., et al., *Apoptosis in leukemias: regulation and therapeutic targeting.* Cancer Treat Res, 2010. **145**: p. 197-217.
37. Joza, N., et al., *AIF: not just an apoptosis-inducing factor.* Ann N Y Acad Sci, 2009. **1171**: p. 2-11.
38. Vahsen, N., et al., *AIF deficiency compromises oxidative phosphorylation.* EMBO J, 2004. **23**(23): p. 4679-89.
39. Steiger-Barraissoul, S. and A. Rami, *Serum deprivation induced autophagy and predominantly an AIF-dependent apoptosis in hippocampal HT22 neurons.* Apoptosis, 2009. **14**(11): p. 1274-88.
40. Cecconi, F. and B. Levine, *The role of autophagy in mammalian development: cell makeover rather than cell death.* Dev Cell, 2008. **15**(3): p. 344-57.
41. Mizushima, N., et al., *Autophagy fights disease through cellular self-digestion.* Nature, 2008. **451**(7182): p. 1069-75.
42. Rosenfeldt, M.T. and K.M. Ryan, *The multiple roles of autophagy in cancer.* Carcinogenesis, 2011. **32**(7): p. 955-63.
43. Lee, J., S. Giordano, and J. Zhang, *Autophagy, mitochondria and oxidative stress: cross-talk and redox signalling.* Biochem J, 2012. **441**(2): p. 523-40.
44. Mah, L.Y. and K.M. Ryan, *Autophagy and cancer.* Cold Spring Harb Perspect Biol, 2012. **4**(1): p. a008821.
45. Wu, Y.T., et al., *Dual role of 3-methyladenine in modulation of autophagy via different temporal patterns of inhibition on class I and III phosphoinositide 3-kinase.* J Biol Chem, 2010. **285**(14): p. 10850-61.
46. Nencioni, A., et al., *Autophagy in blood cancers: biological role and therapeutic implications.* Haematologica, 2013. **98**(9): p. 1335-43.
47. Degenhardt, K., et al., *Autophagy promotes tumor cell survival and restricts necrosis, inflammation, and tumorigenesis.* Cancer Cell, 2006. **10**(1): p. 51-64.
48. Guo, J.Y., et al., *Activated Ras requires autophagy to maintain oxidative metabolism and tumorigenesis.* Genes Dev, 2011. **25**(5): p. 460-470.

49. Mathew, R., V. Karantza-Wadsworth, and E. White, *Role of autophagy in cancer.* Nature Reviews Cancer, 2007. **7**(12): p. 961-967.
50. Liu, J., et al., *Beclin1 controls the levels of p53 by regulating the deubiquitination activity of USP10 and USP13.* Cell, 2011. **147**(1): p. 223-34.
51. Rubinstein, A.D., et al., *The autophagy protein Atg12 associates with antiapoptotic Bcl-2 family members to promote mitochondrial apoptosis.* Mol Cell, 2011. **44**(5): p. 698-709.
52. Ryningen, A., et al., *Inhibition of Mammalian target of rapamycin in human acute myeloid leukemia cells has diverse effects that depend on the environmental in vitro stress.* Bone Marrow Res, 2012. **2012**: p. 329061.
53. Chiarini, F., et al., *A combination of temsirolimus, an allosteric mTOR inhibitor, with clofarabine as a new therapeutic option for patients with acute myeloid leukemia.* Oncotarget, 2012. **3**(12): p. 1615-28.
54. Tamburini, J., et al., *Mammalian target of rapamycin (mTOR) inhibition activates phosphatidylinositol 3-kinase/Akt by up-regulating insulin-like growth factor-1 receptor signaling in acute myeloid leukemia: rationale for therapeutic inhibition of both pathways.* Blood, 2008. **111**(1): p. 379-82.
55. Recher, C., et al., *Antileukemic activity of rapamycin in acute myeloid leukemia.* Blood, 2005. **105**(6): p. 2527-34.
56. Growers, C.A. 2012; Available from: http://www.californiaavocadogrowers.com/.
57. Yasir, M., S. Das, and M.D. Kharya, *The phytochemical and pharmacological profile of Persea americana Mill.* Pharmacogn Rev, 2010. **4**(7): p. 77-84.
58. Ding, H., et al., *Chemopreventive characteristics of avocado fruit.* Semin Cancer Biol, 2007. **17**(5): p. 386-94.
59. Oberlies, N.H., et al., *Cytotoxic and insecticidal constituents of the unripe fruit of Persea americana.* J Nat Prod, 1998. **61**(6): p. 781-5.
60. Leon, L.G., et al., *Antiproliferative effects of novel aliphatic acetogenin analogs against aggressive solid tumor cell lines.* In Vivo, 2011. **25**(2): p. 203-7.
61. Adikaram, N.K.B., et al., *Antifungal compounds from immature avocado fruit peel.* Phytochemistry, 1992. **31**(1): p. 93-96.
62. Schuringa, J.J. and H. Schepers, *Ex vivo assays to study self-renewal and long-term expansion of genetically modified primary human acute myeloid leukemia stem cells.* Methods Mol Biol, 2009. **538**: p. 287-300.
63. Baracca, A., et al., *Rhodamine 123 as a probe of mitochondrial membrane potential: evaluation of proton flux through F-0 during ATP synthesis.* Biochimica Et Biophysica Acta-Bioenergetics, 2003. **1606**(1-3): p. 137-146.
64. Cossarizza, A., et al., *Mitochondrial modifications during rat thymocyte apoptosis: a study at the single cell level.* Exp Cell Res, 1994. **214**(1): p. 323-30.
65. Dam, A.D., et al., *Elevated skeletal muscle apoptotic signaling following glutathione depletion.* Apoptosis, 2012. **17**(1): p. 48-60.
66. Owusu-Ansah, E., A. Yavari, and U. Banerjee, *A protocol for _in vivo_ detection of reactive oxygen species.* 2008.
67. Luo, Y., P. Rana, and Y. Will, *Palmitate Increases the Susceptibility of Cells to Drug-Induced Toxicity: An In Vitro Method to Identify Drugs With Potential Contraindications in Patients With Metabolic Disease.* Toxicological Sciences, 2012. **129**(2): p. 346-362.
68. Spagnuolo, P.A., et al., *The antihelmintic flubendazole inhibits microtubule function through a mechanism distinct from Vinca alkaloids and displays preclinical activity in leukemia and myeloma.* Blood, 2010. **115**(23): p. 4824-33.
69. Sukhai, M.A., et al., *Lysosomal disruption preferentially targets acute myeloid leukemia cells and progenitors.* J Clin Invest, 2012.
70. Sachlos, E., et al., *Identification of drugs including a dopamine receptor antagonist that selectively target cancer stem cells.* Cell, 2012. **149**(6): p. 1284-97.

71. Chou, T.C. and P. Talalay, *Quantitative analysis of dose-effect relationships: the combined effects of multiple drugs or enzyme inhibitors.* Adv Enzyme Regul, 1984. **22**: p. 27-55.
72. Chou, T.C., *Preclinical versus clinical drug combination studies.* Leuk Lymphoma, 2008. **49**(11): p. 2059-80.
73. Spagnuolo, P.A., et al., *Inhibition of intracellular dipeptidyl peptidases 8 and 9 enhances parthenolide's anti-leukemic activity.* Leukemia, 2013.
74. Abe, Y., et al., *TGF-beta1 stimulates mitochondrial oxidative phosphorylation and generation of reactive oxygen species in cultured mouse podocytes, mediated in part by the mTOR pathway.* Am J Physiol Renal Physiol, 2013. **305**(10): p. F1477-90.
75. Pike, L.S., et al., *Inhibition of fatty acid oxidation by etomoxir impairs NADPH production and increases reactive oxygen species resulting in ATP depletion and cell death in human glioblastoma cells.* Biochim Biophys Acta, 2011. **1807**(6): p. 726-34.
76. Angka, L., et al., *Glucopsychosine increases cytosolic calcium to induce calpain-mediated apoptosis of acute myeloid leukemia cells.* Cancer Lett, 2014.
77. Christensen, M.E., et al., *Flow cytometry based assays for the measurement of apoptosis-associated mitochondrial membrane depolarisation and cytochrome c release.* Methods, 2013. **61**(2): p. 138-145.
78. Waterhouse, N.J. and J.A. Trapani, *A new quantitative assay for cytochrome c release in apoptotic cells.* Cell Death Differ, 2003. **10**(7): p. 853-855.
79. Tanaka, Y., et al., *Accumulation of autophagic vacuoles and cardiomyopathy in LAMP-2-deficient mice.* Nature, 2000. **406**(6798): p. 902-6.
80. Lee, A.Y., et al., *Mapping the cellular response to small molecules using chemogenomic fitness signatures.* Science, 2014. **344**(6180): p. 208-11.
81. Carbon, S., et al., *AmiGO: online access to ontology and annotation data.* Bioinformatics, 2009. **25**(2): p. 288-9.
82. McDermott, S.P., et al., *A small molecule screening strategy with validation on human leukemia stem cells uncovers the therapeutic efficacy of kinetin riboside.* Blood, 2012. **119**(5): p. 1200-7.
83. Warner, J.K., et al., *Direct evidence for cooperating genetic events in the leukemic transformation of normal human hematopoietic cells.* Leukemia, 2005. **19**(10): p. 1794-805.
84. Alves HM, C.D., Falshaw CP, Godtfredsen WO, Ollis, WD *The Avocatins - a New Class of Natural Products.* Annals of the Brazilian Academy of Sciences, 1970. **42**: p. 4.
85. *ChemBank*. 2014; Available from: http://chembank.broadinstitute.org/chemistry/viewMolecule.htm;jsessionid=9CC037B2065BFDE714299282DD50A255?cbid=3198534.
86. Konopleva, M., et al., *Mechanisms of antileukemic activity of the novel Bcl-2 homology domain-3 mimetic GX15-070 (obatoclax).* Cancer Res, 2008. **68**(9): p. 3413-20.
87. Guzman, M.L., et al., *The sesquiterpene lactone parthenolide induces apoptosis of human acute myelogenous leukemia stem and progenitor cells.* Blood, 2005. **105**(11): p. 4163-9.
88. Chipuk, J.E., L. Bouchier-Hayes, and D.R. Green, *Mitochondrial outer membrane permeabilization during apoptosis: the innocent bystander scenario.* Cell Death Differ, 2006. **13**(8): p. 1396-402.
89. Dussmann, H., et al., *Outer mitochondrial membrane permeabilization during apoptosis triggers caspase-independent mitochondrial and caspase-dependent plasma membrane potential depolarization: a single-cell analysis.* J Cell Sci, 2003. **116**(Pt 3): p. 525-36.
90. Hashimura, H., et al., *Acetyl-CoA carboxylase inhibitors from avocado (Persea americana Mill) fruits.* Biosci Biotechnol Biochem, 2001. **65**(7): p. 1656-8.
91. Pizer, E.S., et al., *Fatty acid synthase (FAS): a target for cytotoxic antimetabolites in HL60 promyelocytic leukemia cells.* Cancer Res, 1996. **56**(4): p. 745-51.
92. Lupu, R. and J.A. Menendez, *Pharmacological inhibitors of Fatty Acid Synthase (FASN)--catalyzed endogenous fatty acid biogenesis: a new family of anti-cancer agents?* Curr Pharm Biotechnol, 2006. **7**(6): p. 483-93.

93. Pandey, P.R., et al., *Anti-cancer drugs targeting fatty acid synthase (FAS).* Recent Pat Anticancer Drug Discov, 2012. **7**(2): p. 185-97.
94. Noto, A., et al., *Stearoyl-CoA desaturase-1 is a key factor for lung cancer-initiating cells*. Cell Death Dis, 2013. **4**.
95. Carracedo, A., L.C. Cantley, and P.P. Pandolfi, *Cancer metabolism: fatty acid oxidation in the limelight.* Nat Rev Cancer, 2013. **13**(4): p. 227-32.
96. Heiden, M.G.V., L.C. Cantley, and C.B. Thompson, *Understanding the Warburg Effect: The Metabolic Requirements of Cell Proliferation.* Science, 2009. **324**(5930): p. 1029-1033.
97. Kirsch, M. and H. De Groot, *NAD(P)H, a directly operating antioxidant?* FASEB J, 2001. **15**(9): p. 1569-74.
98. Godbout, J.P., et al., *alpha-Tocopherol reduces lipopolysaccharide-induced peroxide radical formation and interleukin-6 secretion in primary murine microglia and in brain.* J Neuroimmunol, 2004. **149**(1-2): p. 101-9.
99. Bejar, D.E.E., et al., *Uncovering Cardioprotective Strategies For Anthracycline Therapy By Analysis Of Redox and Apoptotic Effects.* Blood, 2013. **122**(21).
100. Vejpongsa, P. and E.T.H. Yeh, *Topoisomerase 2 beta: A Promising Molecular Target for Primary Prevention of Anthracycline-Induced Cardiotoxicity.* Clinical Pharmacology & Therapeutics, 2014. **95**(1): p. 45-52.
101. Kersten, S., et al., *Peroxisome proliferator-activated receptor alpha mediates the adaptive response to fasting.* J Clin Invest, 1999. **103**(11): p. 1489-98.
102. Thompson, M.P. and D. Kim, *Links between fatty acids and expression of UCP2 and UCP3 mRNAs.* FEBS Lett, 2004. **568**(1-3): p. 4-9.
103. Desjardins, P., E. Frost, and R. Morais, *Ethidium bromide-induced loss of mitochondrial DNA from primary chicken embryo fibroblasts.* Mol Cell Biol, 1985. **5**(5): p. 1163-9.
104. Hashiguchi, K. and Q.M. Zhang-Akiyama, *Establishment of human cell lines lacking mitochondrial DNA.* Methods Mol Biol, 2009. **554**: p. 383-91.
105. Belanger, A.J., et al., *Hypoxia-inducible factor 1 mediates hypoxia-induced cardiomyocyte lipid accumulation by reducing the DNA binding activity of peroxisome proliferator-activated receptor alpha/retinoid X receptor.* Biochem Biophys Res Commun, 2007. **364**(3): p. 567-72.
106. Cairns, R.A., I.S. Harris, and T.W. Mak, *Regulation of cancer cell metabolism.* Nat Rev Cancer, 2011. **11**(2): p. 85-95.
107. Ito, K. and T. Suda, *Metabolic requirements for the maintenance of self-renewing stem cells.* Nat Rev Mol Cell Biol, 2014. **15**(4): p. 243-56.
108. Fiegl, M., et al., *CXCR4 expression and biologic activity in acute myeloid leukemia are dependent on oxygen partial pressure.* Blood, 2009. **113**(7): p. 1504-1512.
109. Schrauwen, P., et al., *Uncoupling protein 3 as a mitochondrial fatty acid anion exporter.* FASEB J, 2003. **17**(15): p. 2272-4.
110. Reddy, J.K. and T. Hashimoto, *Peroxisomal beta-oxidation and peroxisome proliferator-activated receptor alpha: an adaptive metabolic system.* Annu Rev Nutr, 2001. **21**: p. 193-230.
111. Lee EA, A.L., Rota SG, Hurren R, Wang XM, Gronda M, Bernard D, Minden M, Mitchell A, Joseph JW, Datti A, Wrana J, Quadrilatero J, Schimmer AD, Spagnuolo PA. , *Targeting mitochondria with avocatin B induces selective leukemia cell death* Cancer Research. CAN-14-2676. Revisions Pending, 2014.
112. Rabinowitz, J.D. and E. White, *Autophagy and metabolism.* Science, 2010. **330**(6009): p. 1344-8.
113. Choi, A.M., S.W. Ryter, and B. Levine, *Autophagy in human health and disease.* N Engl J Med, 2013. **368**(7): p. 651-62.
114. Sukhai, M.A., et al., *Lysosomal disruption preferentially targets acute myeloid leukemia cells and progenitors.* J Clin Invest, 2013. **123**(1): p. 315-28.
115. Giaever, G., et al., *Chemogenomic profiling: identifying the functional interactions of small molecules in yeast.* Proc Natl Acad Sci U S A, 2004. **101**(3): p. 793-8.

116. Lee, A.Y., et al., *Mapping the Cellular Response to Small Molecules Using Chemogenomic Fitness Signatures.* Science, 2014. **344**(6180): p. 208-211.
117. Geng, J.F., et al., *Post-Golgi Sec Proteins Are Required for Autophagy in Saccharomyces cerevisiae.* Molecular Biology of the Cell, 2010. **21**(13): p. 2257-2269.
118. Ishihara, N., et al., *Autophagosome requires specific early Sec proteins for its formation and NSF/SNARE for vacuolar fusion.* Molecular Biology of the Cell, 2001. **12**(11): p. 3690-3702.
119. Mizushima, N., T. Yoshimori, and B. Levine, *Methods in mammalian autophagy research.* Cell, 2010. **140**(3): p. 313-26.
120. Scherz-Shouval, R. and Z. Elazar, *Regulation of autophagy by ROS: physiology and pathology.* Trends Biochem Sci, 2011. **36**(1): p. 30-8.
121. Mortensen, M., et al., *The autophagy protein Atg7 is essential for hematopoietic stem cell maintenance.* J Exp Med, 2011. **208**(3): p. 455-67.
122. Nihira, K., et al., *An inhibition of p62/SQSTM1 caused autophagic cell death of several human carcinoma cells.* Cancer Sci, 2014. **105**(5): p. 568-75.
123. Duran, A., et al., *The signaling adaptor p62 is an important NF-kappaB mediator in tumorigenesis.* Cancer Cell, 2008. **13**(4): p. 343-54.
124. Konopleva, M., et al., *Stromal cells prevent apoptosis of AML cells by up-regulation of anti-apoptotic proteins.* Leukemia, 2002. **16**(9): p. 1713-24.
125. Ito, K., et al., *A PML–PPAR-δ pathway for fatty acid oxidation regulates hematopoietic stem cell maintenance.* Nature Medicine, 2012. **18**(9): p. 1350-1360.
126. Agius, L., E.J. Meredith, and H.S. Sherratt, *Stereospecificity of the inhibition by etomoxir of fatty acid and cholesterol synthesis in isolated rat hepatocytes.* Biochem Pharmacol, 1991. **42**(9): p. 1717-20.
127. Postic, C. and J. Girard, *Contribution of de novo fatty acid synthesis to hepatic steatosis and insulin resistance: lessons from genetically engineered mice.* J Clin Invest, 2008. **118**(3): p. 829-38.
128. Kantor, P.F., et al., *The antianginal drug trimetazidine shifts cardiac energy metabolism from fatty acid oxidation to glucose oxidation by inhibiting mitochondrial long-chain 3-ketoacyl coenzyme A thiolase.* Circ Res, 2000. **86**(5): p. 580-8.
129. Fulda, S., L. Galluzzi, and G. Kroemer, *Targeting mitochondria for cancer therapy.* Nature Reviews Drug Discovery, 2010. **9**(6): p. 447-464.
130. Modica-Napolitano, J.S. and K.K. Singh, *Mitochondrial dysfunction in cancer.* Mitochondrion, 2004. **4**(5-6): p. 755-762.
131. Gogvadze, V., S. Orrenius, and B. Zhivotovsky, *Mitochondria in cancer cells: what is so special about them?* Trends Cell Biol, 2008. **18**(4): p. 165-173.
132. Garcea, R., et al., *Phospholipid-Composition of Inner and Outer Mitochondrial-Membranes Isolated from Yoshida Hepatoma Ah-130.* Cancer Lett, 1980. **11**(2): p. 133-139.
133. Kroemer, G. and J. Pouyssegur, *Tumor cell metabolism: Cancer's Achilles' heel.* Cancer Cell, 2008. **13**(6): p. 472-482.
134. Nadege, B., L. Patrick, and R. Rodrigue, *Mitochondria: from bioenergetics to the metabolic regulation of carcinogenesis.* Frontiers in Bioscience, 2009. **14**: p. 4015-4034.
135. Diehn, M., et al., *Association of reactive oxygen species levels and radioresistance in cancer stem cells.* Nature, 2009. **458**(7239): p. 780-3.
136. Tomasello, F., et al., *Outer membrane VDAC1 controls permeability transition of the inner mitochondrial membrane in cellulo during stress-induced apoptosis.* Cell Res, 2009. **19**(12): p. 1363-76.
137. Kroemer, G., L. Galluzzi, and C. Brenner, *Mitochondrial membrane permeabilization in cell death.* Physiol Rev, 2007. **87**(1): p. 99-163.
138. Vander Heiden, M.G., L.C. Cantley, and C.B. Thompson, *Understanding the Warburg effect: the metabolic requirements of cell proliferation.* Science, 2009. **324**(5930): p. 1029-33.

139. Smolkova, K. and P. Jezek, *The Role of Mitochondrial NADPH-Dependent Isocitrate Dehydrogenase in Cancer Cells.* Int J Cell Biol, 2012. **2012**: p. 273947.
140. Gorrini, C., I.S. Harris, and T.W. Mak, *Modulation of oxidative stress as an anticancer strategy.* Nature Reviews Drug Discovery, 2013. **12**(12): p. 931-947.
141. Jo, S.H., et al., *Control of mitochondrial redox balance and cellular defense against oxidative damage by mitochondrial NADP+-dependent isocitrate dehydrogenase.* J Biol Chem, 2001. **276**(19): p. 16168-76.
142. Orrenius, S., V. Gogvadze, and B. Zhivotovsky, *Mitochondrial oxidative stress: implications for cell death.* Annu Rev Pharmacol Toxicol, 2007. **47**: p. 143-83.
143. Chernyak, B.V. and P. Bernardi, *The mitochondrial permeability transition pore is modulated by oxidative agents through both pyridine nucleotides and glutathione at two separate sites.* Eur J Biochem, 1996. **238**(3): p. 623-30.
144. Verrier, F., et al., *Dynamic evolution of the adenine nucleotide translocase interactome during chemotherapy-induced apoptosis.* Oncogene, 2004. **23**(49): p. 8049-64.
145. Puddefoot, J.R., et al., *Non-competitive steroid inhibition of oestrogen receptor functions.* Int J Cancer, 2002. **101**(1): p. 17-22.
146. Buzdar, A.U., et al., *An overview of the pharmacology and pharmacokinetics of the newer generation aromatase inhibitors anastrozole, letrozole, and exemestane.* Cancer, 2002. **95**(9): p. 2006-16.
147. Campbell, R.G. and S.A. Hashim, *Deposition in adipose tissue and transport of odd-numbered fatty acids.* Am J Physiol, 1969. **217**(6): p. 1614-8.
148. Wolk, A., M. Furuheim, and B. Vessby, *Fatty acid composition of adipose tissue and serum lipids are valid biological markers of dairy fat intake in men.* J Nutr, 2001. **131**(3): p. 828-33.
149. Gotoh, N., et al., *Metabolism of odd-numbered fatty acids and even-numbered fatty acids in mouse.* J Oleo Sci, 2008. **57**(5): p. 293-9.
150. Pi-Sunyer, F.X., *Rats enriched with odd-carbon fatty acids. Effect of prolonged starvation on liver glycogen and serum lipids, glucose and insulin.* Diabetes, 1971. **20**(4): p. 200-5.
151. VanItallie, T.B. and A.K. Khachadurian, *Rats enriched with odd-carbon fatty acids: maintenance of liver glycogen during starvation.* Science, 1969. **165**(3895): p. 811-3.
152. Klein, R.A., D. Halliday, and P.G. Pittet, *The use of 13-methyltetradecanoic acid as an indicator of adipose tissue turnover.* Lipids, 1980. **15**(8): p. 572-9.
153. Berg JM, T.J., Stryer L., *Biochemistry. 5th edition*, in *Certain Fatty Acids Require Additional Steps for Degradation.*
2002, W H Freeman: New York.
154. Schrauwen, P. and M.K. Hesselink, *Oxidative capacity, lipotoxicity, and mitochondrial damage in type 2 diabetes.* Diabetes, 2004. **53**(6): p. 1412-7.
155. Schrauwen, P., et al., *Mitochondrial dysfunction and lipotoxicity.* Biochim Biophys Acta, 2010. **1801**(3): p. 266-71.
156. Wang, L.H., X.X. Gu, and R. Cao, *[Separation and identification of pathogens of Panax quinquefolium].* Zhongguo Yi Xue Ke Xue Yuan Xue Bao, 1987. **9**(3): p. 233-4.
157. Li, L., Y.Q. Chen, and S.B. Gibson, *Starvation-induced autophagy is regulated by mitochondrial reactive oxygen species leading to AMPK activation.* Cell Signal, 2013. **25**(1): p. 50-65.
158. Chen, Y.Q. and S.B. Gibson, *Is mitochondrial generation of reactive oxygen species a trigger for autophagy?* Autophagy, 2008. **4**(2): p. 246-248.
159. Qian, W., et al., *Arsenic trioxide induces not only apoptosis but also autophagic cell death in leukemia cell lines via up-regulation of Beclin-1.* 2007(0145-2126 (Print)).
160. Heidari, N., M.A. Hicks, and H. Harada, *GX15-070 (obatoclax) overcomes glucocorticoid resistance in acute lymphoblastic leukemia through induction of apoptosis and autophagy.* Cell Death Dis, 2010. **1**.

161. Kumar, D., S. Shankar, and R.K. Srivastava, *Rottlerin induces autophagy and apoptosis in prostate cancer stem cells via PI3K/Akt/mTOR signaling pathway.* Cancer Lett, 2014. **343**(2): p. 179-189.
162. Nahimana, A., et al., *The NAD biosynthesis inhibitor APO866 has potent antitumor activity against hematologic malignancies.* Blood, 2009. **113**(14): p. 3276-3286.
163. Holubarsch, C.J., et al., *A double-blind randomized multicentre clinical trial to evaluate the efficacy and safety of two doses of etomoxir in comparison with placebo in patients with moderate congestive heart failure: the ERGO (etomoxir for the recovery of glucose oxidation) study.* Clin Sci (Lond), 2007. **113**(4): p. 205-12.
164. Ashrafian, H., J.D. Horowitz, and M.P. Frenneaux, *Perhexiline.* Cardiovasc Drug Rev, 2007. **25**(1): p. 76-97.
165. Passeron, J., *[Effectiveness of trimetazidine in stable effort angina due to chronic coronary insufficiency. A double-blind versus placebo study].* Presse Med, 1986. **15**(35): p. 1775-8.
166. Aldakkak, M., D.F. Stowe, and A.K. Camara, *Safety and Efficacy of Ranolazine for the Treatment of Chronic Angina Pectoris.* Clin Med Insights Ther, 2013. **2013**(5): p. 1-14.
167. Padilla-Camberos E, M.-V.M., Flores-Fernández JM, Villanueva-Rodríguez S, *Acute Toxicity and Genotoxic Activity of Avocado Seed Extract (Persea americana Mill., c.v. Hass).* The Scientific World Journal, 2013. **2013**: p. 4.
168. Shoemaker, R.H., *The NCI60 human tumour cell line anticancer drug screen.* Nature Reviews Cancer, 2006. **6**(10): p. 813-823.